Cosmic Accelerators

Part A) Introduction

- Secondary particle production and nonthermal radiation
- Electromagnetic and hadronic cascades
- Accelerated particles in the Universe
- Collisionless plasma and transport equations
- Fazio-Stecker relation

Part B) Types of particle accelerators

- Magnetic Sun and solar wind
- Supernova Remnant shock waves
- Pulsars and plerions
- Nonthermal AGN: Radiogalaxies and blazars
- Other non-thermal sources

Part C) Particle acceleration

- Diffusive shock acceleration

Part A) Introduction

Relativistic particles and radiation

Mannheim & Schlickeiser A&A (1993)
Rybicki & Lightman „Radiative Processes in Astrophysics“, Cambridge
Schlickeiser „Cosmic Ray Physics“, Springer

- Electrons
  - Coulomb scattering
  - Inverse Compton scattering
  - bremsstrahlung
  - Synchrotron radiation (magneto - bremsstrahlung)
  - Triplet production
- Protons and ions
  - Coulomb scattering
  - Resonance excitation
  - Spallation
  - Pair production (Bethe – Heitler)
  - Pion production

$\sigma_T = 6.7\ 10^{-25}\ cm^2$

$\sigma_N = 3\ 10^{-26}\ cm^2$

$\sigma_\gamma = \alpha\ \sigma_N = 2\ 10^{-28}\ cm^2$

Radiative efficiency

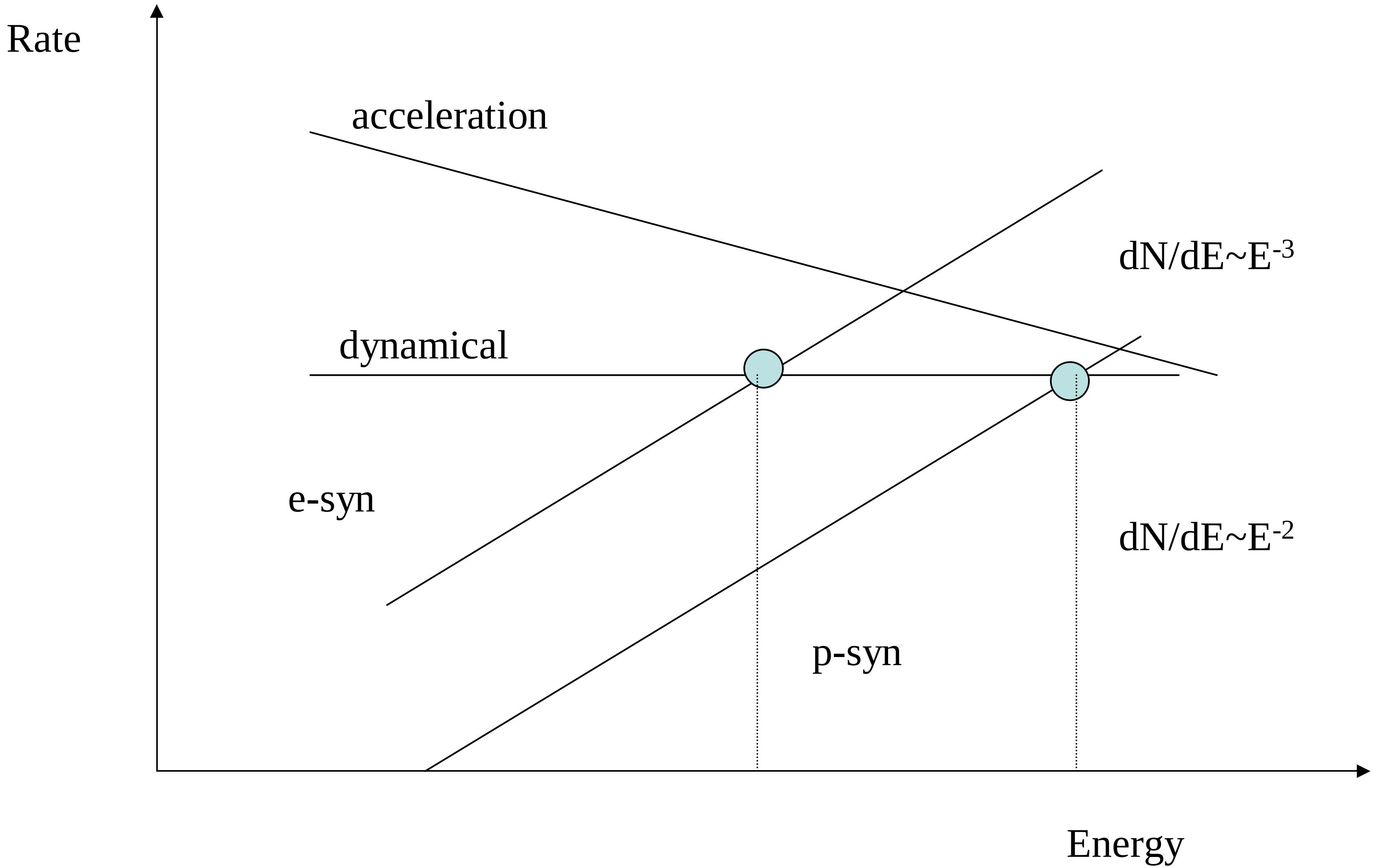

Inverse Compton scattering

$$\gamma_{LE} + e_{HE} \longrightarrow \gamma_{HE} + e_{LowerE}$$

- Inverse Compton scattering (not really a good name)
  - Very important process in HE astrophysics
  - Electron is of high energy:
    1. Go into rest frame of electron (one gamma factor)
    2. Apply Thomson scattering in rest frame of electron
    3. Lorentztransform the result back into the observer'f frame (second gamma factor)
  - Maximum energy transfer:

$$\hbar\omega_{final,\max} = 4 \cdot \gamma^2 \cdot \hbar\omega_{initial}$$

  - Again a gamma^2 factor, similar to ionisation loss energy loss formula

Quasi-klassische Berechnung → Rybicki & Lightman

Exakte QED Berechnung (1. Ordnung) → Jauch & Rohrlich

Neutrino production

$$\Phi_p \sim E^{-2}$$

$$p\gamma \rightarrow \Delta^+$$

$$\Delta^+ \rightarrow \pi^0 p, \quad \pi^0 \rightarrow \gamma\gamma$$

$$\Delta^+ \rightarrow \pi^+ n, \quad n \rightarrow p\, e^- \,\bar{\nu}_e$$

$$\pi^+ \rightarrow \mu^+ \nu_\mu, \quad \mu^+ \rightarrow e^+ \nu_e \bar{\nu}_\mu$$

$$pp \rightarrow \ldots$$

$$E_\nu = \frac{4}{3} E_\gamma$$

$$\frac{\Phi_\gamma}{\Phi_{\nu_\mu}} = \frac{2}{1}$$

$$\frac{\Phi_{\nu_\mu}}{\Phi_{\bar{\nu}_\mu}} = \frac{1}{1}$$

$$\frac{\Phi_{\nu_\mu}}{\Phi_{\nu_e}} = \frac{1}{1}$$

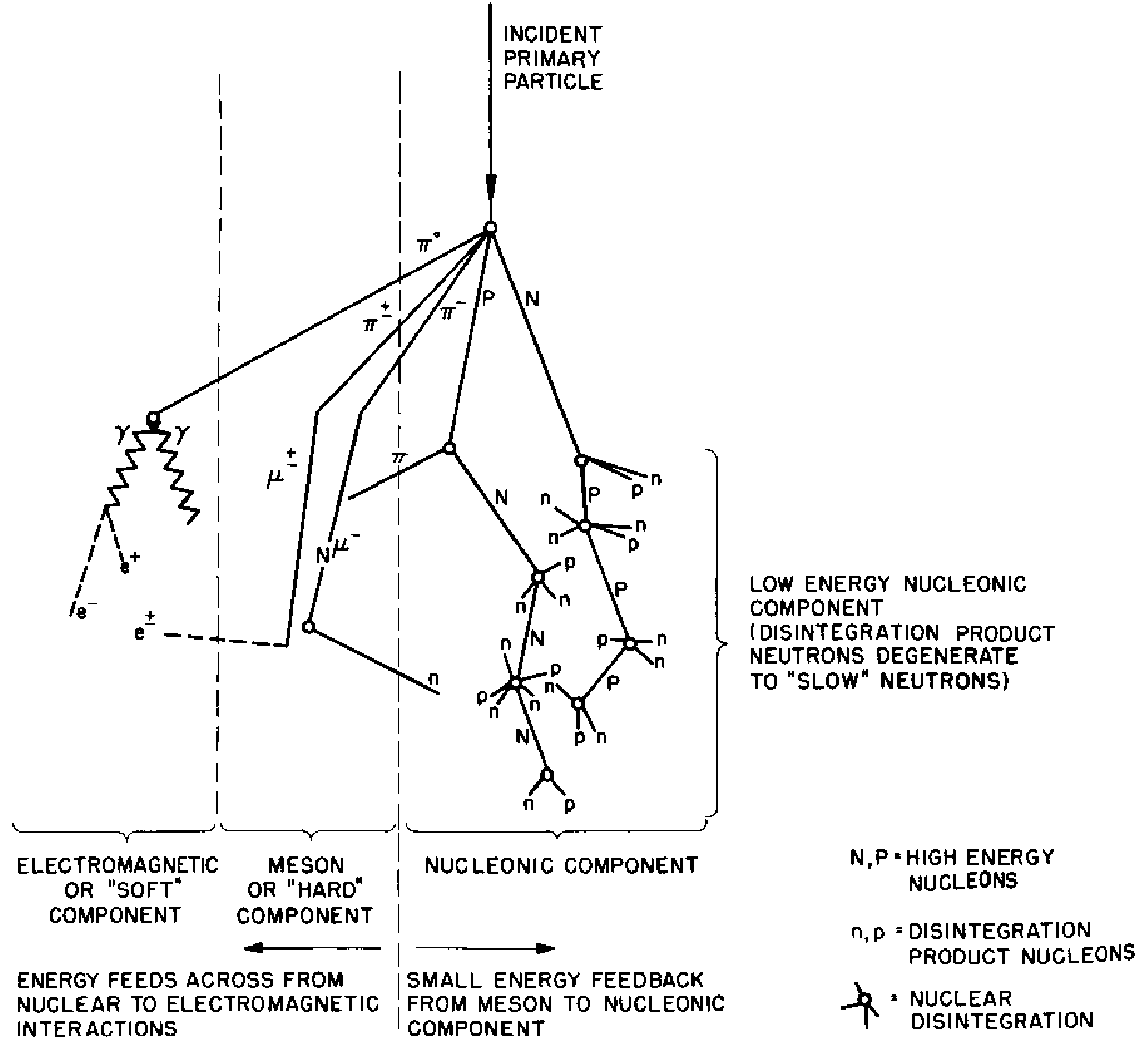

Schematic Diagram of Cosmic Ray Shower

Kaskadengleichungen

- Primärteilchen der KS erzeugt energiereiche Sekundärteilchen in der Atmosphäre
- Die Sekundärteilchen erzeugen lawinenartig weitere Teilchen, bis deren mittlere Energie für Teilchenerzeugung nicht mehr ausreicht (Ionisationsverluste sind dann dominant)
- Gekoppelte Transportgleichungen (Rossi & Greisen 1941)

Fluß der Nukleonen (Protonen und Neutronen)in der atmosphärischen Tiefe X

$$\frac{dN(E,X)}{dX} = -\frac{N(E,X)}{\lambda_N(E)} + \int_E^\infty \frac{N(E',X)}{\lambda_N(E',X)} F_{NN}(E,E') \frac{dE'}{E}$$

wobei die vertikale Schichtdicke

$$X_v = \int_h^\infty \rho(h')dh'$$

abhängig vom Verlauf der atmosphärischen Dichte $\rho(h)$ mit der Höhe h. Die mittlere freie Weglänge der Nukleonen ist

$$\lambda_N = \frac{\rho}{\rho_N \sigma_N^{(Luft)}} = \frac{Am_p}{\sigma_N^{(Luft)}}$$

Für $\sigma_N \approx 300mb$ (Nukleonen Wechselwirkungsquerschnitt bei TeV Energien) ist $\lambda_N \approx 80$g cm^{-2}.

Die Funktion $F(E,E')$ ist der dimensionslose inklusive Wirkungsquerschnitt (integriert über den Transversalimpuls) für die Kollision eines Primärteilchens der Energie E' mit dem Ergebnis eines Sekundärnukleons der Energie E. Mit Feynman Scaling gilt

$$F_{ac}(E_c,E_a) = E_c \frac{dn_c(E_c,E_a)}{dE_c} \simeq F_{ac}(E_c/E_a) = F_{ac}(x)$$

Randbedingungen

$$N(E,0) = N_0(E) = \frac{dN}{dE} \approx 1.8E^{-2.7}(cm^2\ s\ st\ GeV/A)^{-1}$$

für die Messung der Ereignissrate und

$$N(E,0) = A\delta(E - E_0/A)$$

für single-shower Trigger.

Elementarlösungen mit Faktorisierungsansatz

$$N(E,X) = G(E)g(X)$$

und Feynman Scaling liefert

$$Gg' = -\frac{Gg}{\lambda_N} + g\int_0^1 \frac{G(E/x)F_{NN}(x,E)}{\lambda_N(E/x)}\frac{dx}{x^2}$$

Dies ergibt

$$\frac{g'}{g} = -\frac{1}{\lambda_N(E)} + \frac{1}{G(E)}\int_0^1 \frac{g(E/x)F(x/E)}{\lambda_N(E/x)}\frac{dx}{x^2}$$

$$\rightarrow g(X) = g(0)\exp[-X/\Lambda]$$

mit der Integrationskonstanten Λ.

Approximation A

- Vernachlässige die Ionisationsverluste
- $\lambda(E) = \lambda$
- Scaling $F(E',E) \rightarrow F(x)$(für Paarbildung und Bremsstrahlung)

$$\boxed{N(E,X) = g(0)e^{-X/\Lambda}E^{-(p+1)}}$$

$$\frac{1}{\Lambda} = \frac{1}{\lambda_N}\left[1 - \int_0^1 x^{p-1}F_{NN}(x)dx\right]$$

Spektrum-gewichtetes Moment des inklusiven Wirkungsquerschnitts

$$Z_{ac} = \int_0^1 x^{p-1}F_{ac}(x)dx$$

Gekoppelte Kaskadengleichungen

- Die verlorene Energie $E_a - E_c = \kappa E_a$ geht zum Teil in Sekundärteilchen (und in den Rückstoß des getroffenen Kerns)
- Die Sekundärteilchen kaskadieren weiter und erzeugen dabei auch wieder Teilchen der Primärteilchenspezies (z.B. γ, e)
- Kopplung der Transportgleichungen für alle Teilchenspezies a,b,c,…
- Wegen der diskreten Natur der Wechselwirkungen (Fluktuationen) und der beschränkten Gültigkeit des Scalings werden bevorzugt Monte-Carlo Simulationen benützt (z.B. CORSIKA)

Spectrum of cosmic rays

$dN/dE \sim E^{-2.75}$

$E_{max} = 3\ 10^{11}$ GeV

Solar modulation below ~GeV energies

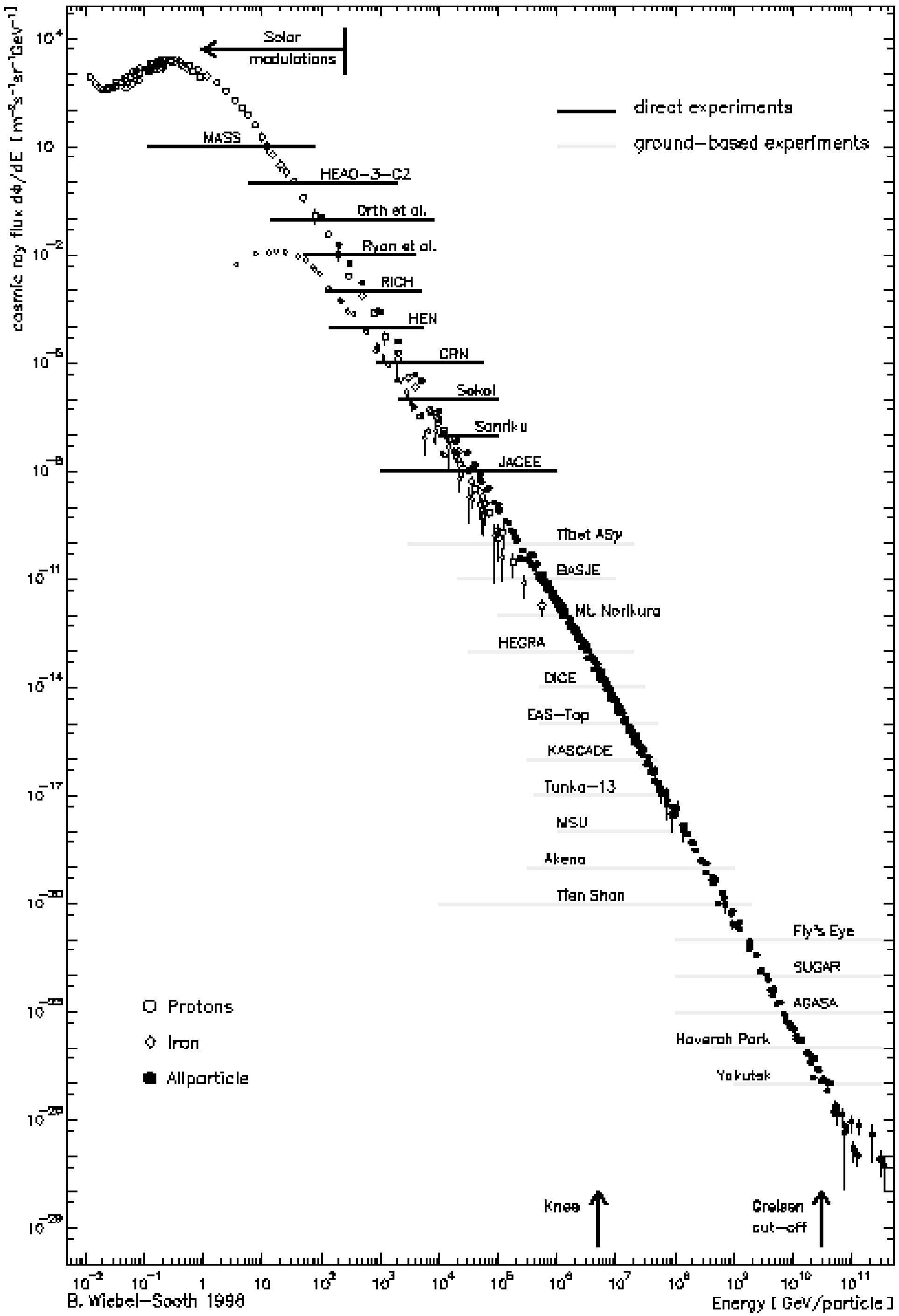

Diffusive transport of cosmic rays in the Galactic Disk (ISM): secondary pair production, inverse Compton, and bremstrahlung

At GeV energies:

Secondary cosmic rays: (10-15) g/cm^2 decreasing with energy

Be7 clock: (1-2)x10^7 a age of cosmic rays

→ Matter density traversed ~ (0.2-0.3) cm^{-3} i.e. much less than thick disk density

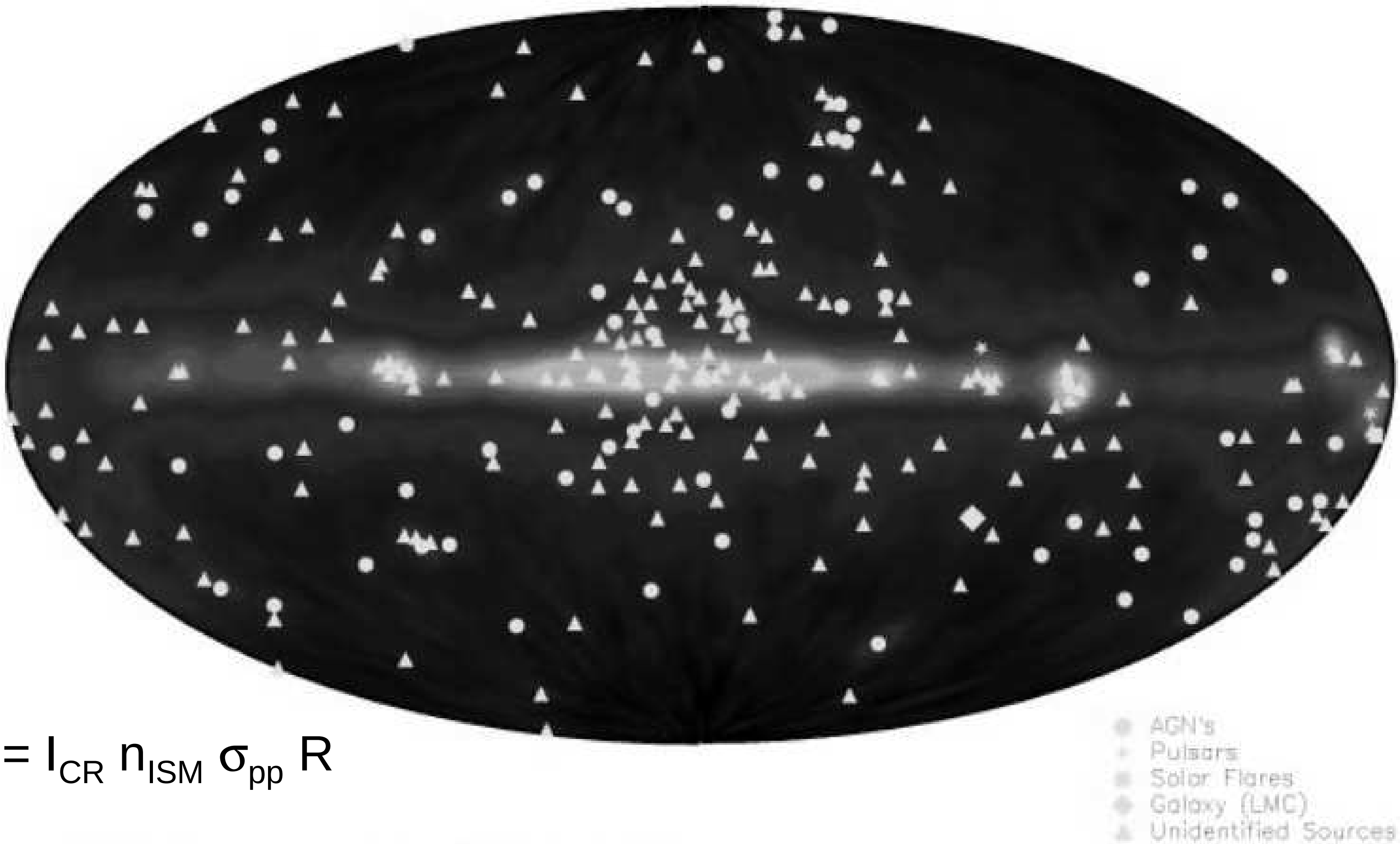

$$I_\gamma = \tau_{pp} I_{CR} = I_{CR}\, n_{ISM}\, \sigma_{pp} R$$

100 MeV

pion + IC

406 MHz

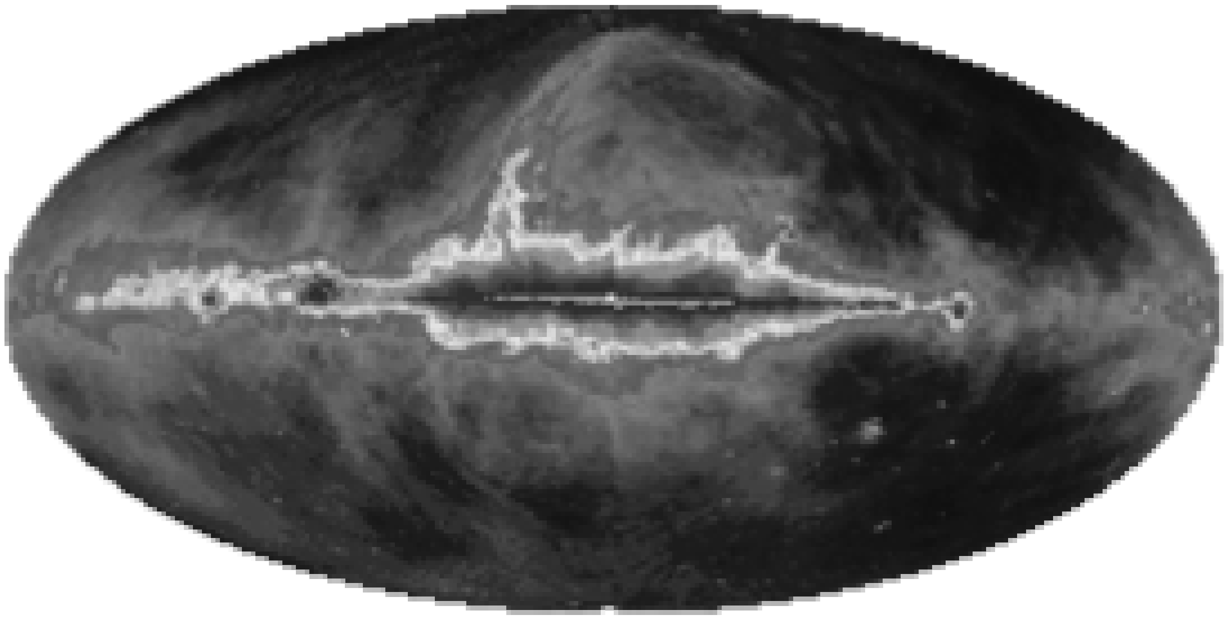

synchrotron

Diffusive-advective transport

- Collisionless plasma
- Quasilinear approximation

→Schlickeiser „Cosmic Rays Physics“

Berezinsky et al., „Cosmic Ray Physics“

→Reviews by Kirk, Drury, Ellison, Baring, Lerche, Zank, Webb, Axford, Völk, Biermann

Bewegungsgleichung für n nichtrelativistische Elektronen und Ionen (ohne Gravitation, mit Lorentzkraft)

$$m_j \frac{d\mathbf{v}_j}{dt} = q_j \left(\mathbf{E}(\mathbf{x}_j, t) + \frac{\mathbf{v}_j \times \mathbf{B}(\mathbf{x}_j, t)}{c} \right) \qquad (j = 1, 2, ..., n)$$

$$\frac{d\mathbf{x}_j}{dt} = \mathbf{v}_j$$

Wenn Anfangsbedingungen bekannt, liefert Integration der Bewegungsgleichungen Teilchentrajektorien $\mathbf{x}_j(t)$. Generell sind aber die Anfangsbedingungen unbekannt, definiere daher Phasenraumdichte, so daß Wahrscheinlichkeit, Teilchen mit Anfangsgeschwindigkeit $-\infty < \mathbf{v}_j(0) < \mathbf{v}$ am Ort $\mathbf{x}$ gegeben ist durch $0 < F_j(\mathbf{x}, \mathbf{v}) < 1$ mit der Phasenraumdichte

$$f_j(\mathbf{x}, \mathbf{v}) = \frac{\partial^3 F_j}{\partial v_x \partial v_y \partial v_z}$$

Ohne Teilchenverluste oder Quellen muß f_j im Phasenraum erhalten bleiben, d.h.

$$\frac{df_j}{dt} = \frac{\partial f_j}{\partial t} + \dot{\mathbf{x}} \cdot \frac{\partial f_j}{\partial \mathbf{x}} + \dot{\mathbf{v}} \cdot \frac{\partial f_j}{\partial \mathbf{v}} = 0$$

Die Beschleunigung $\dot{\mathbf{v}}$ wird durch zwei Arten von elektromagnetsichen Felder verursacht: (i) E.m. Feld, das durch die kollektive Bewegung sämtlicher anderer Teilchen zustande kommt. (ii) E.m. Feld, das durch Bewegungen der Ladungen innerhalb der Stoßdistanz r zustandekommt. Für kleine Plasmaparamter g ist der Aufenthalt in Reichweite der Stoßdistanz eines anderen Teilchens extrem unwahrscheinlich. Werden nun noch Quellen und Senken berücksichtigt, erhält man allgmein (Subskript j kann wegfallen, da $\mathbf{x}$ nicht mehr Ortkoordinate des Teilchens j)

$$\frac{df}{dt} = \frac{\partial f}{\partial t} + \dot{\mathbf{x}} \cdot \frac{\partial f}{\partial \mathbf{x}} + \frac{q}{m} \left[\mathbf{E}(\mathbf{x}, t) + \frac{\mathbf{v} \times \mathbf{B}(\mathbf{x}, t)}{c} \right] \cdot \frac{\partial f}{\partial \mathbf{v}} = S(\mathbf{x}, \mathbf{v}, t)$$

Dichte von Teilchen der Sorte j am Ort $\mathbf{x}$ ist definiert durch

$$n_j(\mathbf{x}, t) = n_j \int_{-\infty}^{\infty} d^3v f_j(\mathbf{x}, \mathbf{v}, t)$$

wobei n_j die Volumen-gemittelte Dichte darstellt.

Gesamte Ladungsdichte

$$\rho(\mathbf{x}, t) = \Sigma_j n_j q_j \int_{-\infty}^{\infty} d^3v f_j(\mathbf{x}, \mathbf{v}, t)$$

Gesamte Stromdichte

$$\mathbf{J}(\mathbf{x}, t) = \Sigma_j n_j q_j \int_{-\infty}^{\infty} d^3v \mathbf{v} f_j(\mathbf{x}, \mathbf{v}, t)$$

Maxwellgleichungen

$$\nabla \times \mathbf{B} = \frac{1}{c}\frac{\partial \mathbf{E}}{\partial t} + \frac{4\pi}{c}\left[\mathbf{J} + \mathbf{J}_{\text{ext}}\right]$$

$$\nabla \cdot \mathbf{B} = 0$$

$$\nabla \times \mathbf{E} = -\frac{1}{c}\frac{\partial \mathbf{B}}{\partial t}$$

$$\nabla \cdot \mathbf{E} = 4\pi\left[\rho + \rho_{\text{ext}}\right]$$

Näherungslösungen

- Um Vlasov-Gleichung zu lösen, werden E und B Felder benötigt
- Um E und B Felder aus Maxwellgleichungen zu bestimmen, werden die Ladungsdichten und der Strom benötigt, die Lösungen der Vlasov-Gleichung sind
- Nichtlineare Kopplung aufheben für
  - Testteilchen (Annahme vorgegebener elektromagnetischer Felder, z.B. Kolomogorov-Turbulenz, und Lösung nach Teilchenverteilungsfunktion)
  - Testwellen (Annahme einer festen Teilchenverteilungsfunktion als Ausgangspunkt)
- Magnetohydrodynamische Gleichungen (MHD) für Dynamik auf Skalen >> mittlere freie Weglänge für Stöße (durch Momentenbildung aus Vlasovgleichung)
- Zwei-Flüssigkeits-Näherung: Thermisches Plasma (MHD) + nicht-thermisches Plasma
- Diffusionsnäherung der quasilinearen Gleichung (Fokker-Planck)

MHD: Momentengleichungen (0. Ordnung ist die Teilchenzahl, 1. Ordnung in v, usw.) sind Impuls-, Energie- und Massenerhaltung

ideale MHD: Maxwellverteilung der Teilchen

Geschwindigkeitsmoment

$$\mathbf{V}_j(\mathbf{x},t) = \frac{\int_{-\infty}^{\infty} d^3v \mathbf{v} f_j(\mathbf{x},\mathbf{v},t)}{n_j(\mathbf{x},t)}$$

Drucktensor

$$\Pi_{j,ik}(\mathbf{x},t) = m_j \int_{-\infty}^{\infty} d^3v f_j(\mathbf{x},\mathbf{v},t)(v_i - V_i)(v_k - V_k)$$

Quasilineare Theorie für Testteilchen:

$$\mathbf{B} = \mathbf{B}_\circ + \delta\mathbf{B}(\mathbf{x},t) \qquad \mathbf{E} = \delta\mathbf{E}(\mathbf{x},t)$$

mit homogenem Hintergrundmagnetfeld $\mathbf{B}_\circ = B_\circ \mathbf{e}_z$ in z-Richtung. Bewegung des Führungzentrums der Teilchengyration

$$\mathbf{R} = (X, Y, Z) = \mathbf{x} + \frac{\mathbf{v} \times \mathbf{e}_z}{\epsilon\Omega}$$

wobei Ω die Gyrofrequenz und ϵ das Vorzeichen der Teilchenladung angeben. Mit sphärische Koordinaten im Impulsraum (p, μ, Φ)

$$p_x = p\cos\Phi\sqrt{1-\mu^2}, \quad p_y = p\sin\Phi\sqrt{1-\mu^2}, \quad p_z = p\mu$$

erhält man

$$\frac{\partial f}{\partial t} + v\mu\frac{\partial f}{\partial Z} - \epsilon\Omega\frac{\partial f}{\partial \Phi} + \frac{1}{p^2}\frac{\partial}{\partial x_\sigma}(p^2 g_{x_\sigma} f) = S(\mathbf{x},\mathbf{p},t)$$

mit dem generalisierten Kraft-Term g_{x_σ}, der die Wirkung der fluktuierenden Felder enthält ($g_{x_\sigma} = 0$ sind ungestörte Orbits). Die Bezeichnung x_σ gibt die Phasenraum-Koordinate (p, μ, Φ, X, Y, Z) an.

Ensemble-Mittelung der Vlasovgleichung $< f >= F$ (so daß die Fluktuationen gegeben sind durch $\delta f = f - F$) ergibt wegen $< \partial B >=< \partial E >= 0$ und $< B >= B_\circ$ im Rahmen der Störungstheorie erster Ordnung

$$\frac{\partial \delta f}{\partial t} + v\mu\frac{\partial \delta f}{\partial Z} - \epsilon\Omega\frac{\partial \delta f}{\partial \Phi} = -g_{x_\sigma}\frac{\partial F}{\partial x_\sigma} - g_{x_\sigma}\frac{\partial \delta f}{\partial x_\sigma} + \langle g_{x_\sigma}\frac{\partial \delta f}{\partial x_\sigma}\rangle$$

Fokker-Planck-Gleichung:

$$\frac{\partial F}{\partial t} + v\mu\frac{\partial F}{\partial Z} - \epsilon\Omega\frac{\partial F}{\partial \Phi} = S + \frac{1}{p^2}\frac{\partial}{\partial x_\sigma}\left(p^2 D_{x_\sigma,x_\nu}\frac{\partial F}{\partial x_\nu}\right)$$

mit den Fokker-Planck-Koeffizienten

$$D_{x_\sigma,x_\nu} = \int_0^t ds\langle\bar{g}_{x_\sigma}(t)\bar{g}_{x_\nu}(s)\rangle$$

(Integrale der fluktuierenden Kraftfelder entlang der ungestörten Teilchenorbits)

Diffusions-Konvektionsgleichung mit Quellterm durch inelastische Wechselwirkungen und Entweichterm („leaky box“)

$$\frac{\partial N}{\partial t} =$$

$$\nabla \cdot (D_i \nabla N_i) - \frac{\partial}{\partial E}(b_i(E) N_i(E)) - \nabla \cdot u N_i(E) + Q_i(E,t) - p_i N_i + \frac{v\rho}{m} \Sigma_{k \geq i} \int \frac{d\sigma_{i,k}(E,E')}{dE} N_k(E') dE'$$

Self-Confinement

- KS strömt durch ISM (Advektion + Diffusion)
- Pitchwinkelstreuung an Plasmaturbulenz (Alfvénwellen ohne Landaudämpfung)
- Plasmaturbulenz wird durch die Zweistrominstabilität angeregt
- Selbst wenn in schmalen Wellenzahlenbereichen Dämpfung (z.B. Ion-Neutral) überwiegend, führen nichtlineare Kaskadenprozesse zu einem Auffüllen der Intensität in den Fluktuationen des B-Feldes
- Im relaxierten Zustand wird so ein Kolmogorov-Spektrum der Turbulenz angeregt $I \sim k^{-5/3}$
- In der Nähe von Flares bzw. Stoßwellen Kraichnan Spektrum $I \sim k^{-3/2}$
- Nachweis durch interstellare Szintillation (Radiobeobachtungen von Pulsaren)

Energiedichte

Fluß kosmischer Strahlung

$$F_{KS} = \frac{\rho_{KS} \beta c}{4\pi}$$

Protonenkomponente (im solaren Minimum)

$$\rho_E = 4\pi \int_0^\infty \frac{dN}{dE} \frac{dE}{\beta c} = \int_0^\infty \frac{e\pi E^2}{\beta c} \frac{dN}{dE} d \ln E = 0.83 \text{ eV cm}^{-3}$$

$$rho_E(\alpha + \text{Kerne}) = 0.27 \text{ eV cm}^{-3}$$

Zum Vergleich: Magnetische Energiedichte im interstellaren Medium (mit $B_{ISM} = 3\mu\text{G}$

$$\rho_B = \frac{B^2}{8\pi} = 0.25 \text{ eV cm}^{-3}$$

Hillas-plot
(candidate sites for E=100 EeV and E=1 ZeV)

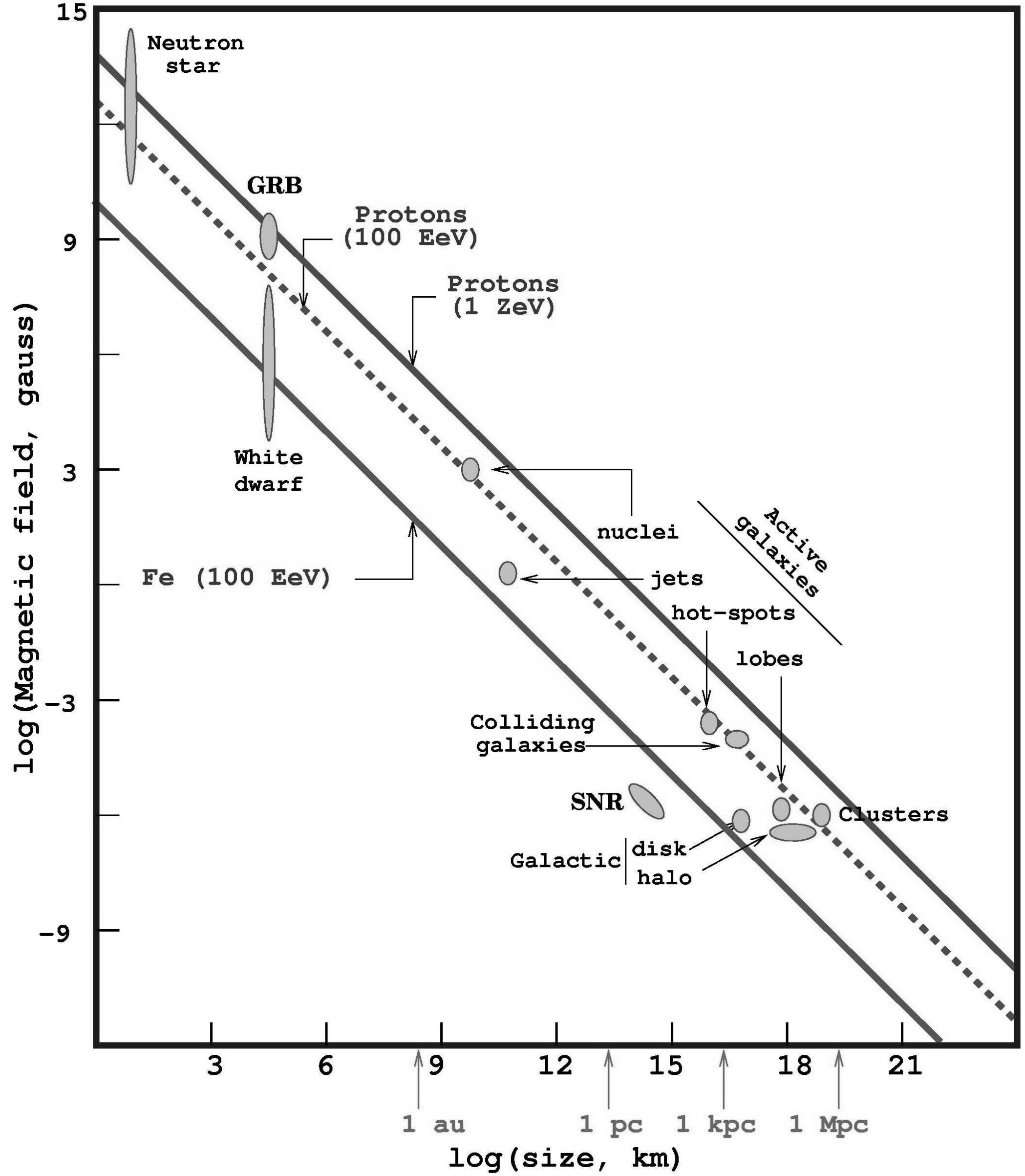

$E_{max} \sim ZBL$ (Fermi)

$E_{max} \sim ZBL\Gamma$ (Ultra-relativistic shocks-GRB)

Kosmische Strahlung

Quelle	Energie [ergs]	Rate [1/a]	E ~ r B [GeV]
Supernovaüberreste (s=2.2+0.5)	10^{51}	1/30	10^{6}
Radiogalaxien (s=2.0)	10^{61}	$1/3\times10^{5}$	10^{11}

($W_{rg}\,R_{rg} = N_{rg} V_{rg} L_{rg}$ mit $N_{rg} = 10^{-6}\ \mathrm{Mpc}^{-3}$ und $L_{rg} = 10^{45}$ erg/s)

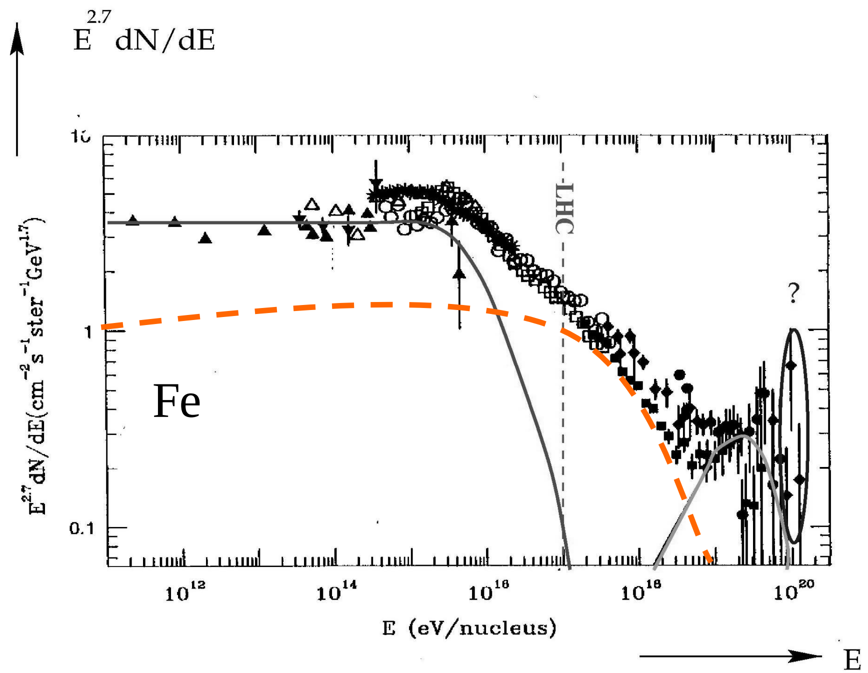

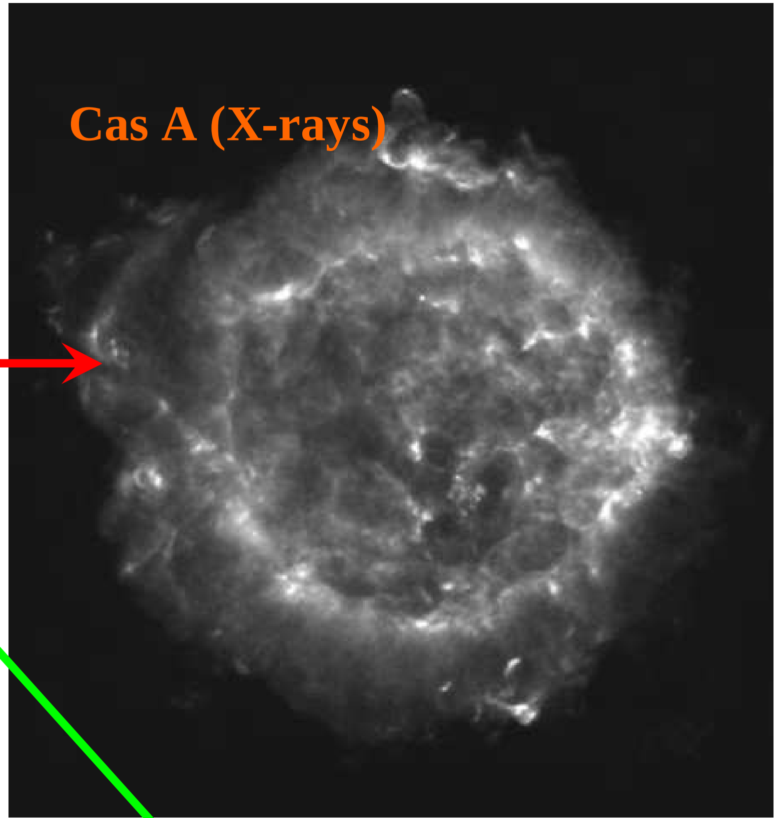

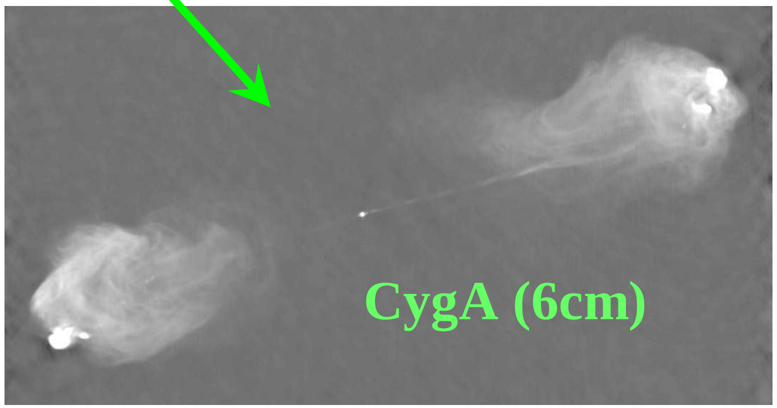

Cosmological horizons for cosmic rays, gamma rays, and neutrinos

- Cosmic rays: Greisen-Zatsepin-Kuzmin cutoff due to photo-pion production in 2.7K
- Gamma rays: Fazio-Stecker cutoff due to pair production in FIR-to-UV metagalactic radiation field (MRF)

  MRF → mostly of thermal origin, nonthermal component in radio and gamma-ray bands
- Neutrinos: Weiler dip due to resonant Z

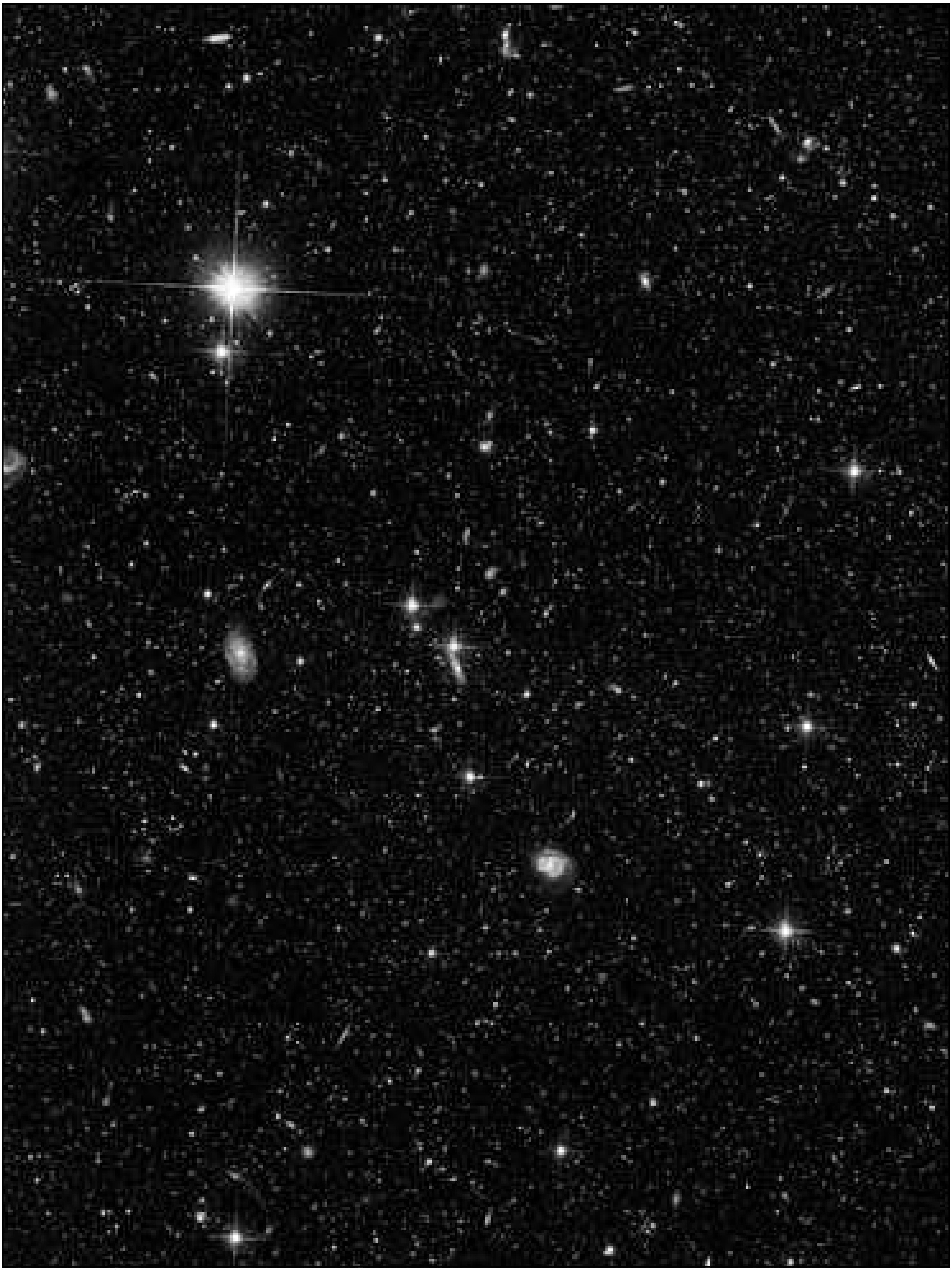

Tegmark 2003

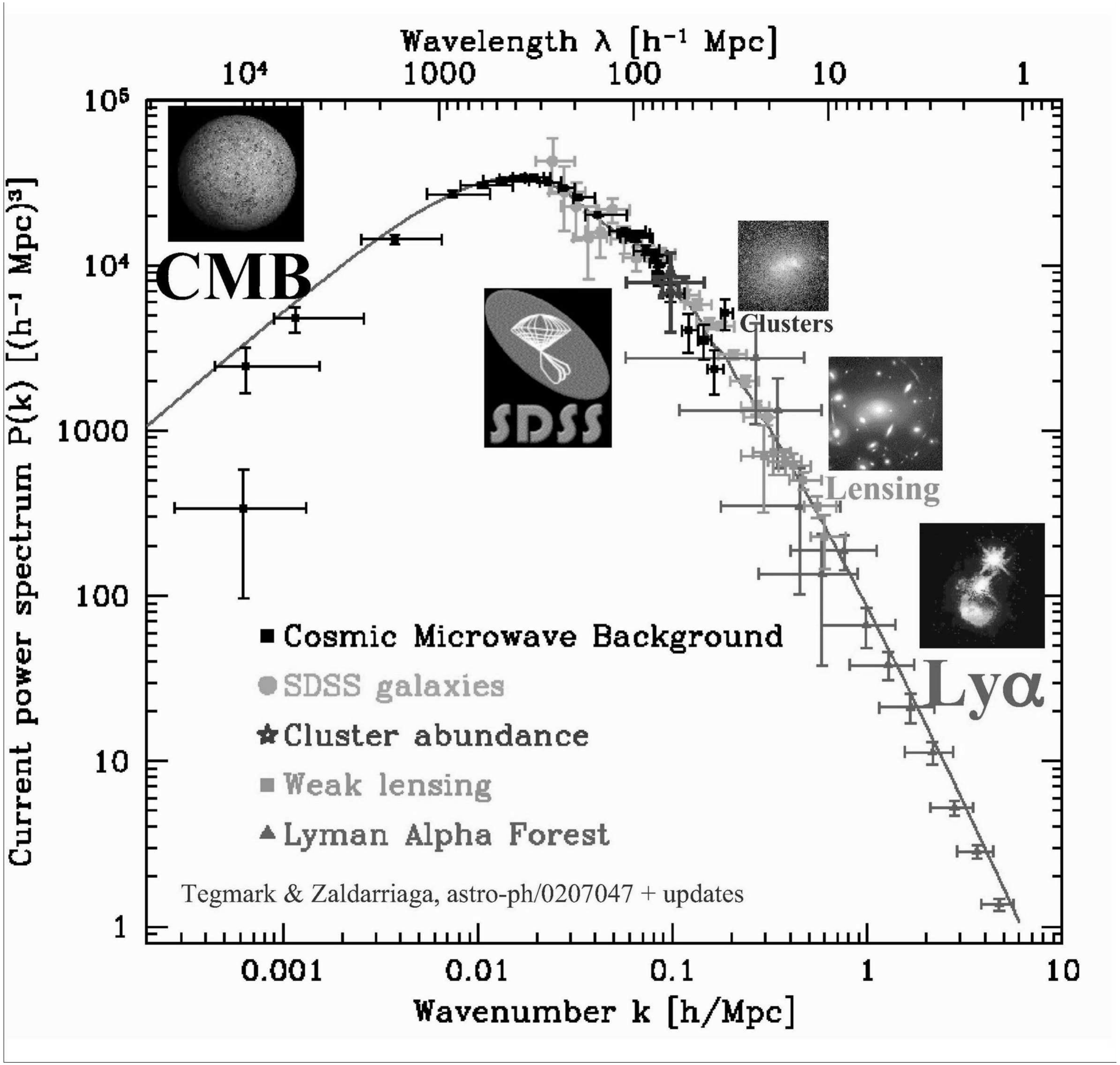

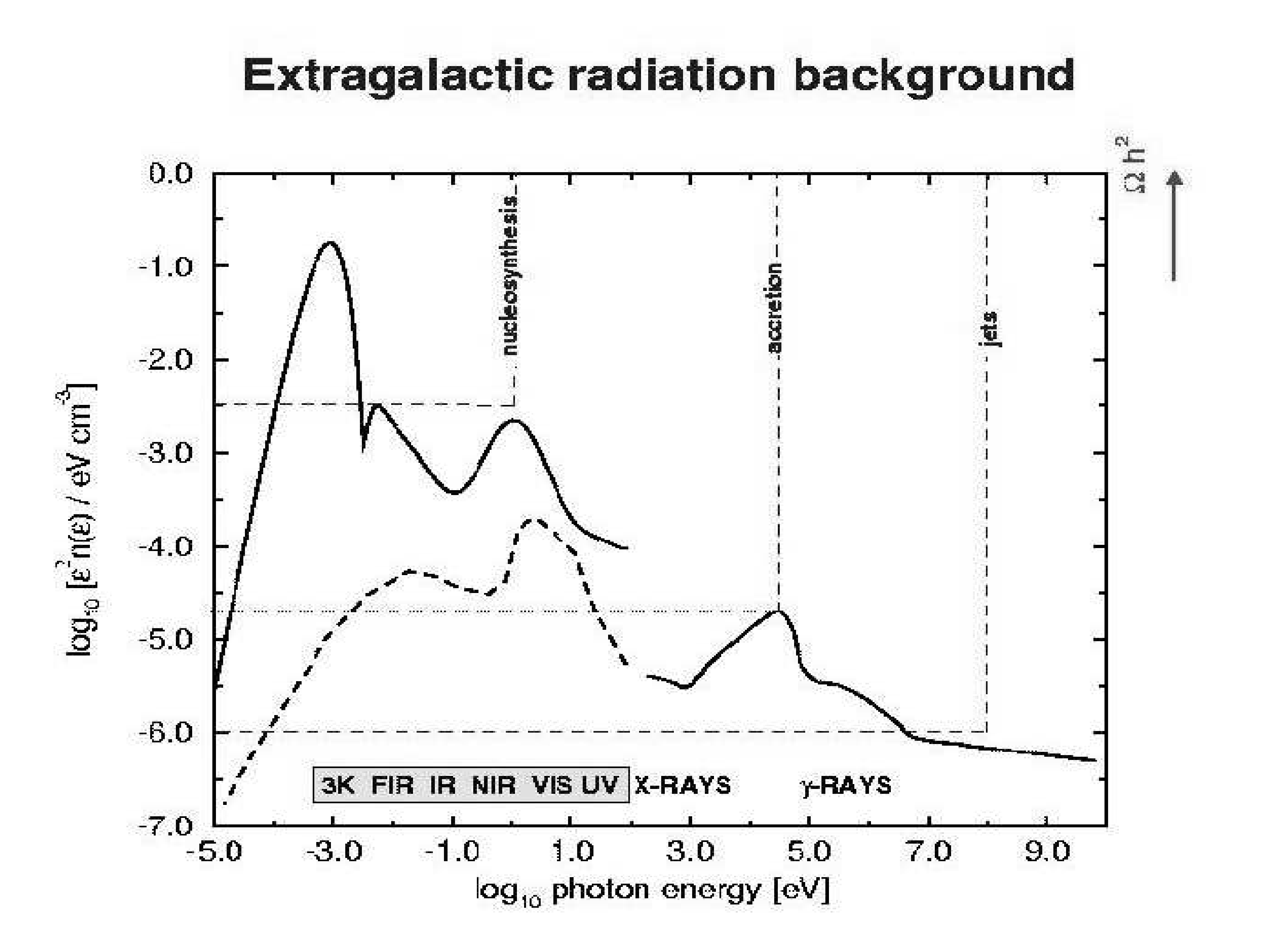

Extragalactic radiation background
0.0
-1.0
-2.0
-3.0
-4.0
-5.0
-6.0
-7.0
-5.0
-3.0
-1.0
1.0
3.0
5.0
7.0
9.0
log10 photon energy [eV]
log10 [ε² n(ε) / eV cm⁻³]
nucleosynthesis
accretion
jets
Ω h²
3K FIR IR NIR VIS UV
X-RAYS
γ-RAYS

Kneiske, et al., A&A 2002, 2004: EBL model based on galaxy counts

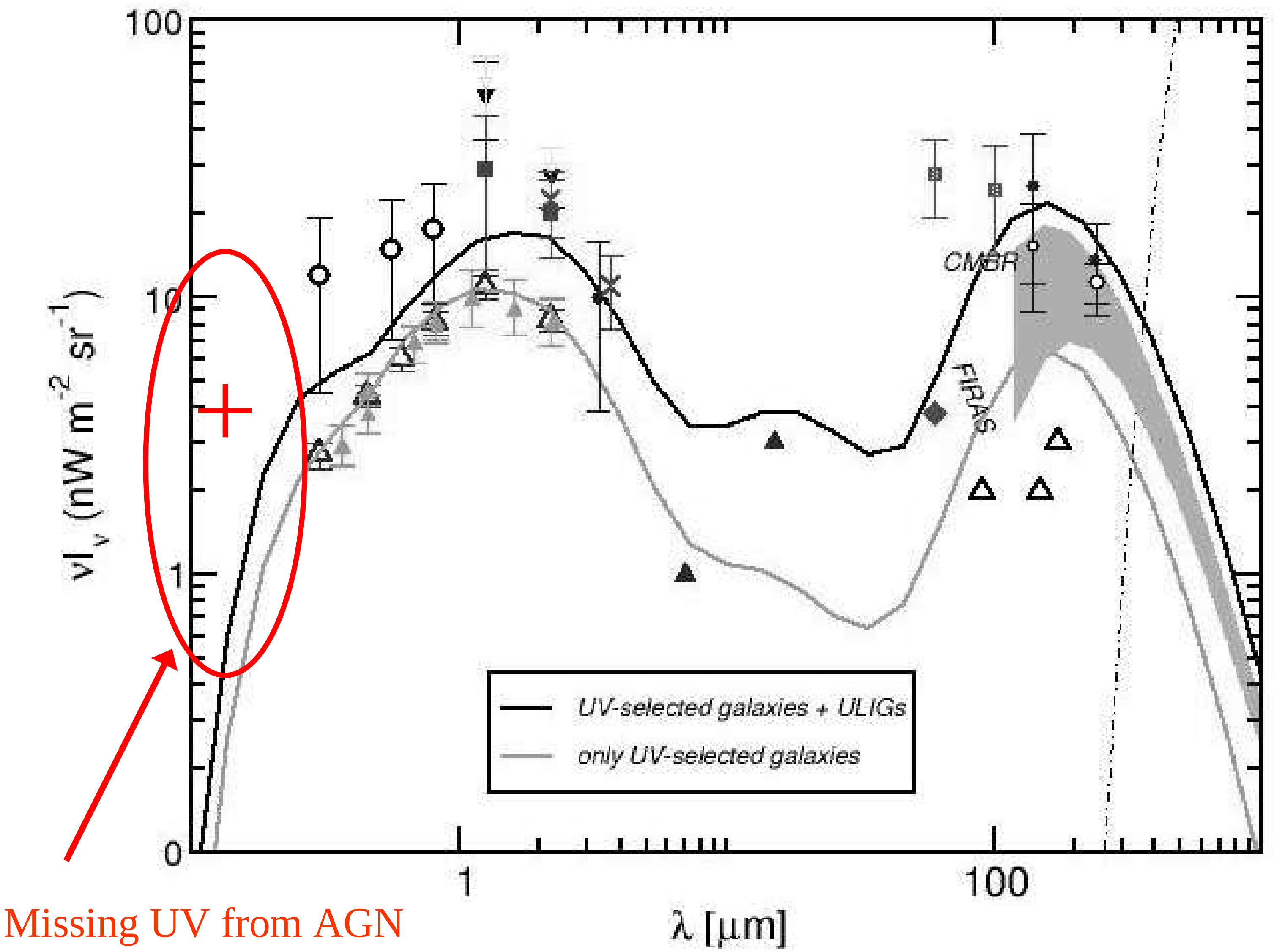

Fazio-Stecker relation

Pair absorption cutoff energy as a function of redshift (Fazio &Stecker, 1975, Nature; Kneiske et al., A&A, 2002)

→ **z~1 activity region becomes visible below ~100 GeV**

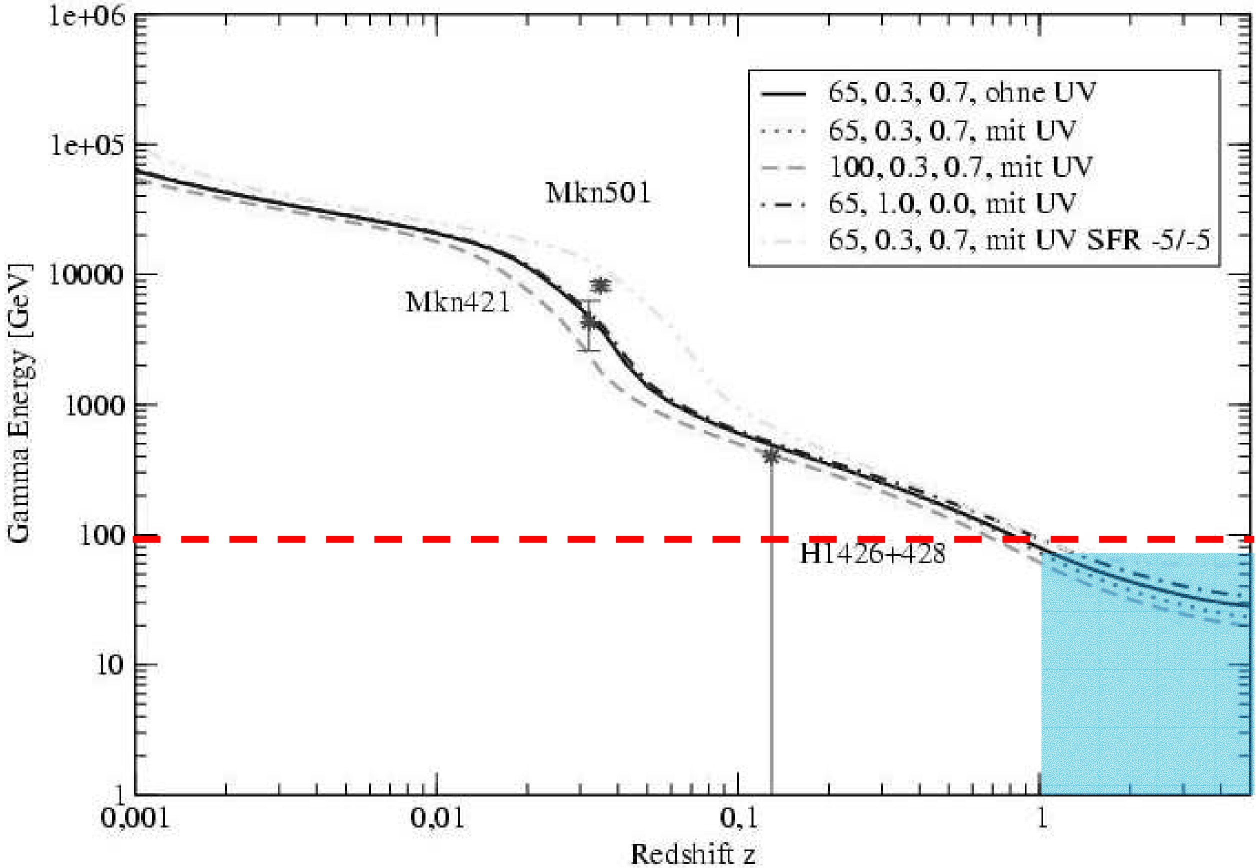

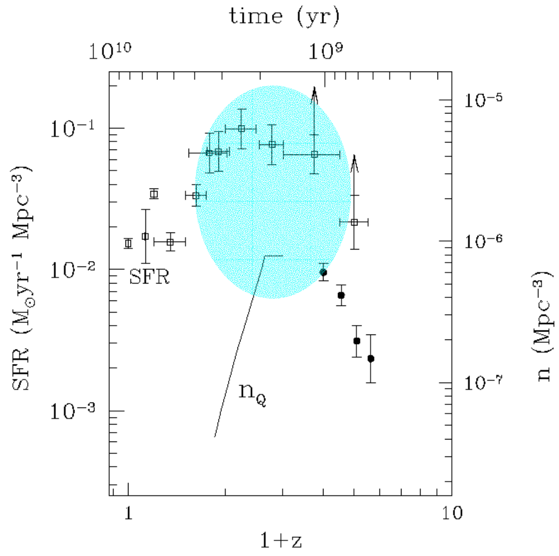

Kneiske et al. 2002, 2004

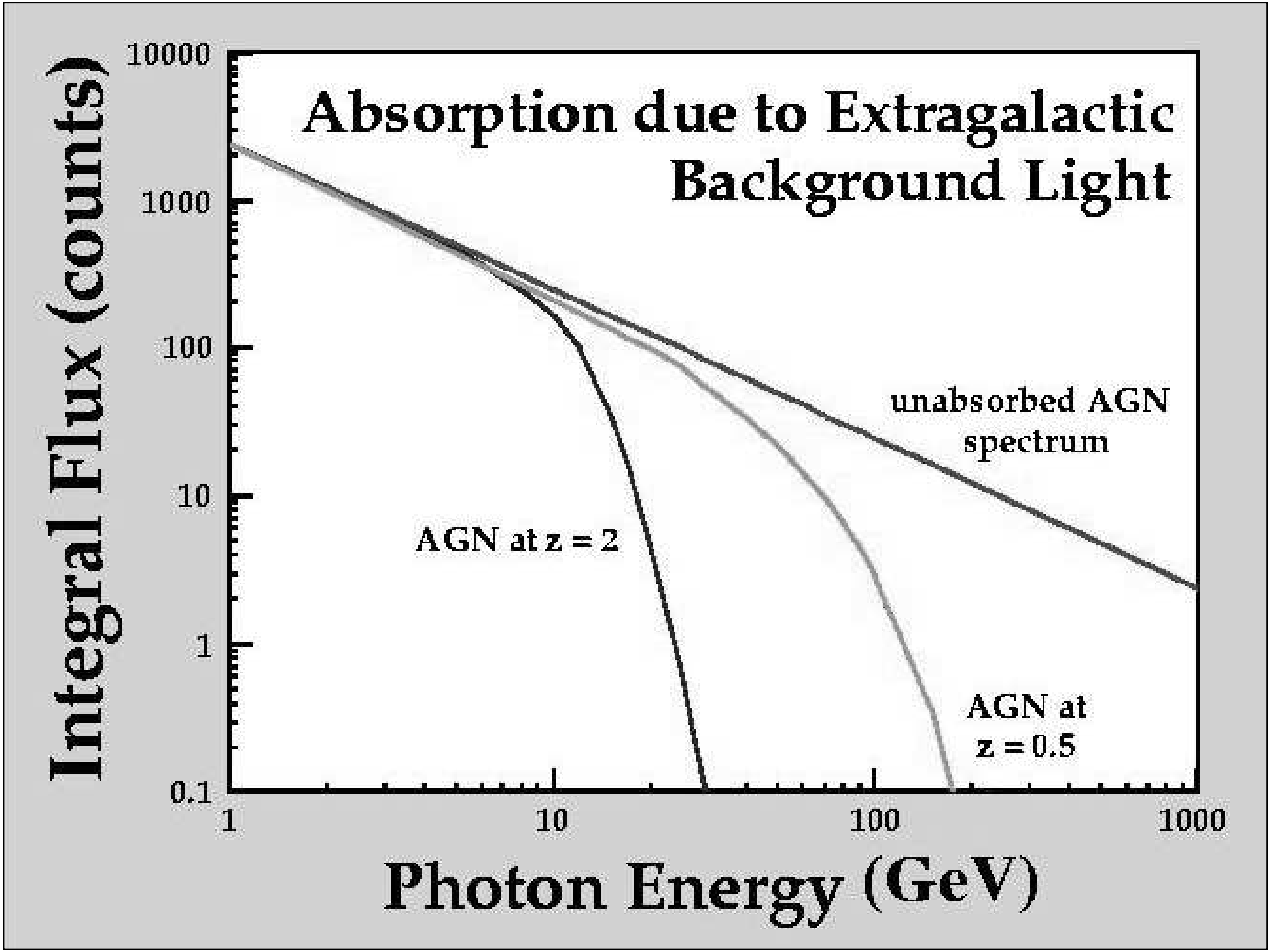
Absorption due to Extragalactic
Background Light
Integral Flux (counts)
10000
1000
100
10
1
0.1
1
10
100
1000
Photon Energy (GeV)
unabsorbed AGN
spectrum
AGN at z = 2
AGN at
z = 0.5

Extragalactic X ray/gamma ray background

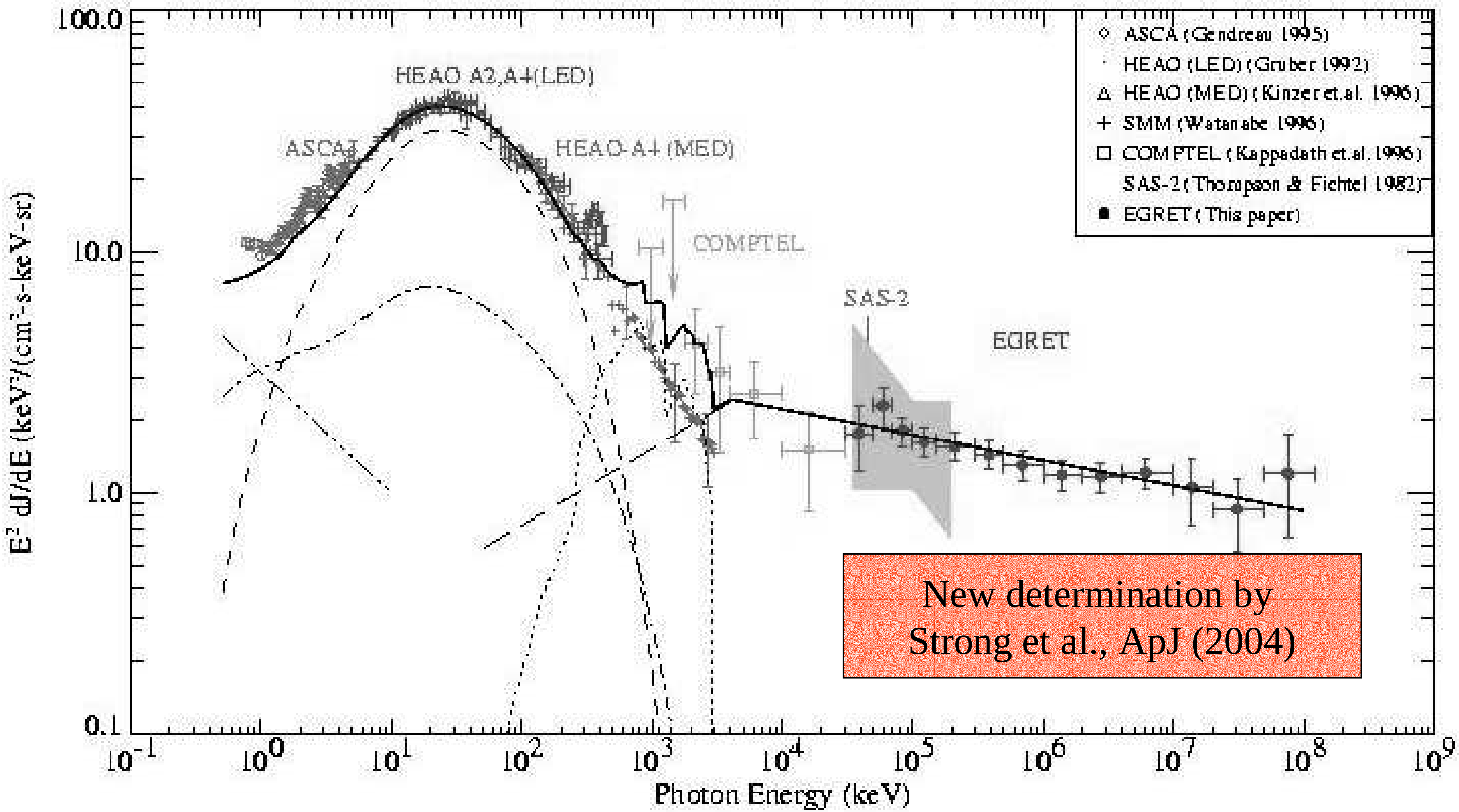

New determination by Strong et al., ApJ (2004)

- Extragalactic gamma-ray background light (EBL) = present-day metagalactic radiation field due to faint, unresolved gamma-ray sources: Mukherchee & Chiang, ApJ 1998; Stecker, ApJ 1998

- Energy container for radiation power produced by accelerated particles. VHE gamma rays cascade until transparent (→ Fazio-Stecker relation): Aharonian & Coppi, Mannheim, Protheroe

- Bolometric flux of gamma-ray EBL related to neutrino EBL and UHE cosmic ray flux if particle acceleration limited by energy losses (pion production and decay kinematics):
  - Mannheim (AGN as sources of UHE cosmic rays)
  - Waxman & Bahcall (GRB as sources of UHE cosmic rays)

- Cosmic ray flux below ankle ($\sim 10^{18.5}$ eV) of galactic origin (chemical composition) and particle acceleration limited by age and size of emission region rather than energy losses → diffuse galactic neutrino and gamma-ray flux much smaller than cosmic ray flux

Part B) Types of particle accelerators

- Different types of high-energy sources
  - Atmospheric (secondary) emission
    → neutrinos, muons, air showers
  - Sun and solar system
  - Galactic point sources
    → pulsars, plerions, supernovae, X-ray binaries (microquasars, magnetic CVs,…)
  - Galactic (> arcmin) extended sources
    → SNR, OB ass., molecular clouds
  - Galactic diffuse emission
    → ISM, galactic wind, halo
  - Extragalactic point sources
    → (jetted) active galactic nuclei, GRB
  - Extragalactic extended sources
    → clusters of galaxies, intergalactic shocks
  - Extragalactic diffuse, isotropic emission
    → unresolved, faint point sources

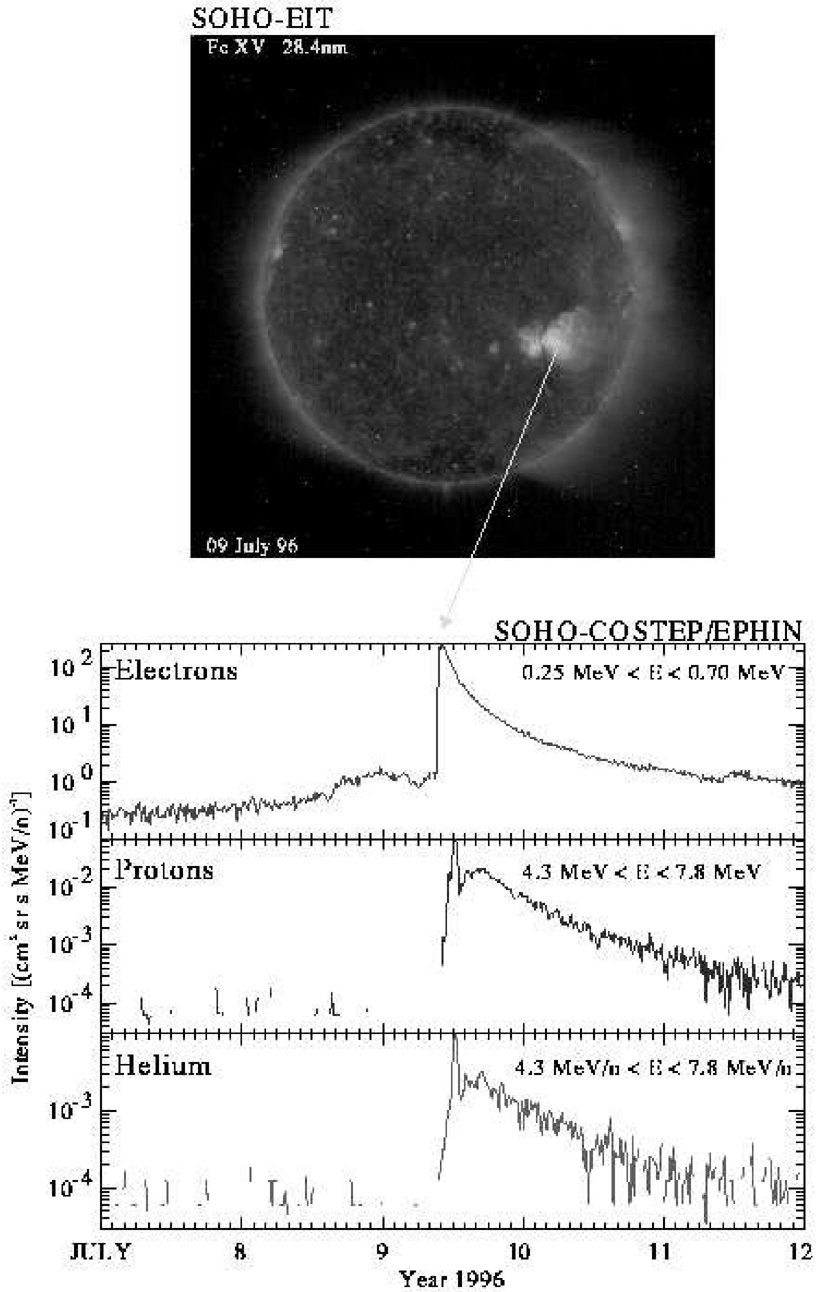
SOHO-EIT
Fe XV 28.4nm
09 July 96
SOHO-COSTEP/EPHIN
Electrons
0.25 MeV < E < 0.70 MeV
Protons
4.3 MeV < E < 7.8 MeV
Helium
4.3 MeV/n < E < 7.8 MeV/n
Intensity [(cm² sr s MeV/n)⁻¹]
JULY
8
9
10
11
12
Year 1996


2002/01/12 18:25

SNR Cas A

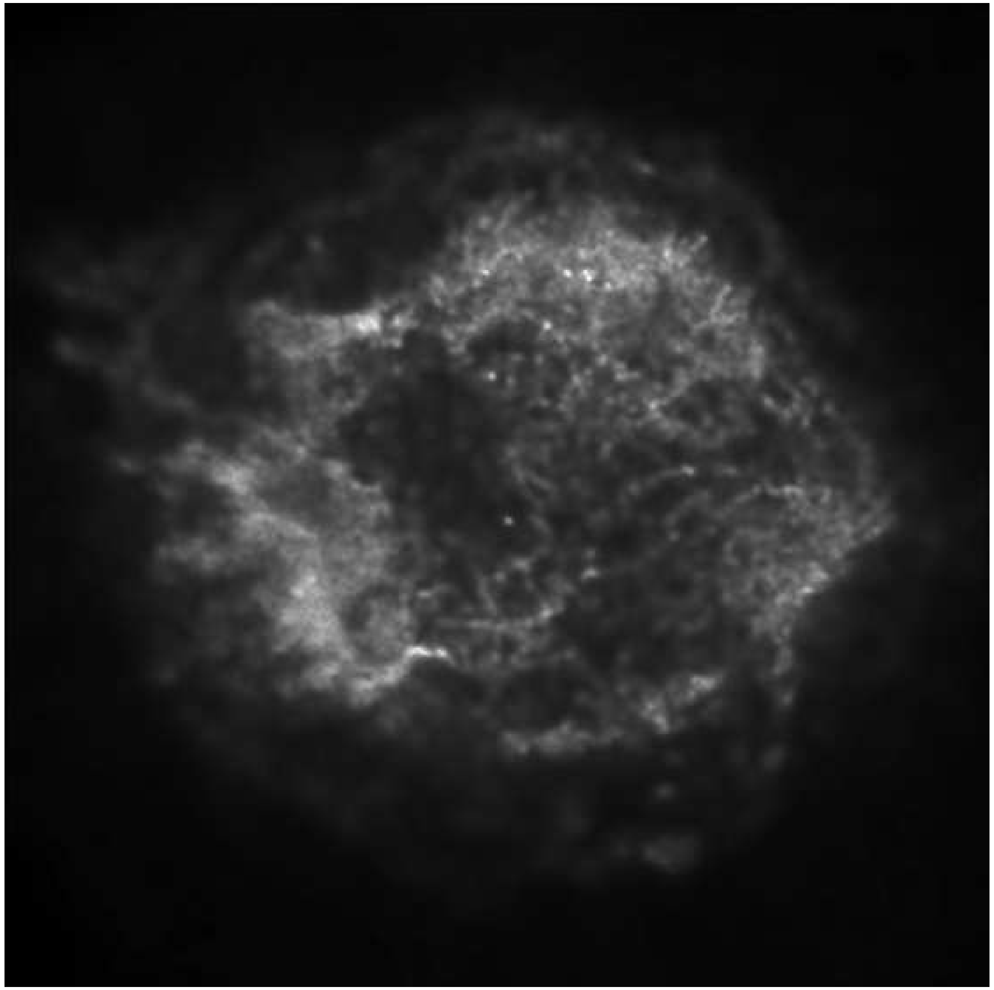

Ginzburg hypothesis: origin of galactic cosmic rays

Successes:

a) Energetics
b) Diffusive shock acceleration model
c) Chemical composition (enrichment of volatile elements → dust sputtering)

Supernova Remnant Cas A: Bremsstrahlung of an interstellar shock wave. Pion component (HEGRA)?

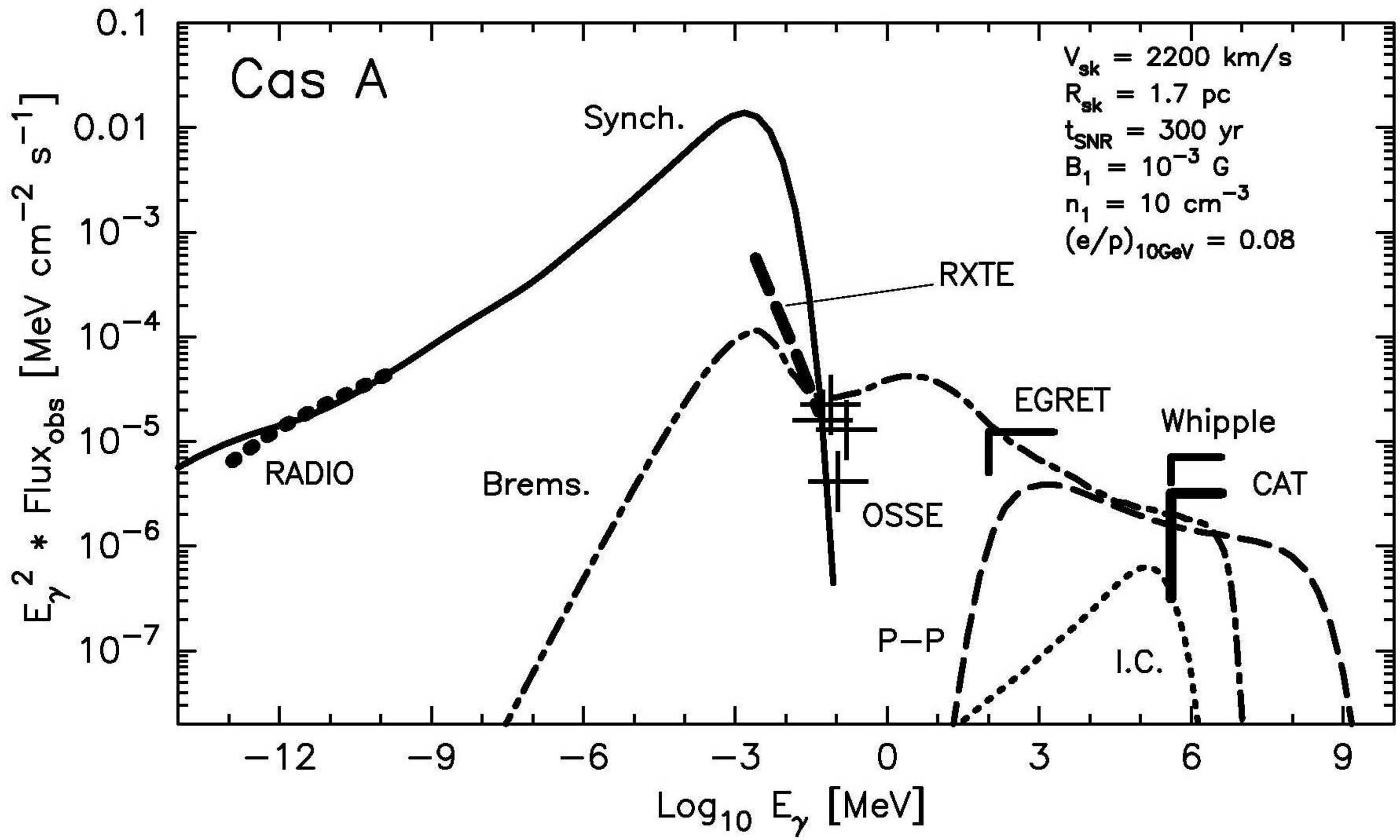

Predictions of the nonlinear diffusive shock-acceleration model from radio to TeV γ-rays as compared to observations (see Ellison et al. (1999) for details and references therein). The present result is shown together with the Whipple upper limit of Lessard (1999).

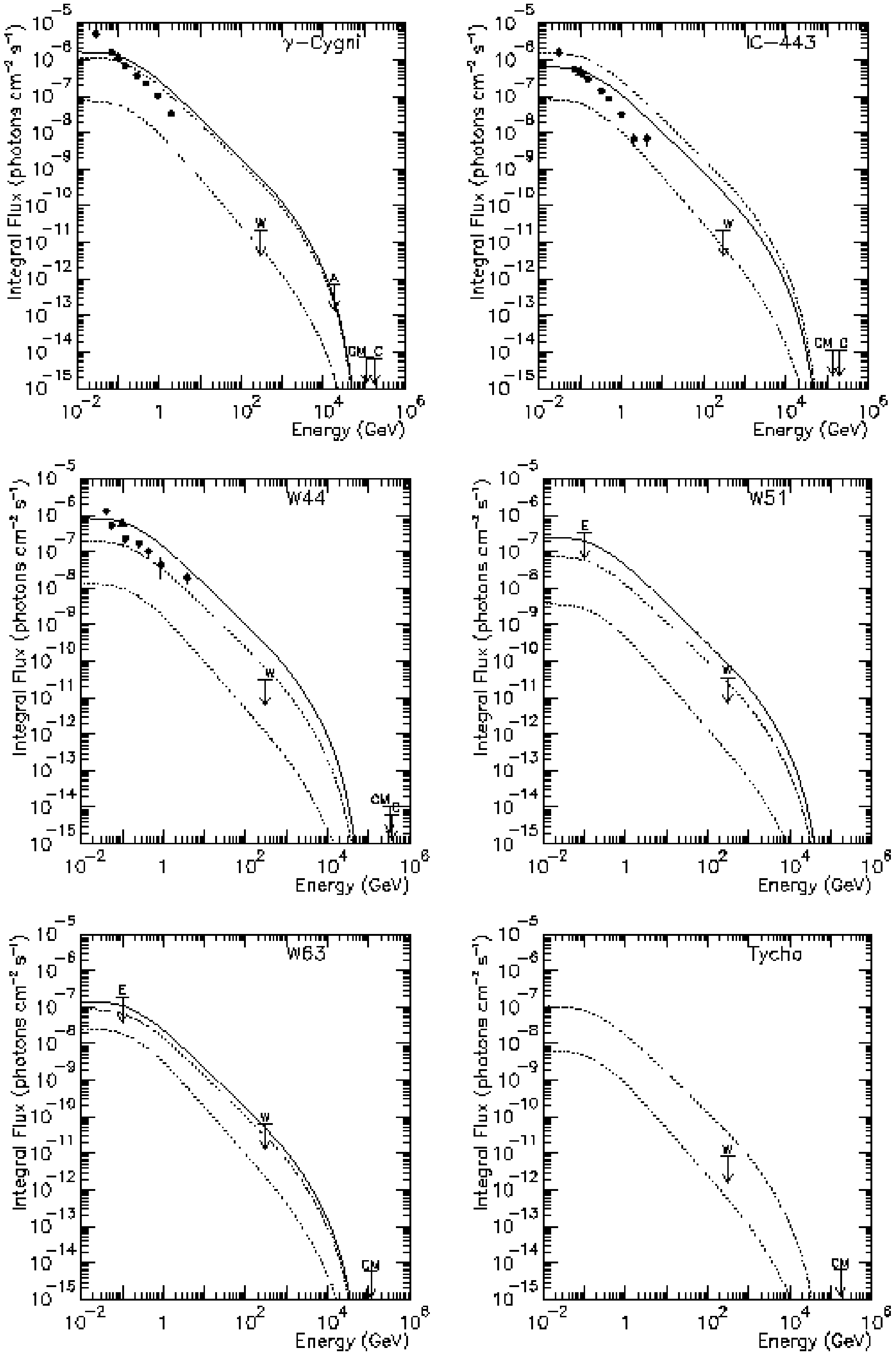

Problems with the standard lore:

a) Lack of TeV emission from EGRET SNR (which may contain pulsars/plerions)

b) Source distribution with galactocentric radius too flat

→ up to now issue of galactic CRs still not settled

Synchrotron sources:
Pulsar wind in Crab-Nebel (Chandra/HST)
Moving wisps

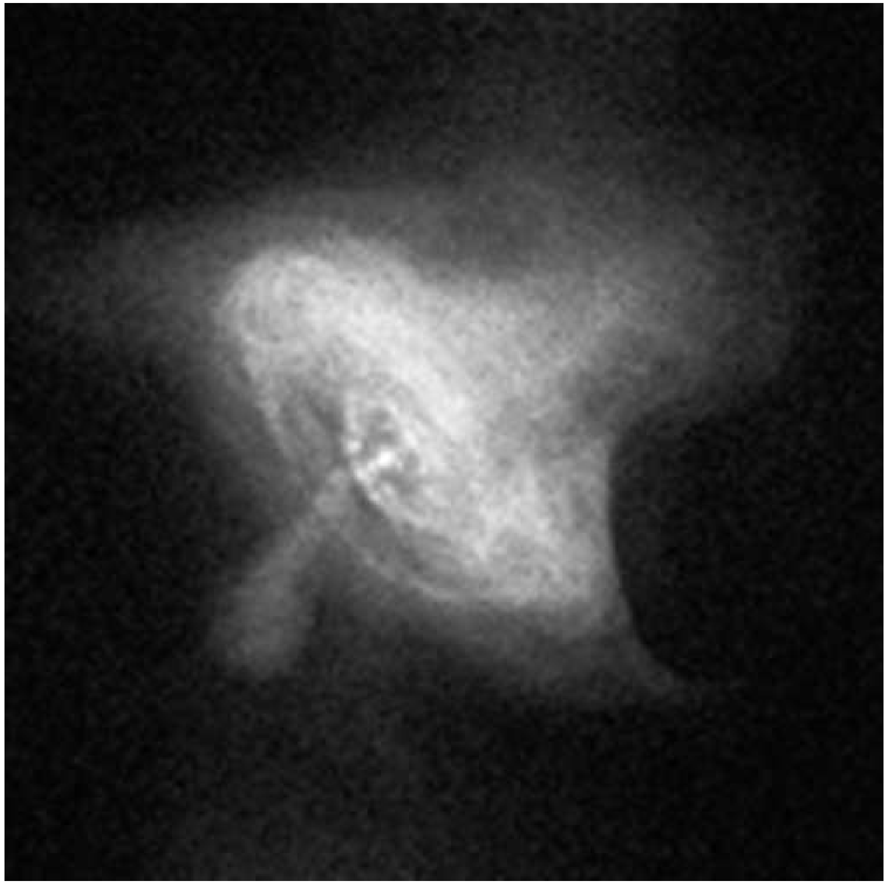

Spectral energy distribution of the Crab nebula (Harding & Stecker) – Models vs. Multiwavelength Observations

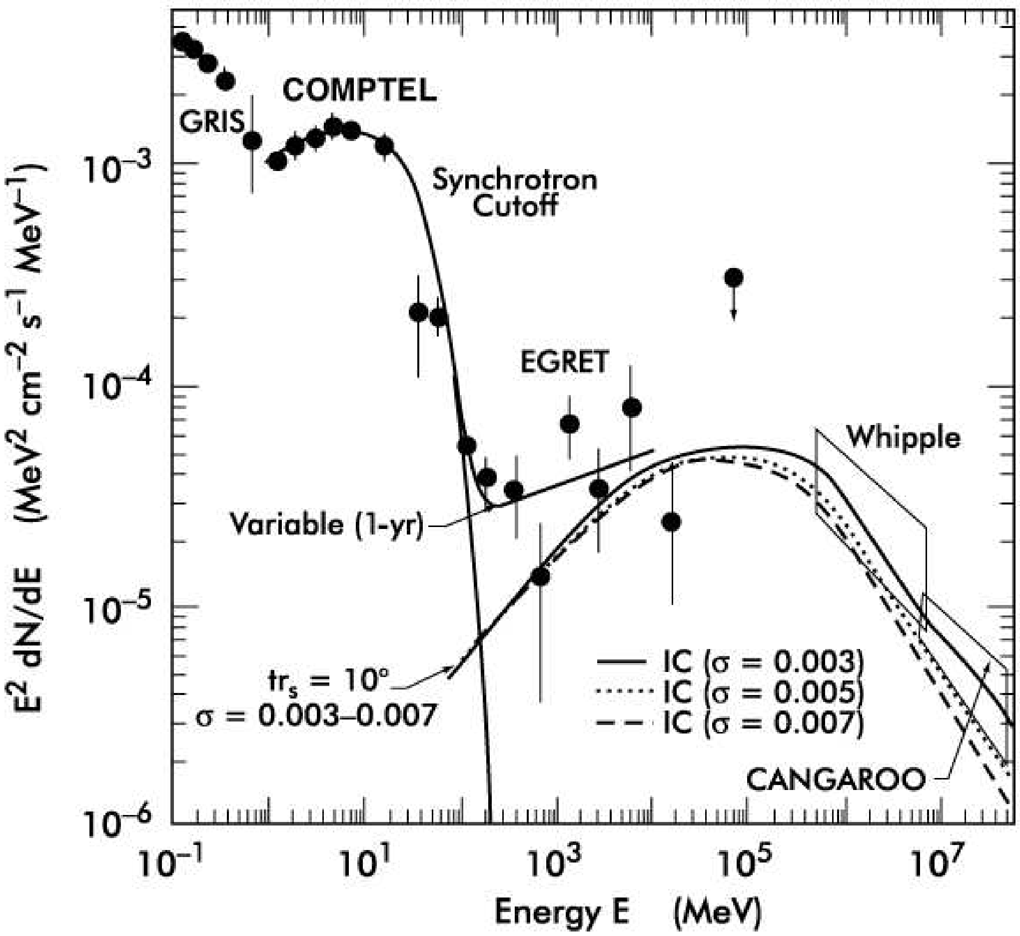

Pulsar - Magnetosphere

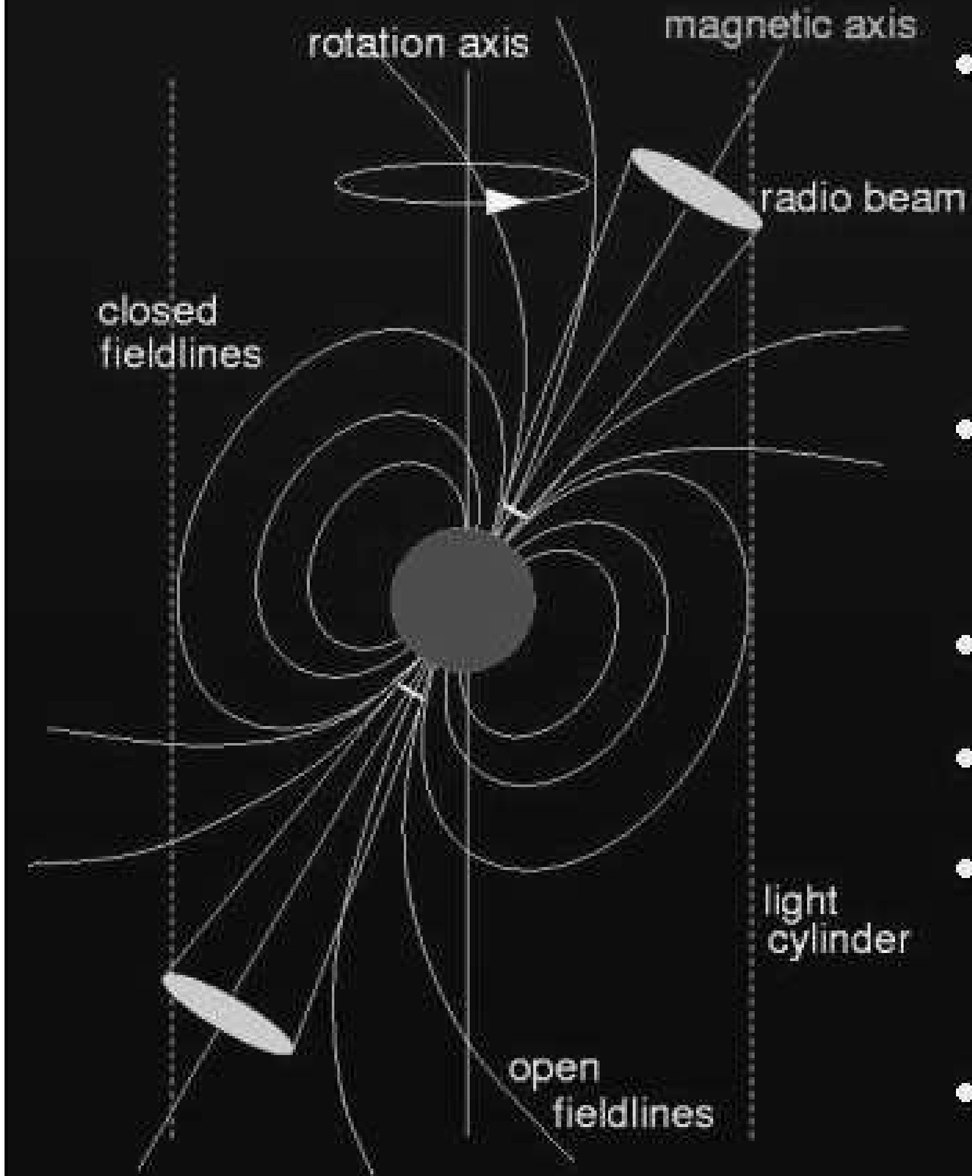

- rotation induces electric quadrupole field

$$F_{el} / F_{grav} = 10^{12}$$

- charges pulled out of surface, shielding force
- plasma fills surrounding
- co-rotation with pulsar
- light cylinder:

$$v = R_L \Omega = c$$

- open and closed fieldlines

Old pulsars – high gama ray luminosity

Low magnetic fields (recycled =msec pulsars) – high gamma ray maximum energy

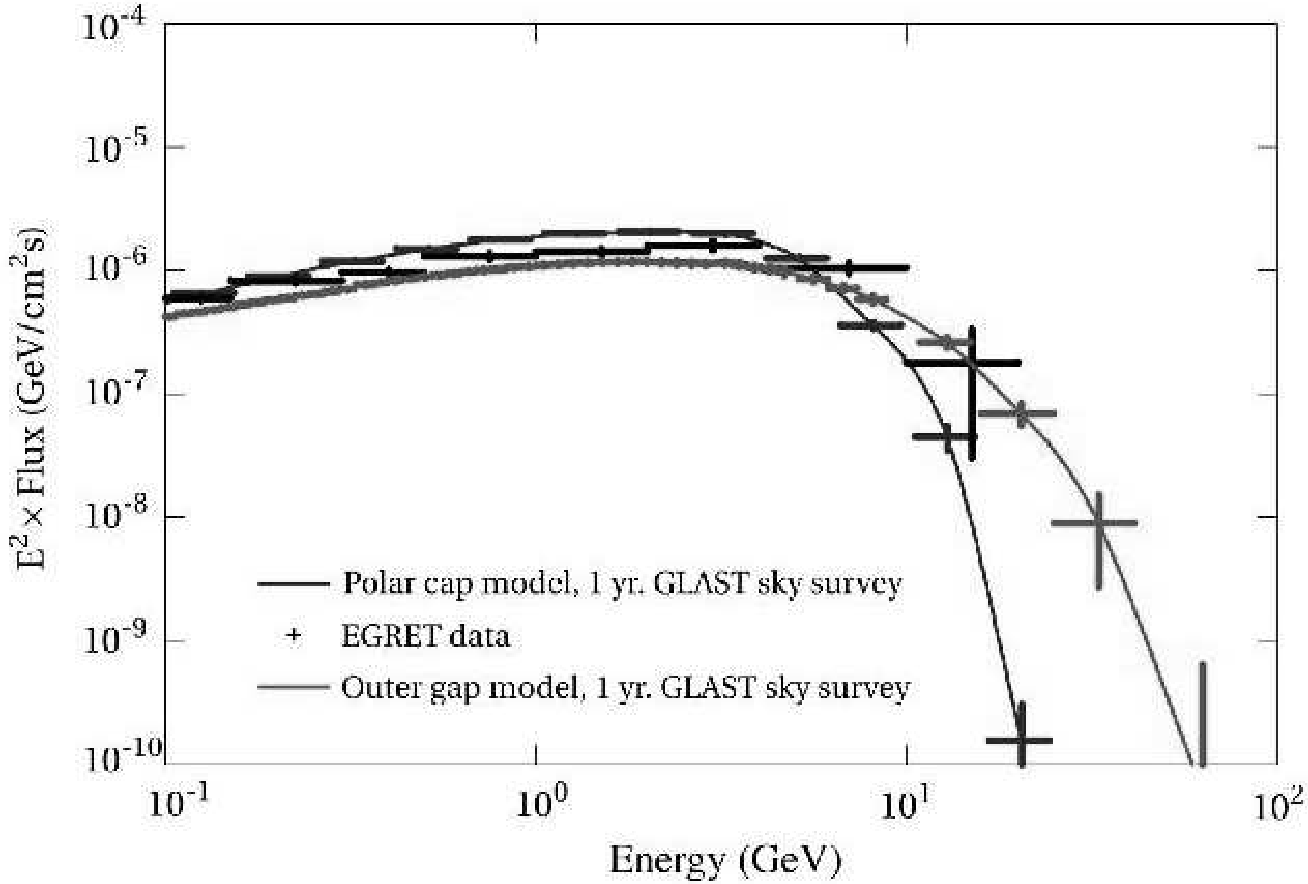

Active Galactic Nuclei: produce most nonthermal power in the Universe = most efficient accelerators

1. "An Introduction to Active Galactic Nuclei", B.P. Peterson, 1997, Cambridge University Press
2. "Quasars and Active Galactic Nuclei", A. Kembhavi & J. Narlikar, 1999, Cambridge University Press
3. "Astrophysics of Gaseous Nebulae and Active Galactic Nuclei", Osterbrock, University Science Books, 1996
4. "Active Galactic Nuclei", Krolik, Cambridge UP, 2000

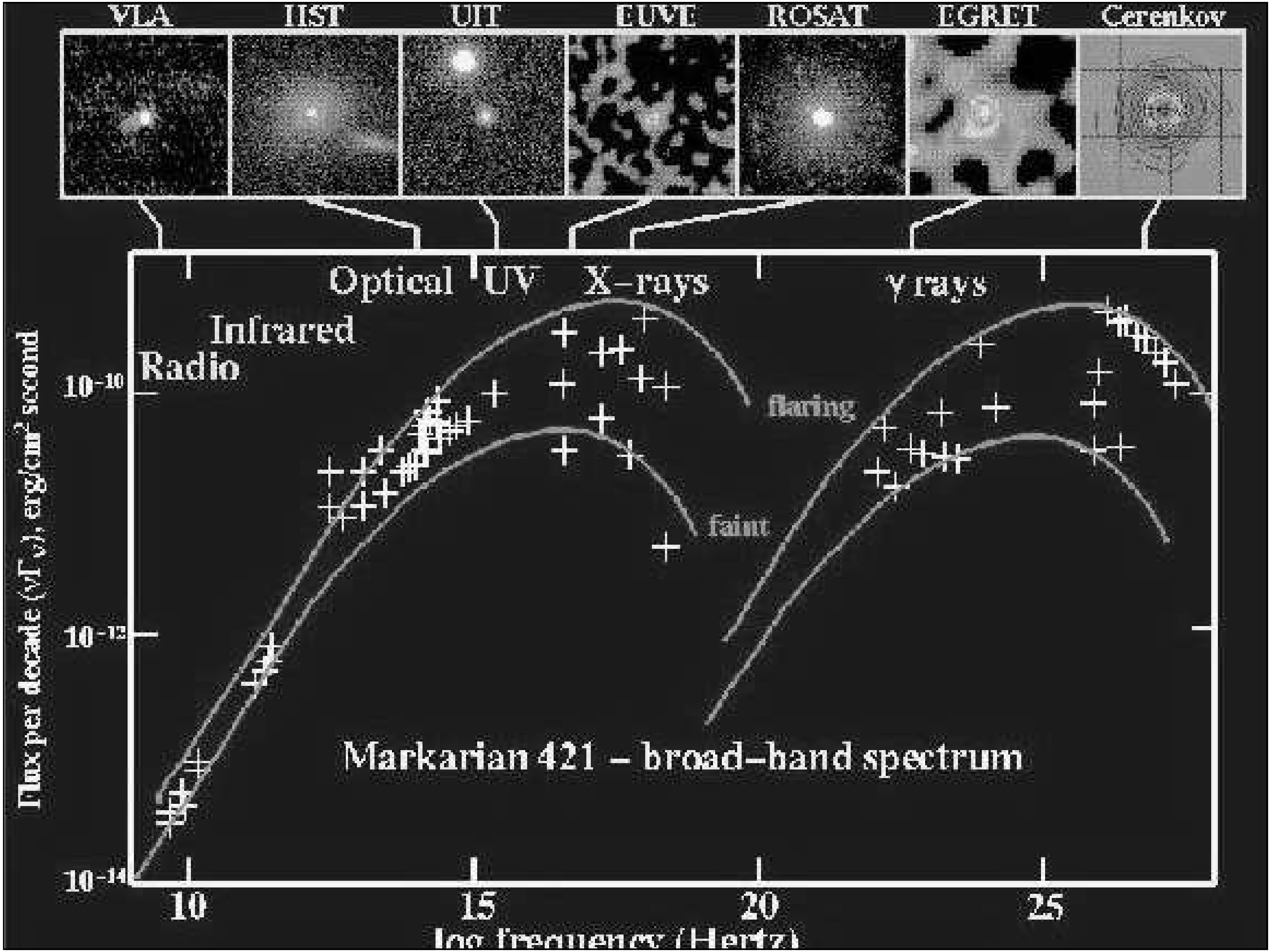
VLA
HST
UIT
EUVE
ROSAT
EGRET
Cerenkov
Radio
Infrared
Optical
UV
X-rays
γ rays
flaring
faint
Markarian 421 – broad-band spectrum
10^{-10}
10^{-12}
10^{-14}
10
15
20
25
Flux per decade (νF_ν), erg/cm^2 second
log frequency (Hertz)

AGN Taxonomy and Unification

Classification of AGN
AGN vs other emission line galaxies
Unification
Pros and cons of unification
Evidence for obscuring tori

AGN taxonomy

“Active” is used to refer to energetic processes that are not related to the normal evolution of stars.

However, the nucleus of a galaxy is defined as an AGN when it has certain optical spectroscopic characteristics. The definition does not address the mechanism responsible for the peculiarities of the spectra.

AGN are a very heterogeneous group:

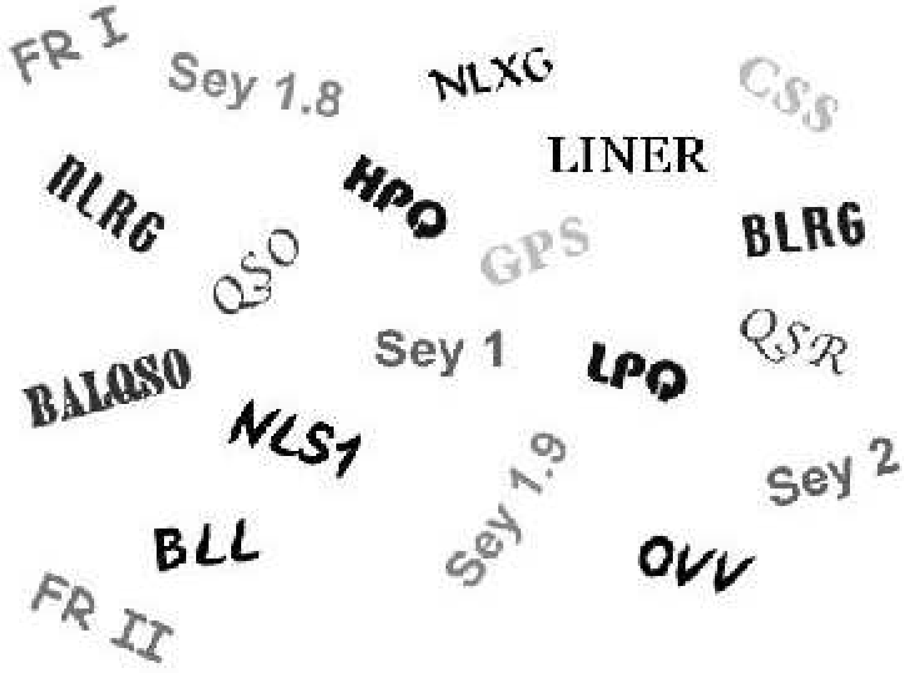

(Goodrich 2001)

AGN taxonomy

Seyfert galaxy: galaxy (usually a spiral) with a high surface brightness nucleus that reveals unusual emission-lines (Seyfert 1943).

(Paul van der Werf's web-page, see also Kraemer & Crenshaw 2000)

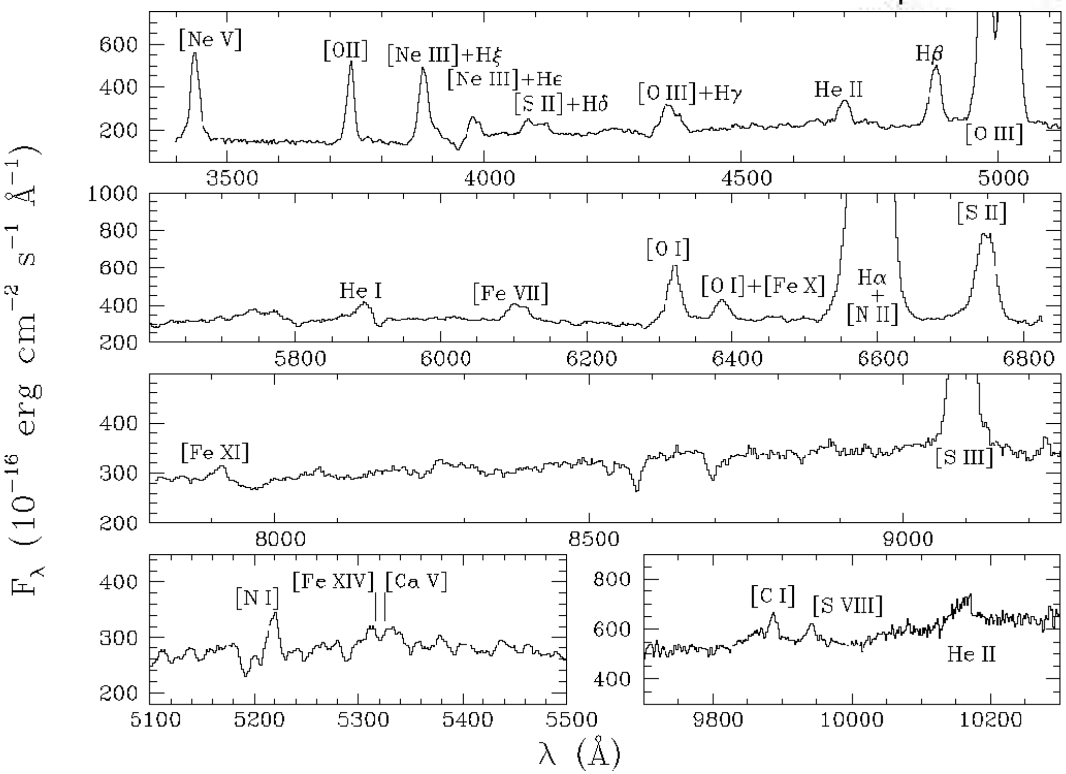

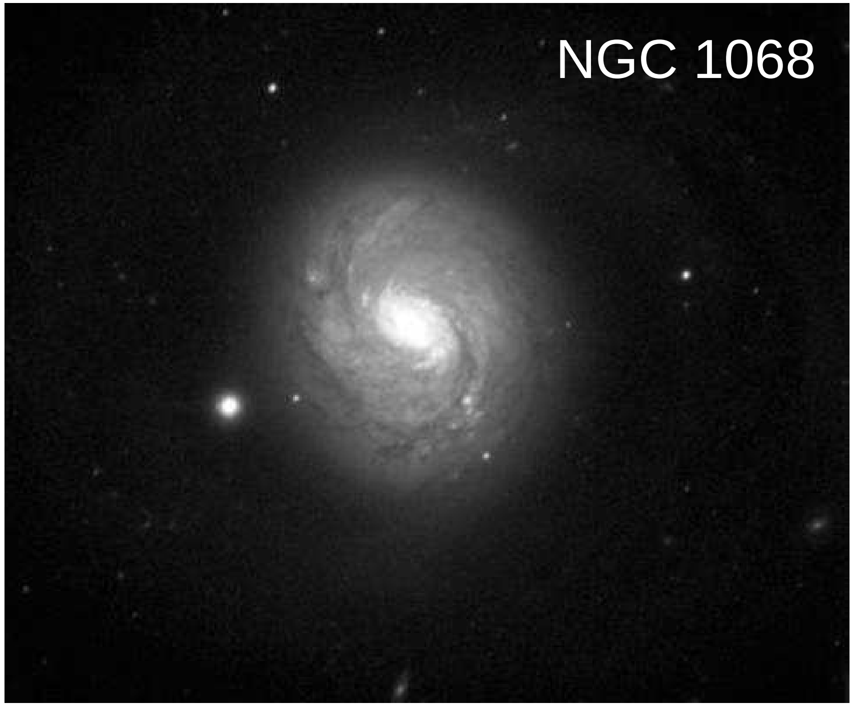

©NOAO

The definition has evolved to underline the presence of strong high-ionization lines, and even coronal lines (although not all AGN have them).

AGN diagnostic diagrams

The BPT diagrams are used in narrow-line emission systems, to distinguish between hard and soft radiation (Balwin, Phillips & Terlevich 1981, Veilleux & Ostrebrock 1987), which is usually ascribed to non-stellar and stellar activity, respectively.

Some people erronously take [O III] / Hβ > 3 as the criterium for AGN

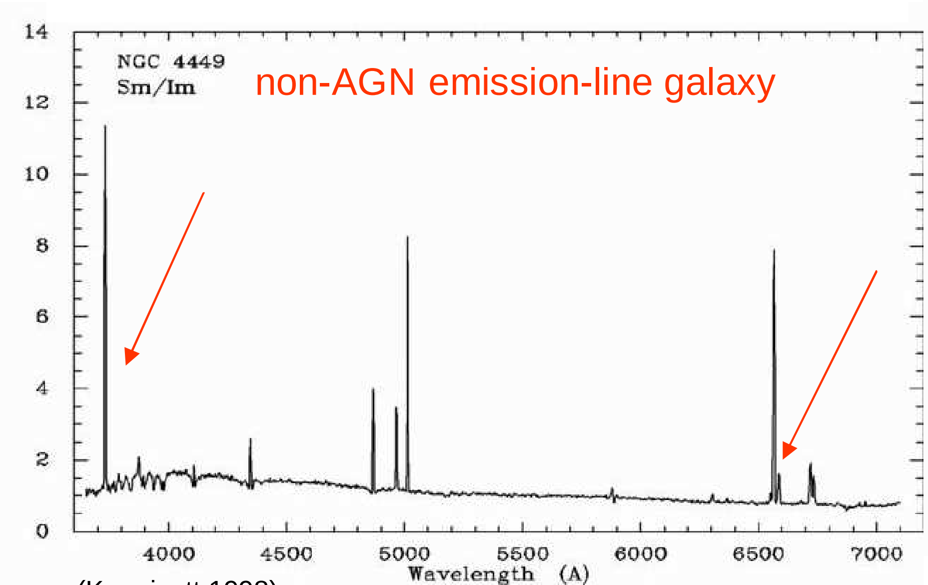

(Kennicutt 1998)

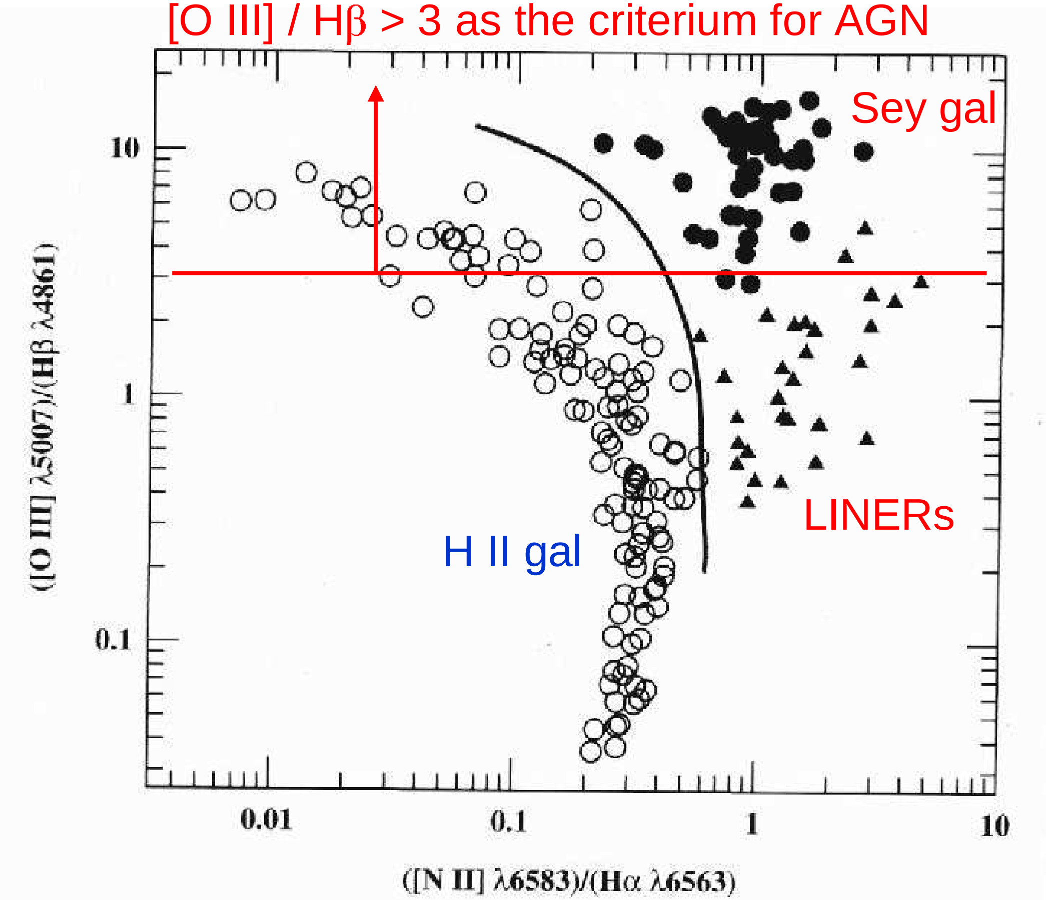

(Peterson 1997)

AGN diagnostic diagrams

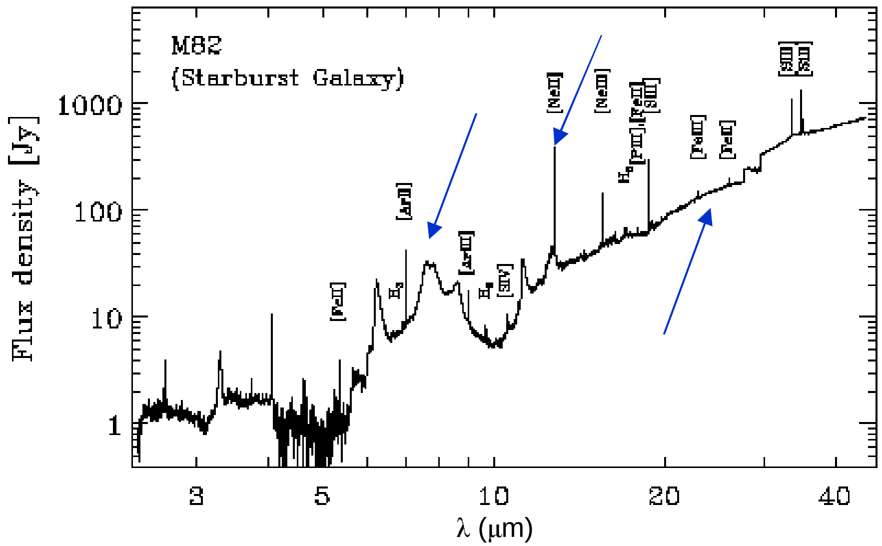

Policyclic aromatic hidrocarbons (PAHs), create bumps in the MIR spectrum, which easily identify soft-UV radiation fields that irradiate hot dust. They get destroyed by hard radiation. ULIRGs have radiation fields closer to starburst galaxies than to AGN. From this diagnostic diagram, it is estimated that 70-80% of the MIR radiation is powered by obscured starbursts and 20-30% by AGN (Genzel et al. 1998).

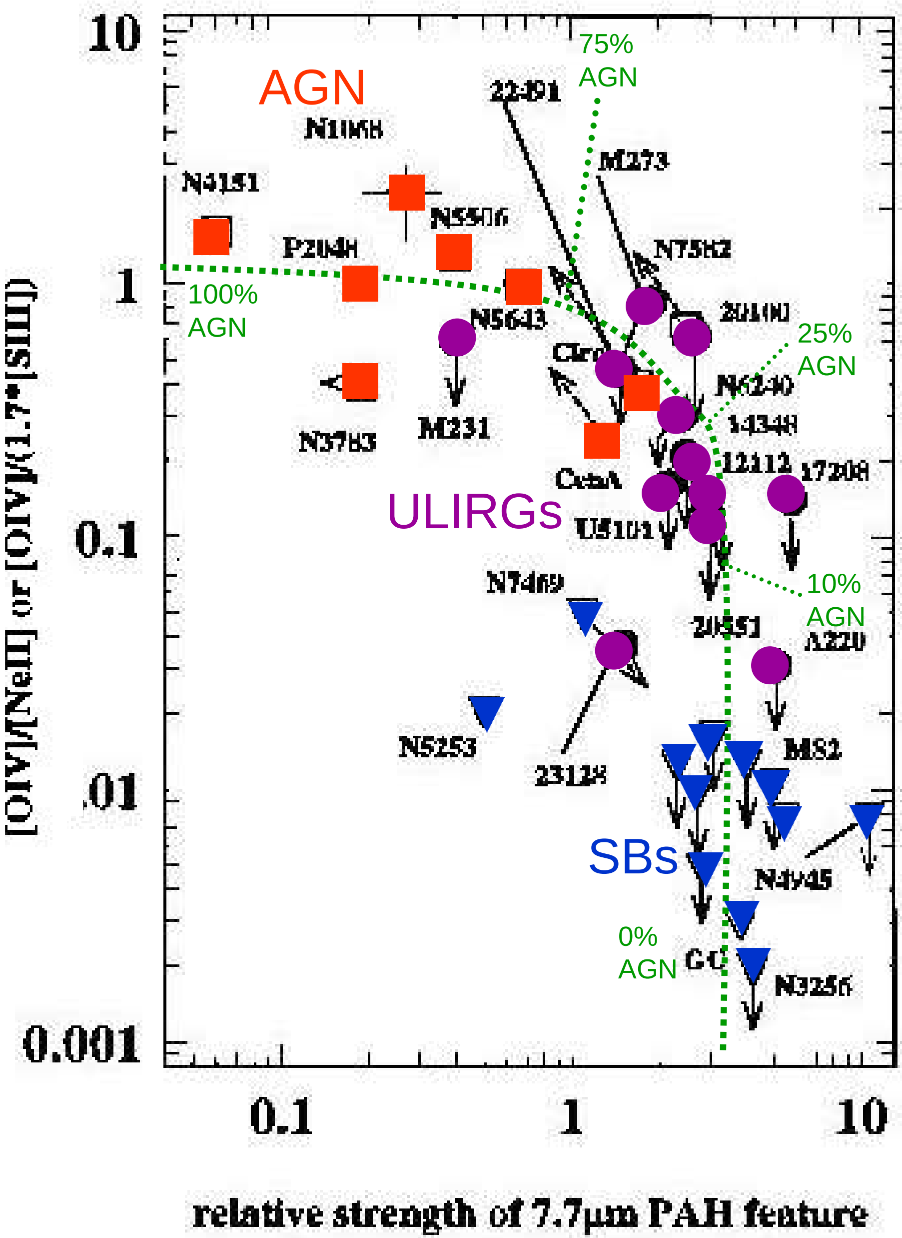

AGN taxonomy: Seyfert galaxies

Seyfert types: depending on the width of the optical emission lines (Khachikian & Weedman 1974, Osterbrock 1981):

- Sy 2: narrow emission lines of FWHM ≤ few x 100 km s^{-1}
- Sy 1: broad permitted emission lines (Hα, He II, ...), of FWHM $\lesssim 10^4$ km s^{-1} that originate in a high-density medium ($n_e \geq 10^9$ cm^{-3}), and narrow-forbidden lines ([O III], [N II], …) that originate in a low-density medium ($n_e \approx 10^3 - 10^6$ cm^{-3}).
- Sy1.x (1.9, 1.8, ...): they graduate with the width of the Hα and Hβ lines.
- NL Sy1: subclass of Sy 2 with X-ray excess and optical Fe II in emission.

But the classification for a single object can change with time, due to AGN variability!

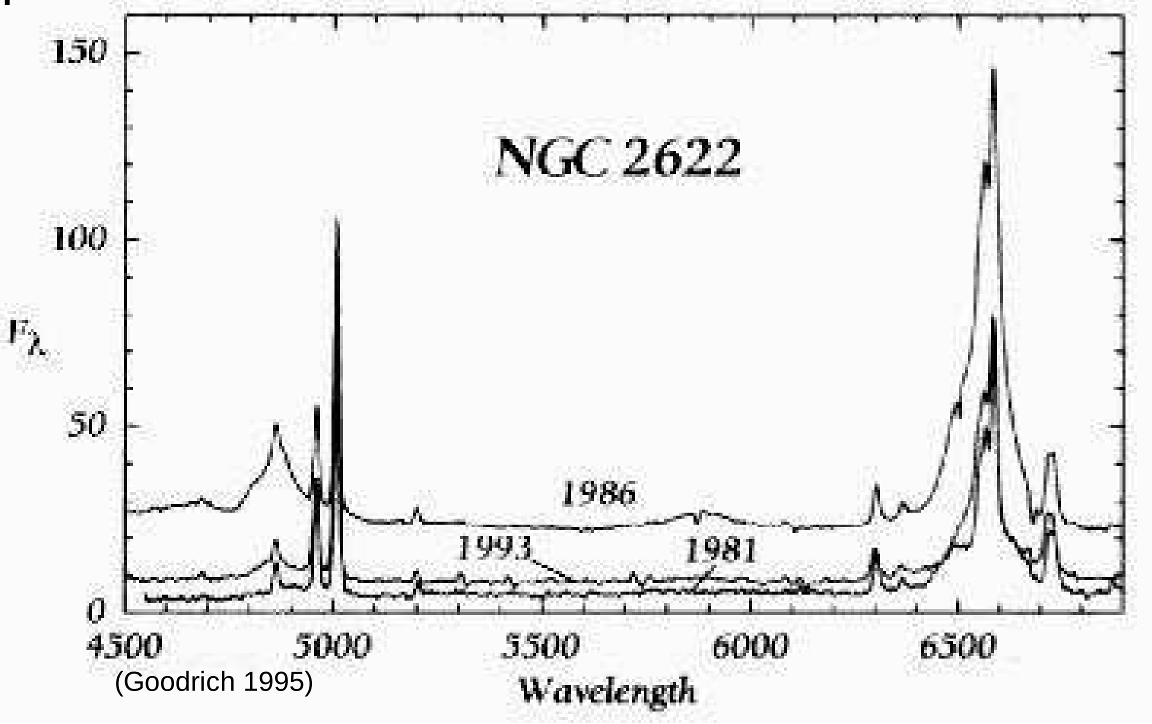

(Goodrich 1995)

AGN taxonomy: Quasars and QSOs

Quasar = Quasi Stellar Radio-source , QSO = Quasi-Stellar Object

Scaled-up version of a Seyfert, where the nucleus has a luminosity $M_B < -21.5 + 5 \log h_0$ (Schmidt & Green 1983). The morphology is, most often, star-like. The optical spectra are similar to those of Sy 1 nuclei, with the exception that the narrow lines are generally weaker.

©HST

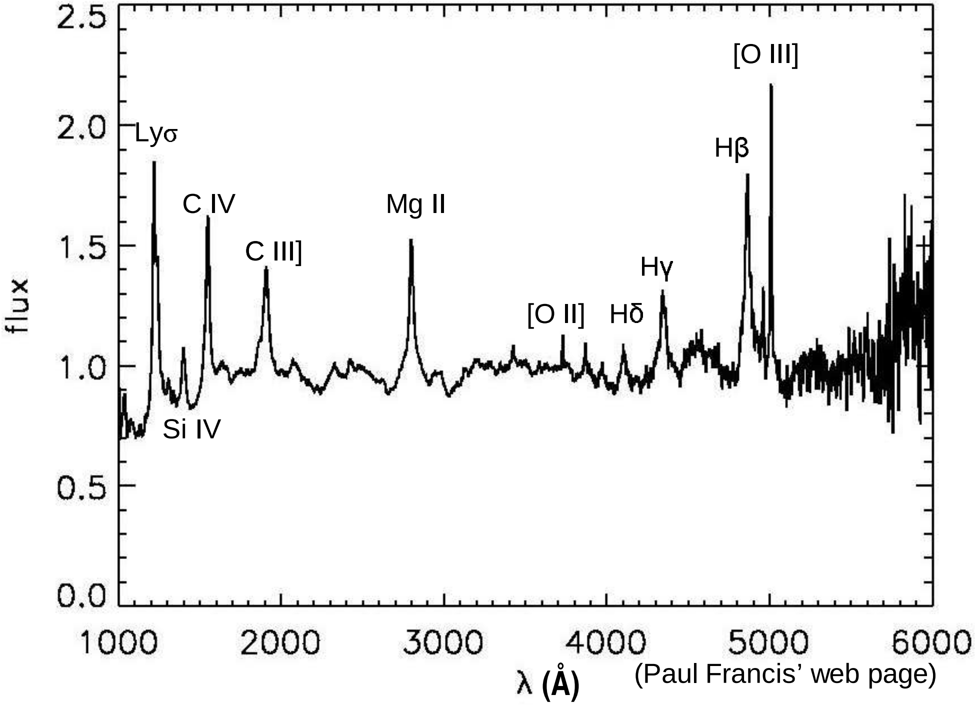

(Paul Francis' web page)

There are two varieties: radio-loud QSOs (quasars or RL QSOs) and radio-quiet QSOs (or RQ QSOs) with a dividing power at $P_{5GHz} \approx 10^{24.7}$ W Hz^{-1} sr^{-1} .

RL QSOs are 5−10% of the total of QSOs.

AGN taxonomy: Quasars and QSOs

There is a big gap in radio power between RL and RQ varieties of QSOs
(Kellerman et al. 1989, Miller et al. 1990)

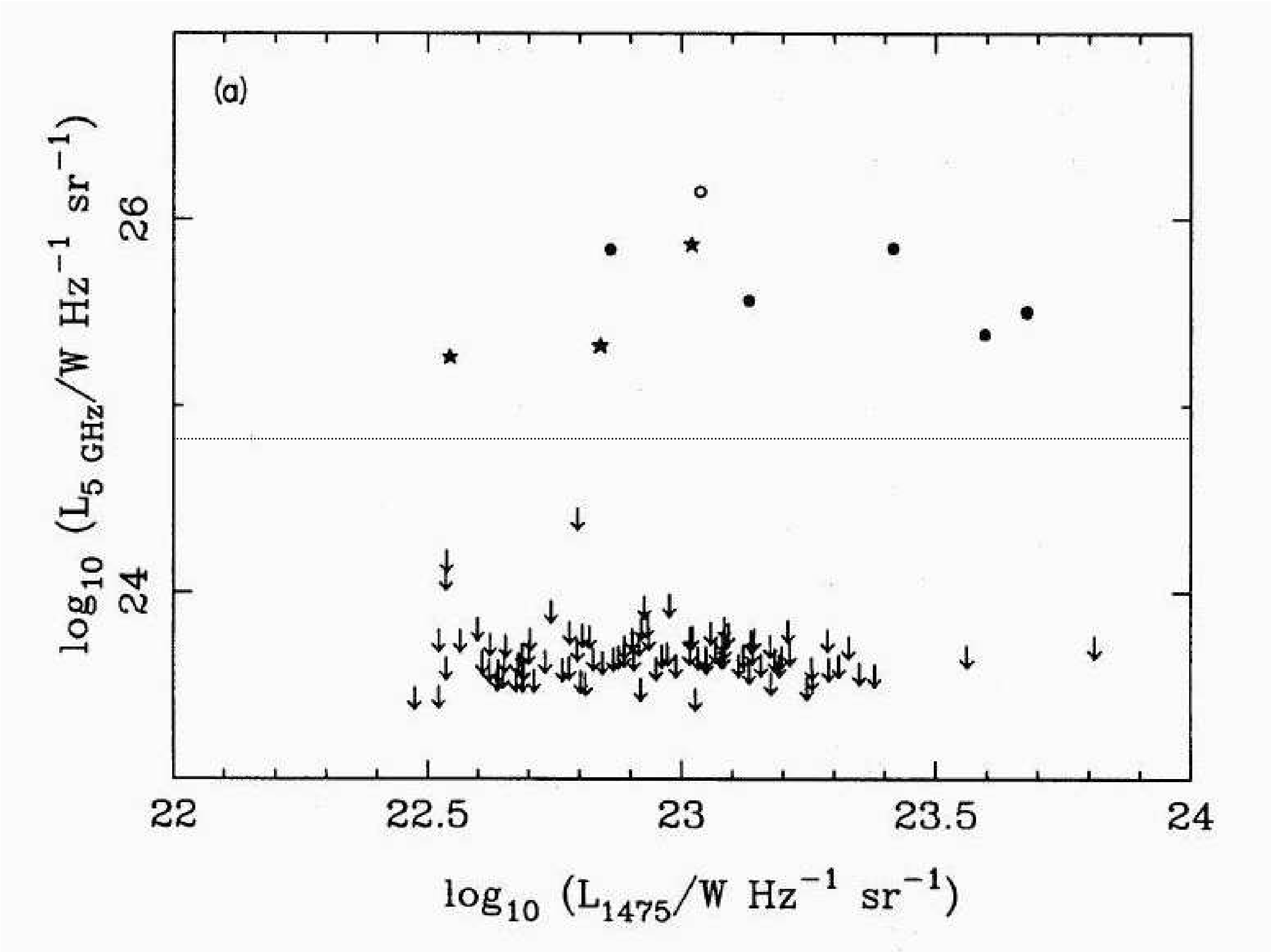

(Miller et al. 1990)

AGN taxonomy: BAL QSOs

BAL QSOs = Broad Absorption Line QSOs

Otherwise normal QSOs that show deep blue-shifted absorption lines corresponding to resonance lines of C IV, Si IV, N V.

All of them are at $z \geq 1.5$ because the phenomenon is observed in the rest-frame UV. At these redshifts, they are about 10% of the *observed* population.

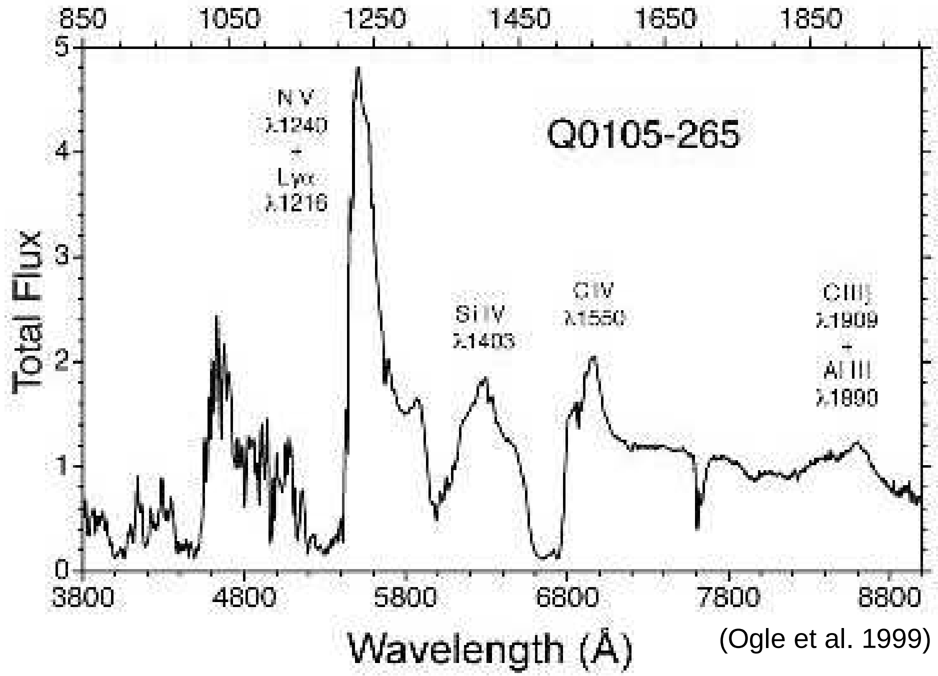

(Ogle et al. 1999)

BAL QSOs tend to be more polarized than non-BAL QSOs.

AGN taxonomy: Radio galaxies

Strong radio sources associated with giant elliptical galaxies, with optical spectra similar to Seyfert galaxies.

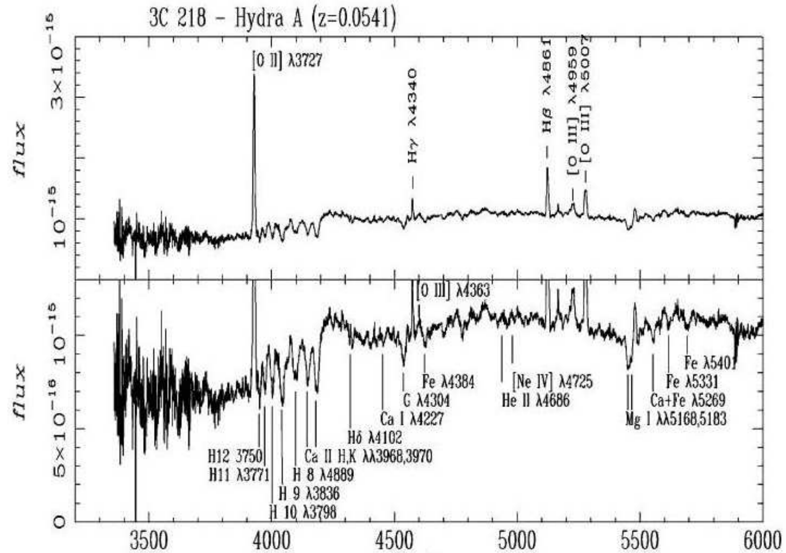

(Aretxaga et al. 2001)

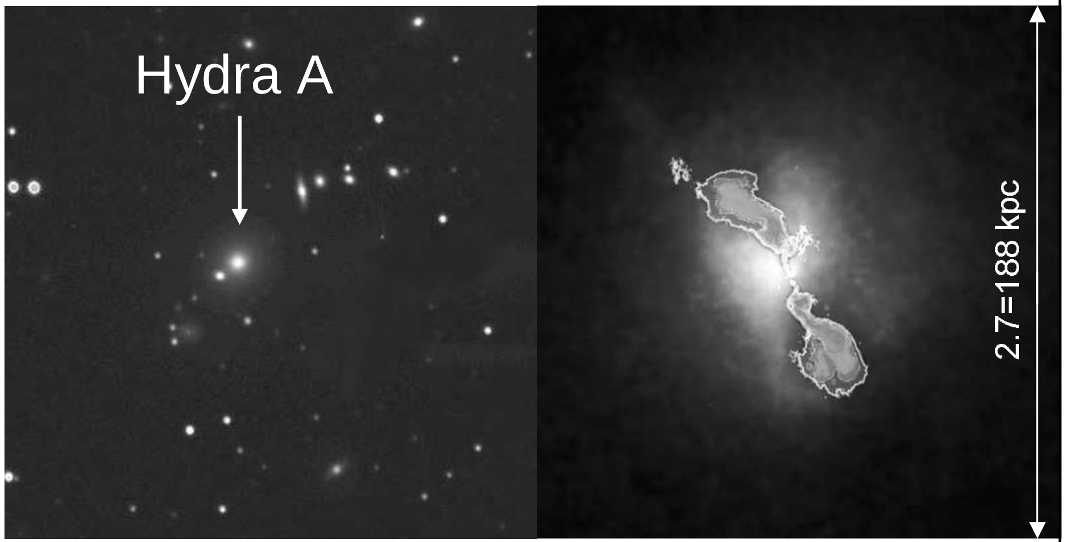

©Chandra

Sub-classification according to

♦ optical spectra: NLRG = narrow-line radio galaxy, and BLRG = broad-line radio galaxy, with optical spectra similar to Sy 2 and Sy 1, respectively.

♦ spectral index (α, such that $F_\nu = \nu^\alpha$) at ν=1GHz: steep or flat separated by α=−0.4

♦ radio morphology (Fanaroff & Riley 1974): measured by the ratio of the distance between the two brightest spots and the overall size of the radio image.
FR I with R<0.5 and FR II with R>0.5

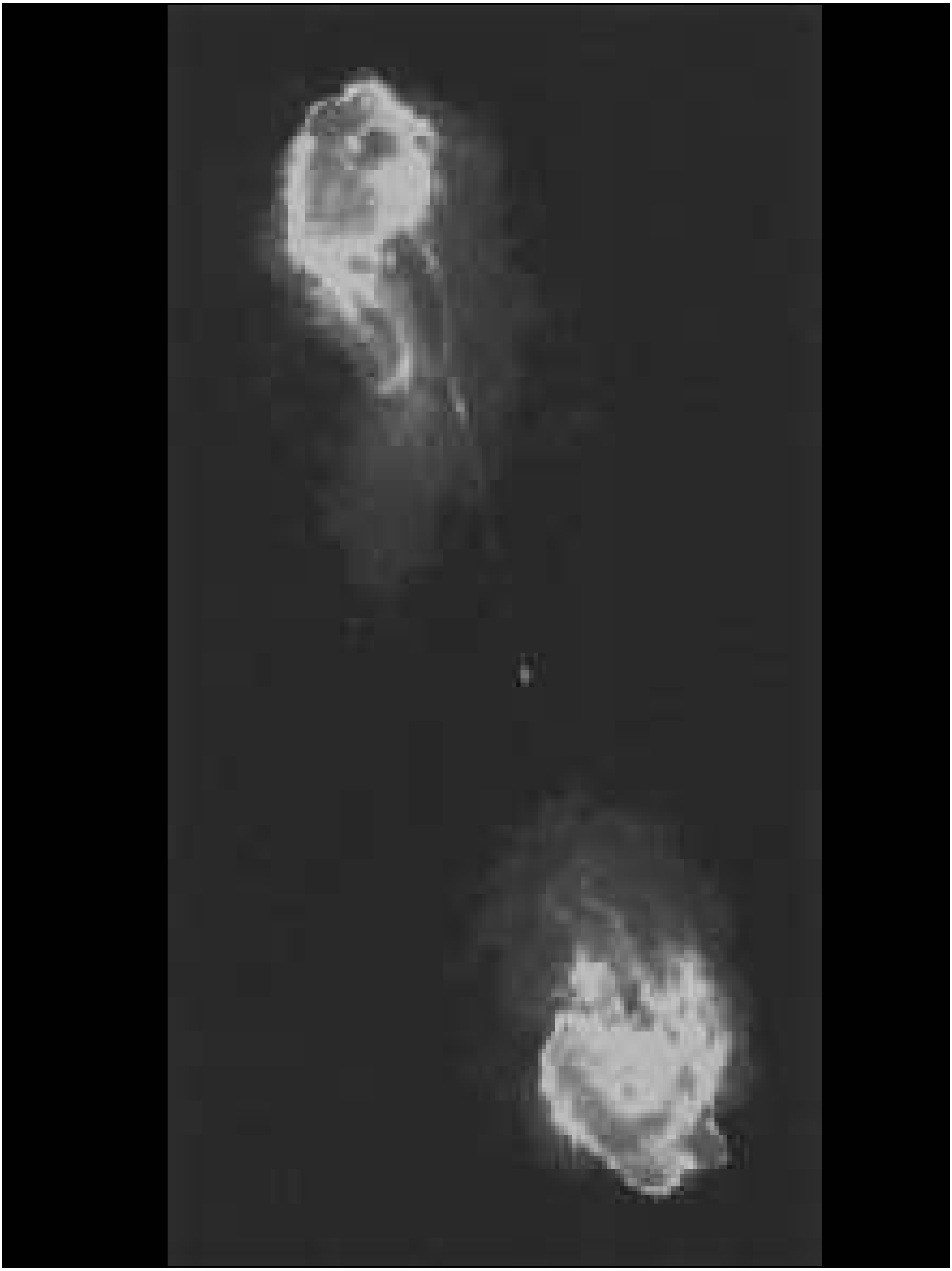

AGN taxonomy: BL Lacs

BL Lac is the prototype of its class, an object, stellar in appearance, with very weak emission lines and variable, intense and highly polarized continuum. The weak lines often just appear in the most quiescent stages. Blazars encompass BL Lacs and optically violent-variable (OVV) QSOs. These are believed to be objects with a strong relativistically beamed jet in the line of sight.

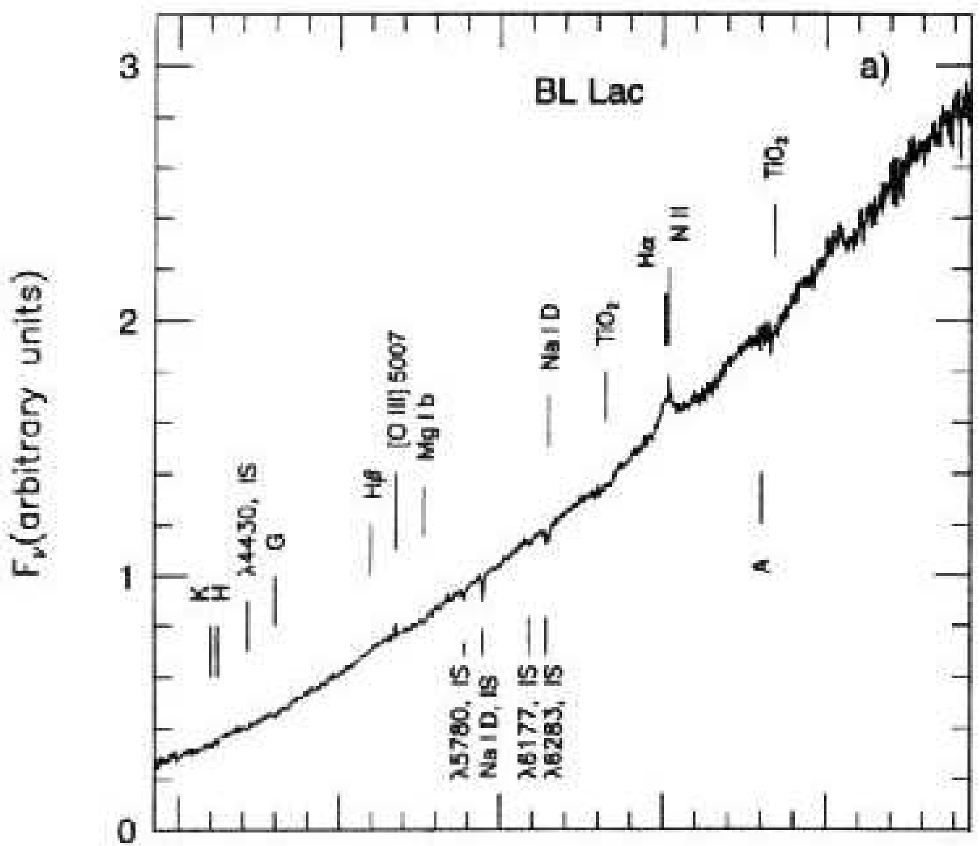

(Vermeulen et al. 1994)

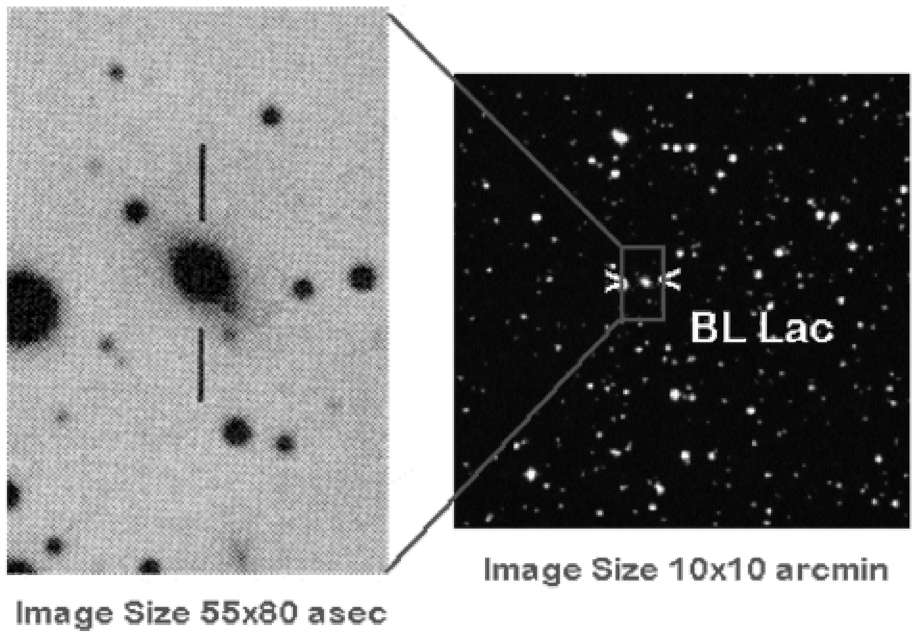

AGN gallery and densities

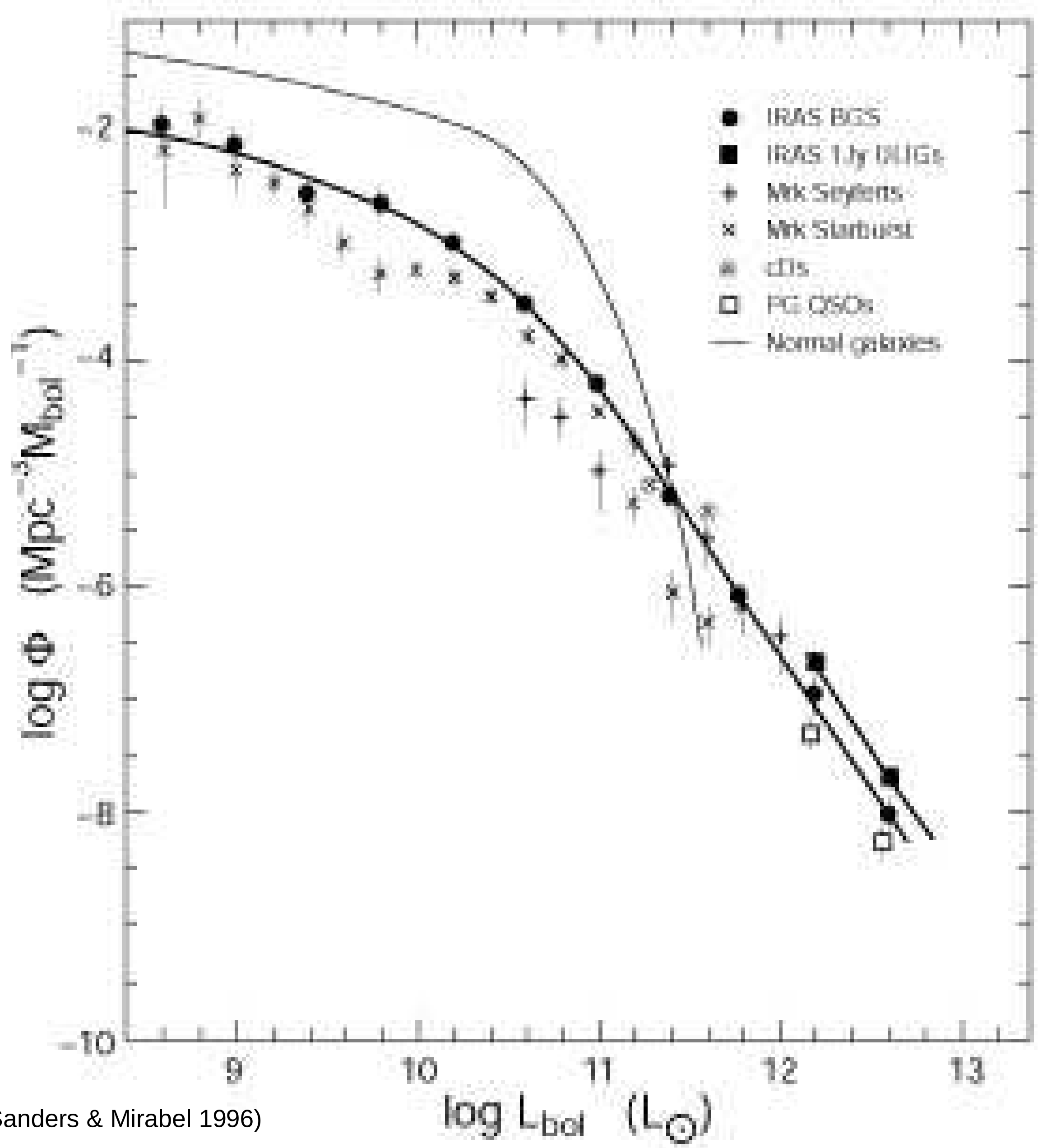

(Sanders & Mirabel 1996)

Space densities in the local Universe

(Wotjer 1990)

Radio-quiet

Sy 2: 8 x 10^5 h_0^3 Gpc^{-3}

Sy 1: 3 x 10^5 h_0^3 Gpc^{-3}

QSOs: 800 h_0^3 Gpc^{-3}

Radio-loud

FR I: 2 x 10^4 h_0^3 Gpc^{-3}

BL Lac: 600 h_0^3 Gpc^{-3}

FR II: 80 h_0^3 Gpc^{-3}

Quasars: 20 h_0^3 Gpc^{-3}

Phenomenology of AGN: variability

Broad-line varieties (Sy 1s, QSOs, BLRGs) are usually variable, where as narrow-line varieties (Sy 2s, LINERs, NLRGs) are usually quiescent.

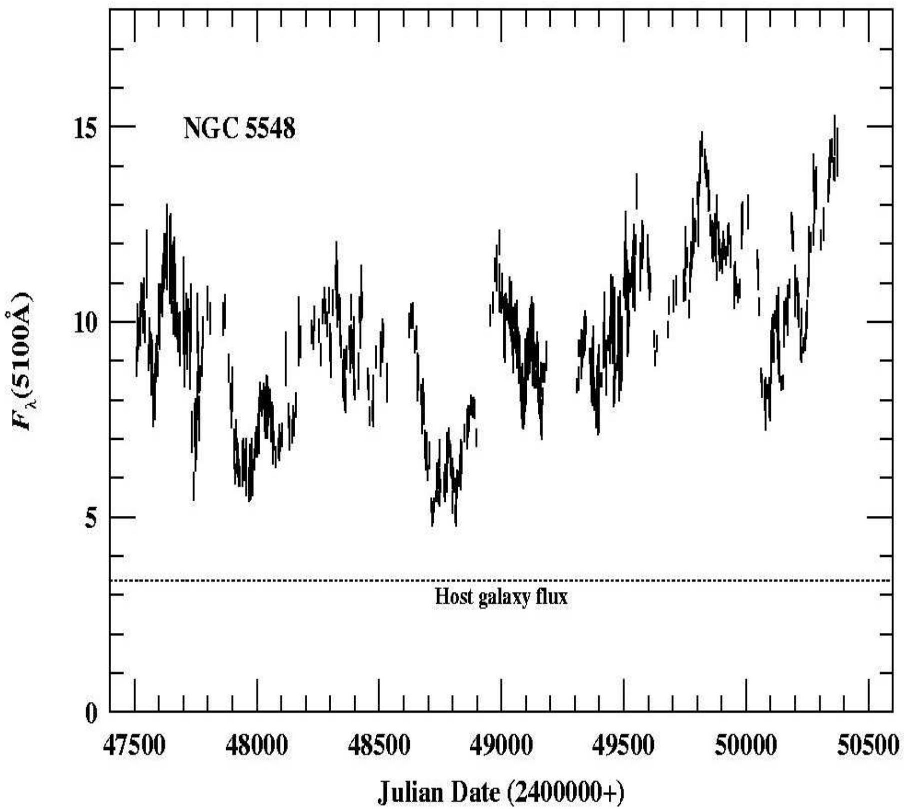

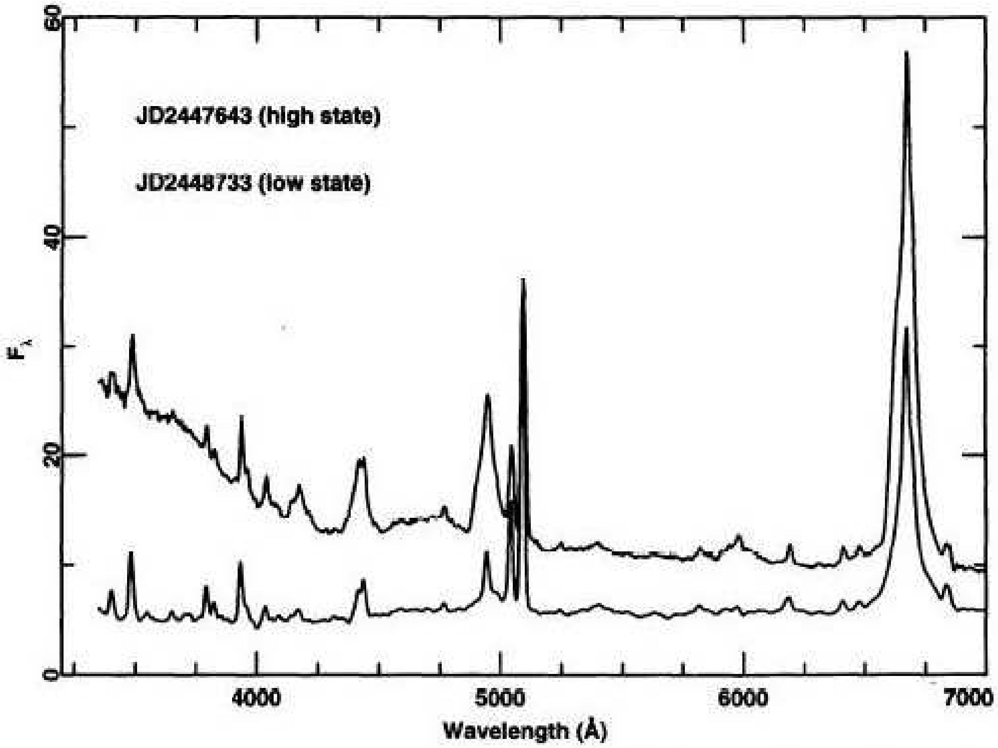

(Peterson et al. 1994, Peterson 2001)

But there are outstanding exceptions....

Phenomenology of AGN: energetics

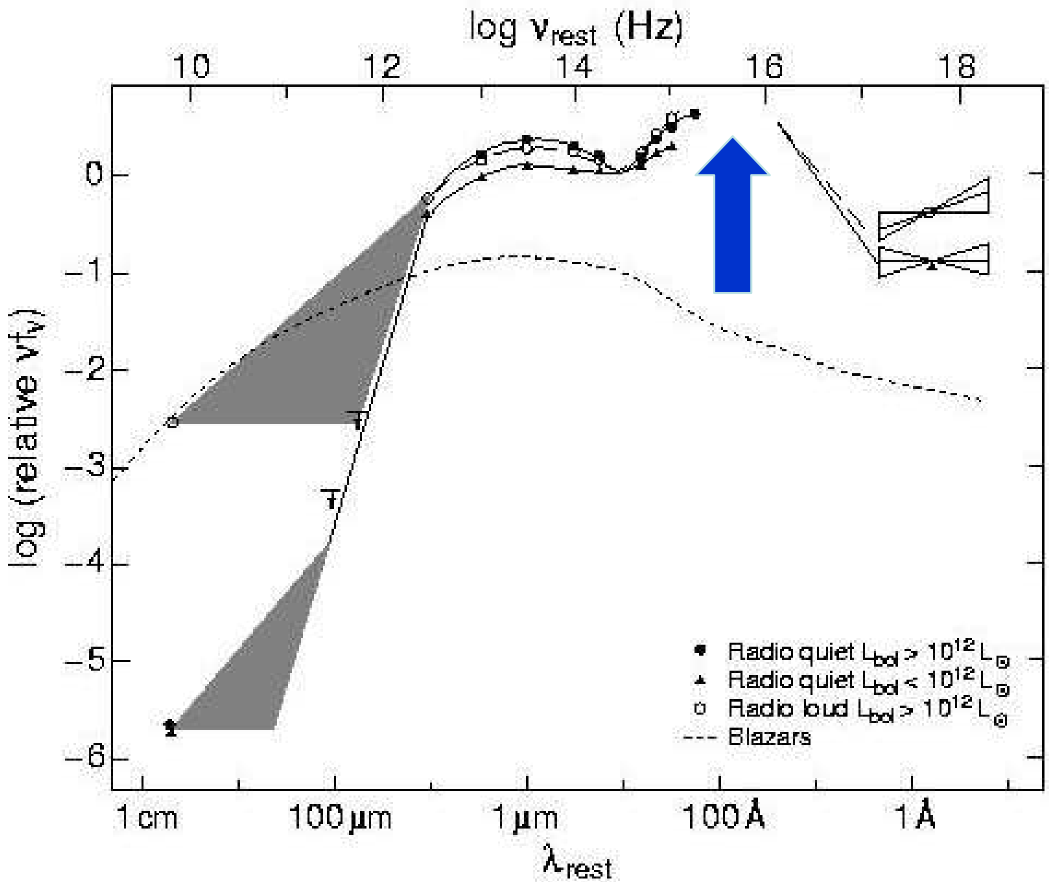

(Sanders & Mirabel 1996)

Most of the energy emitted by QSOs is associated with the big blue bump. One needs to understand the emission mechanism in this region to understand what makes AGN unique.

The extreme luminosities emitted by AGN

bolometric $L_{Sy} \approx 10^{44}$ erg s^{-1}

$L_{QSO} \approx 10^{46}$ erg s^{-1}

made it clear that the easiest way to explain them was through the release of gravitational energy. In the mid-60s the concept of a supermassive black hole (**SMBH**) surrounded by a viscous disk of accreting matter gained popularity (Zeldovich & Novikov 1964), and has become the standard model for AGN, still used today.

The standard model of AGN

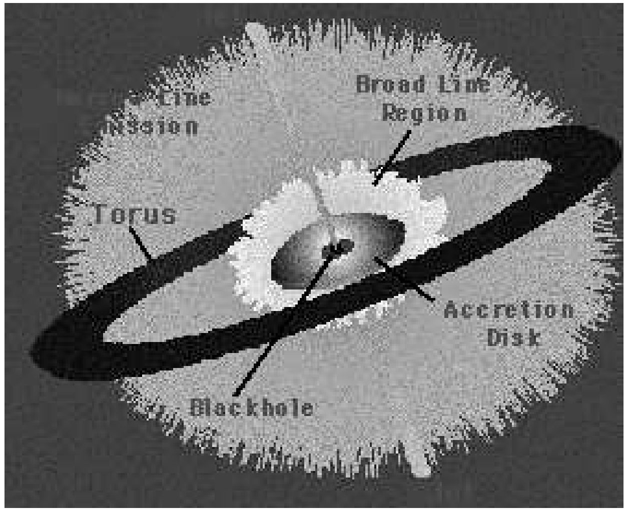

Components:

accretion disk: $r \sim 10^{-3}$ pc $n \sim 10^{15}$ cm^{-3}

$v \sim 0.3c$

Broad Line Region (BLR):

$r \sim 0.01 - 0.1$ pc $n \sim 10^{10}$ cm^{-3}

$v \sim$ few x 10^{3} km s^{-1}

torus: $r \sim 1 - 100$ pc $n \sim 10^{3} - 10^{6}$ cm^{-3}

Narrow Line Region (NLR):

$r \sim 100 - 1000$ pc $n \sim 10^{3} - 10^{6}$ cm^{-3}

$v \sim$ few x 100 km s^{-1}

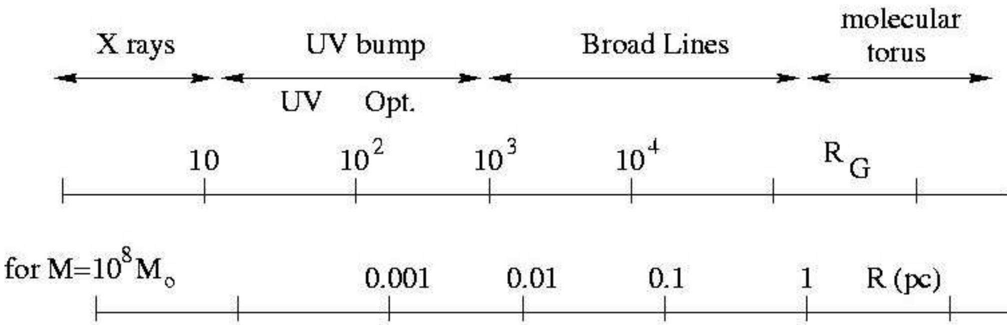

Jet:

From 10^{-3} pc to 100 kpc

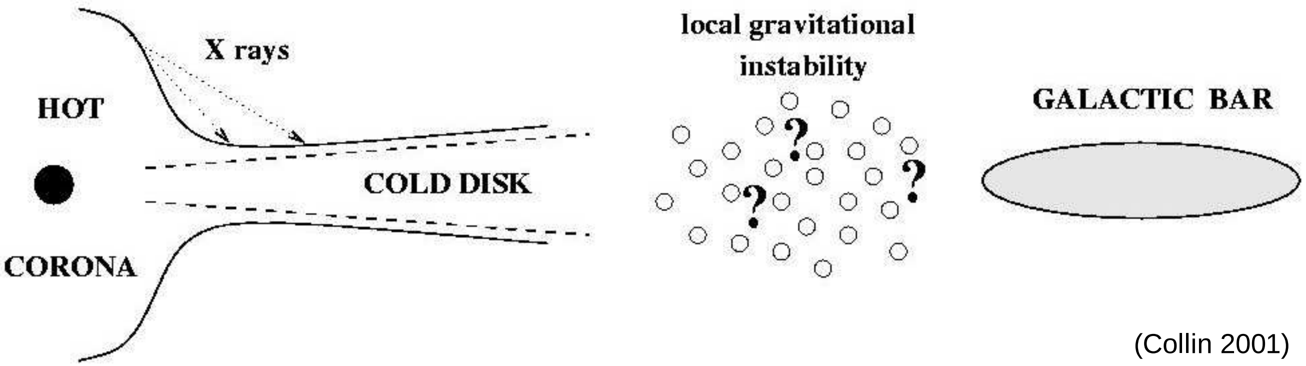

(Collin 2001)

Blandford-Znajek Mechanism

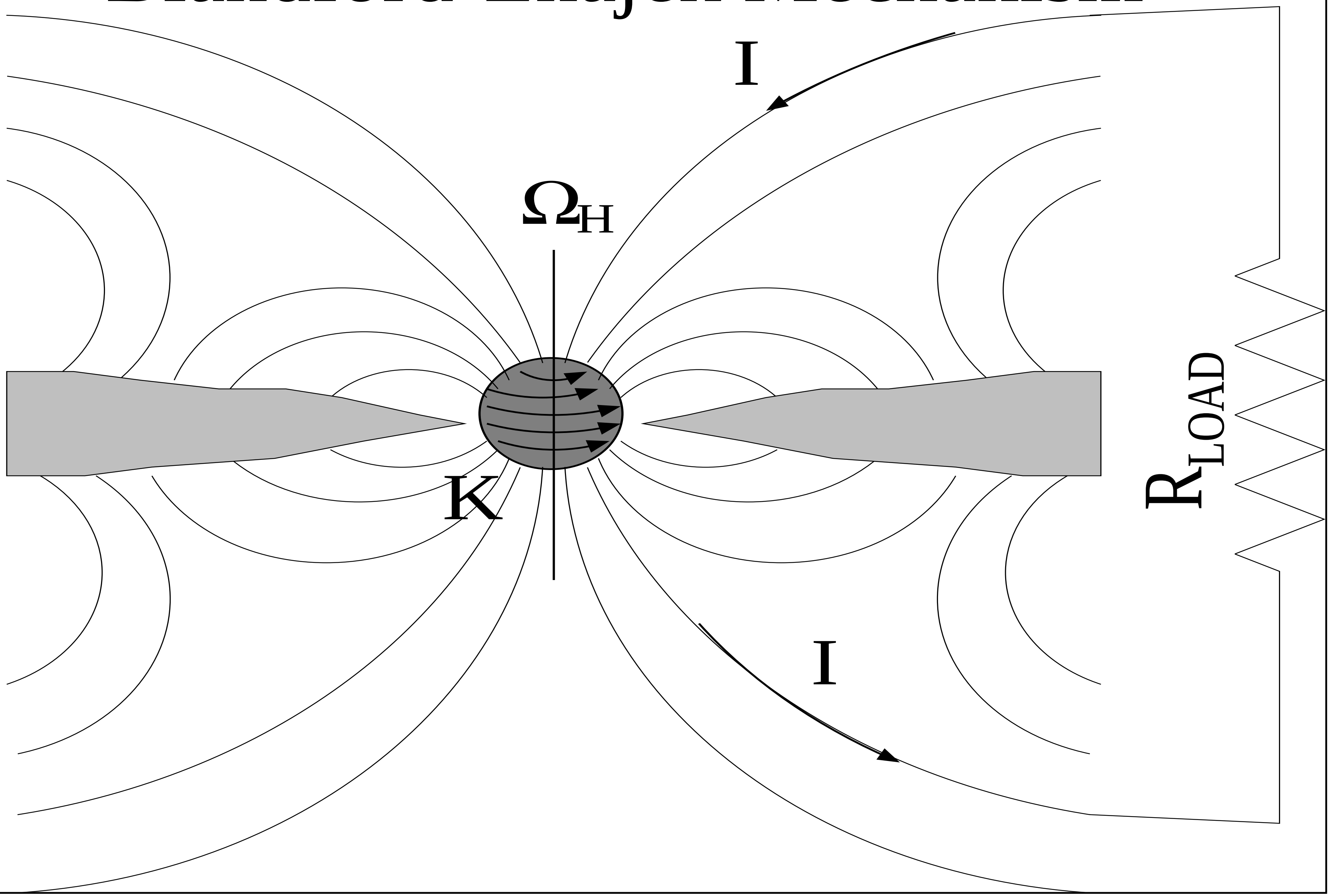

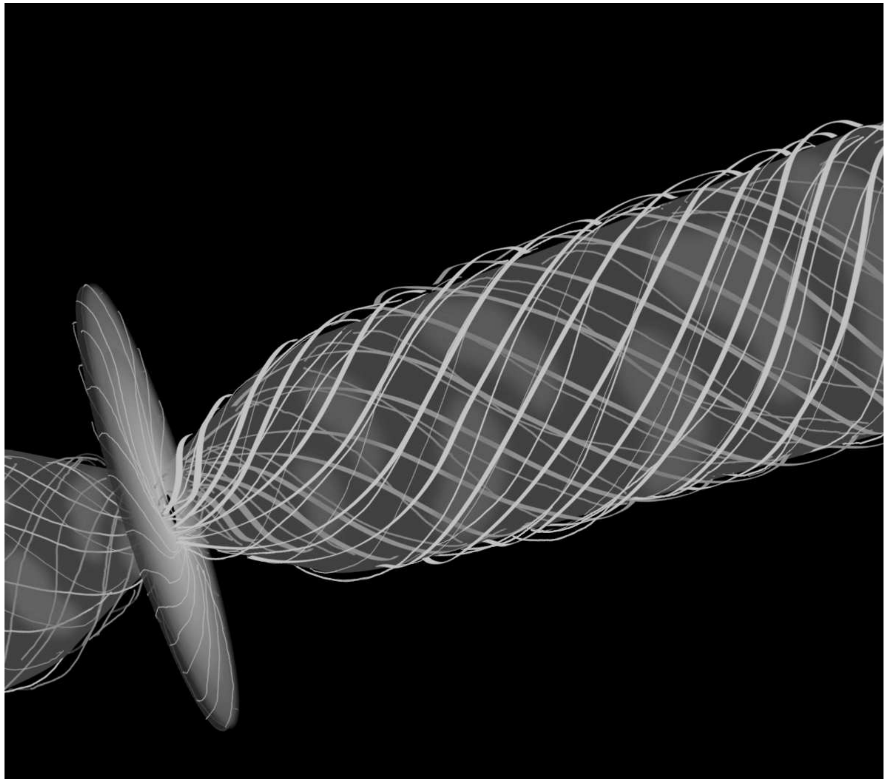

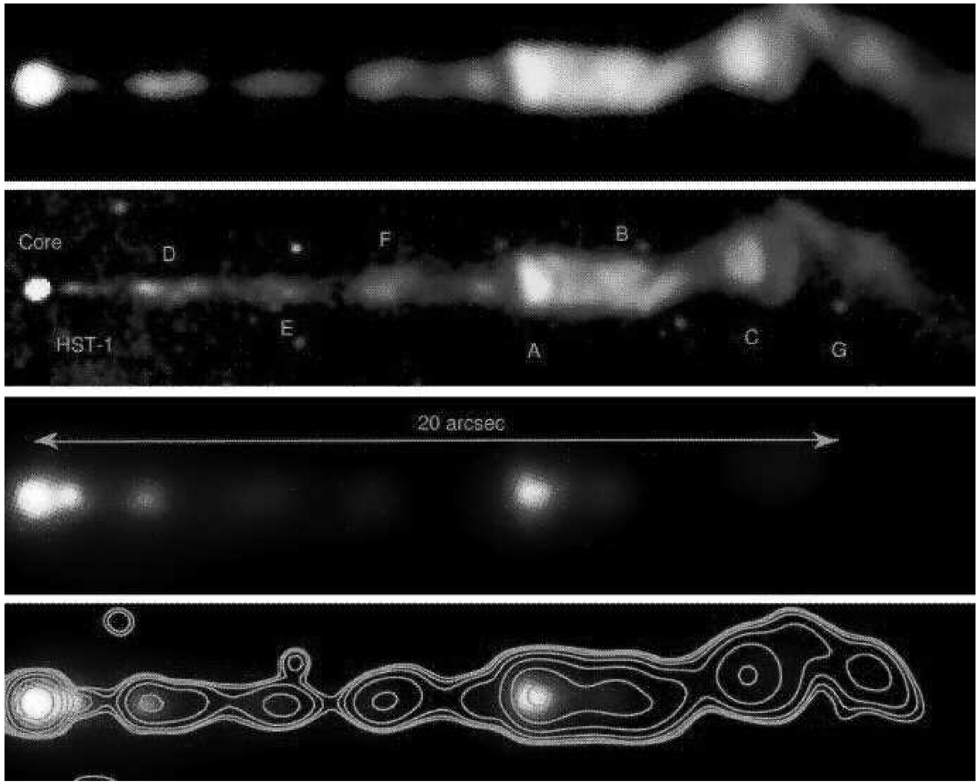
Core
D
F
B
HST-1
E
A
C
G
20 arcsec

Unification in AGN

All AGN are the same type of object but looked at from a different point of view

	Face-on	Edge-on
Radio-quiet	Sy 1	Sy 2
	QSO	FIR gal?
Radio-loud	BL Lac	FR I
	BLRG	NLRG
	quasar	FR II

This idea dates back to, at least, Rowan-Robinson (1977), and became popular in the mid-80s (reviews by Lawrence 1987, Antonucci 1993, Urry & Padovani 1997, Goodrich 2001).

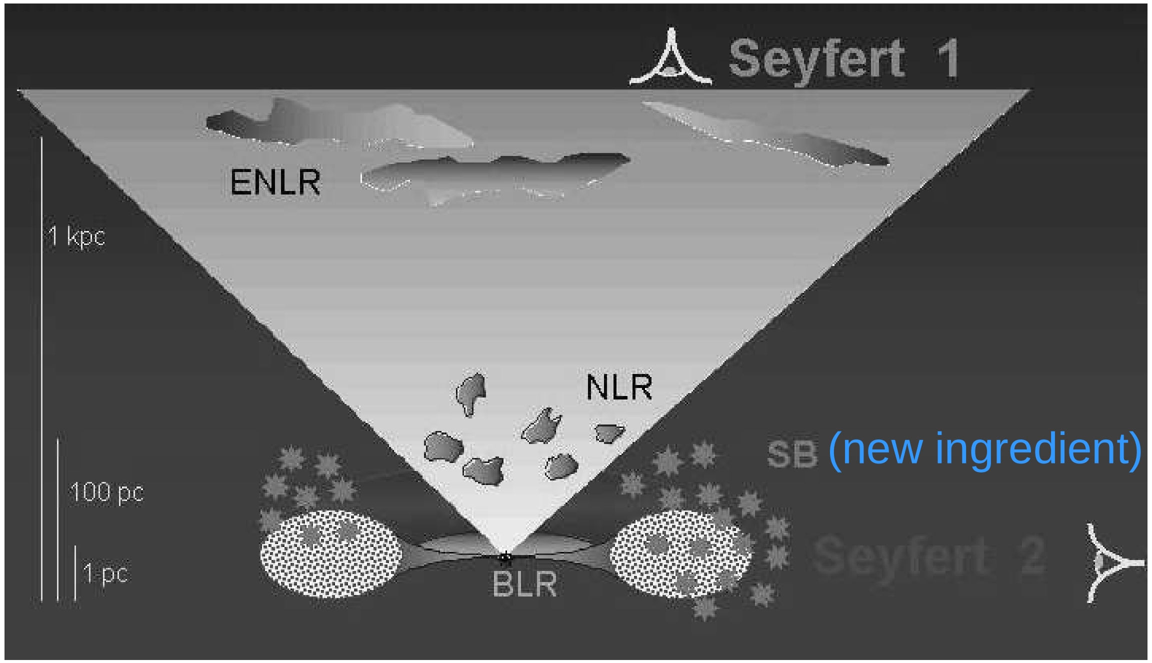

(Rosa González-Delgado´s web page)

Support for unification: hidden emission lines

Some Sy 2s show broad lines in polarized light (Antonucci & Miller 1995, Goodrich & Miller 1990, ...): the fraction is still unclear since the observed samples are biased towards high-*P* broad-band continuum objects.

The polarization level of the continuum flux is roughly constant up to λ1500Å (Code et al. 1993), which implies that hot electrons are the scattering source near the nucleus, but dust dominates the outskirts.

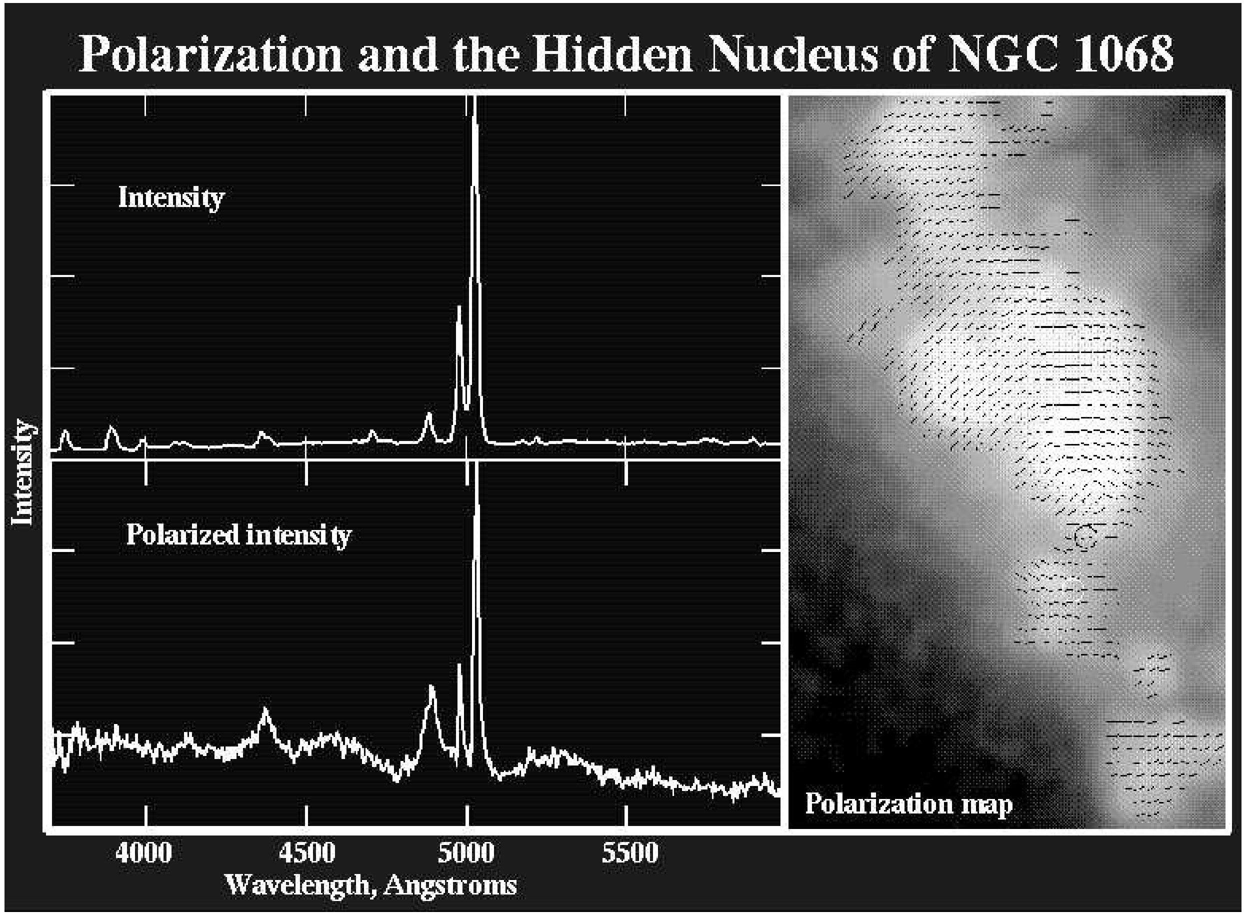

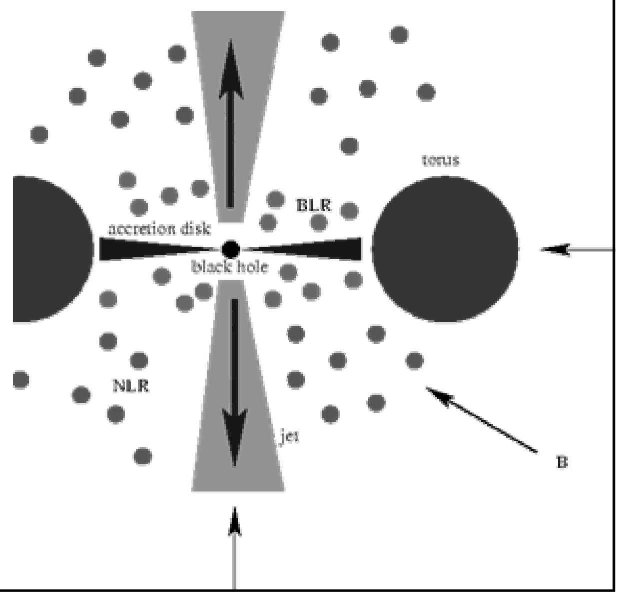

(Bill Keel´s web page with data from Miller, Goodrich & Mathews 1991, Capetti et al. 1995)

Support for unification: ionization cones

A number of Sy 2s also show clear anisotropy in the highly ionized emission lines (like [O III]) which, often, resemble a cone (Pogge 1988): the ionization cone is “collimated” by the obscuring torus.

One can readily assess that the radiation field is anisotropic (Neugebauer et al. 1980, Wilson et al. 1988, Storchi-Bergmann et al. 1992):

The number of ionizing photons to produce Hβ:

$$N(H\beta) = \frac{L(H\beta)}{h\nu_{H\beta}} \frac{\alpha_B}{\alpha_{H\beta}^{eff}} \approx 2.1\times10^{52} L_{40}(H\beta) \text{ photons s}^{-1}$$

This can be compared with the ionizing production rate inferred from the continuum:

$$N(H) = 4\pi d^2 \int_{\nu_1}^{\nu_2} \frac{F_\nu d\nu}{h\nu}$$

which yields N(H)/N(Hβ) < 1, and suggests that the ionization cone sees a more luminous continuum than we do.

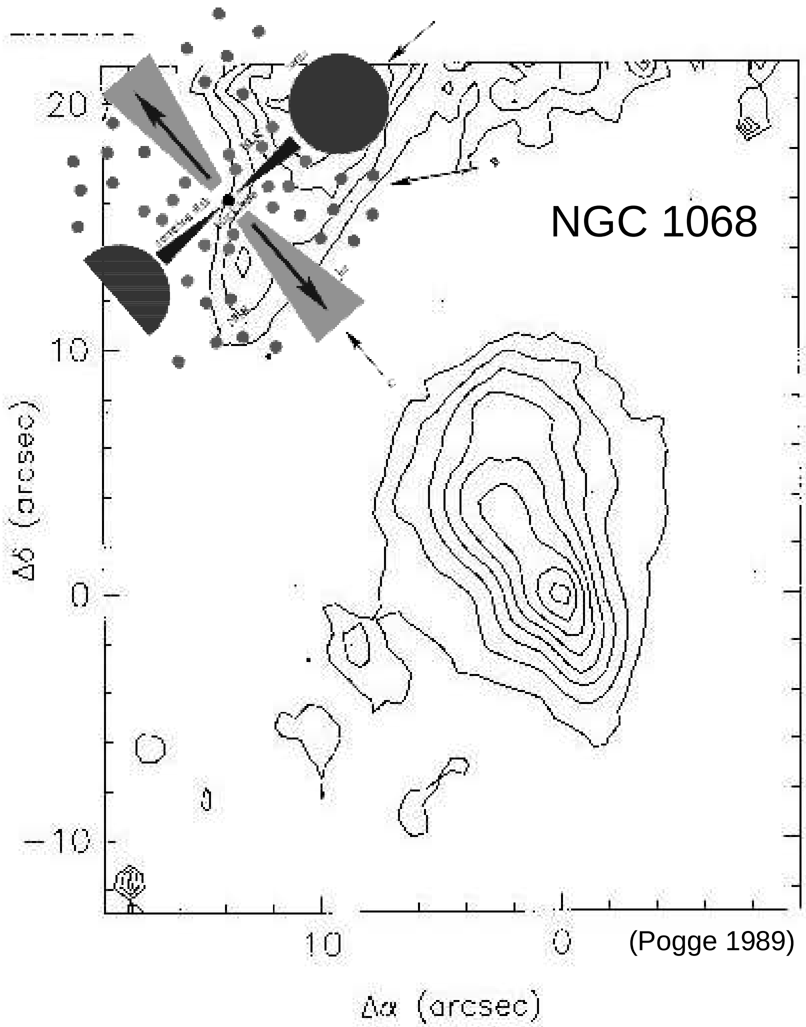

(Pogge 1989)

Support for unification: IR and N_H excess

One can measure the column of neutral H that absorbs the soft X-rays emitted by the nucleus. The gas is associated with the dust in the molecular torus, and thus provides a rough estimate of the dust content and the attenuation this provides.

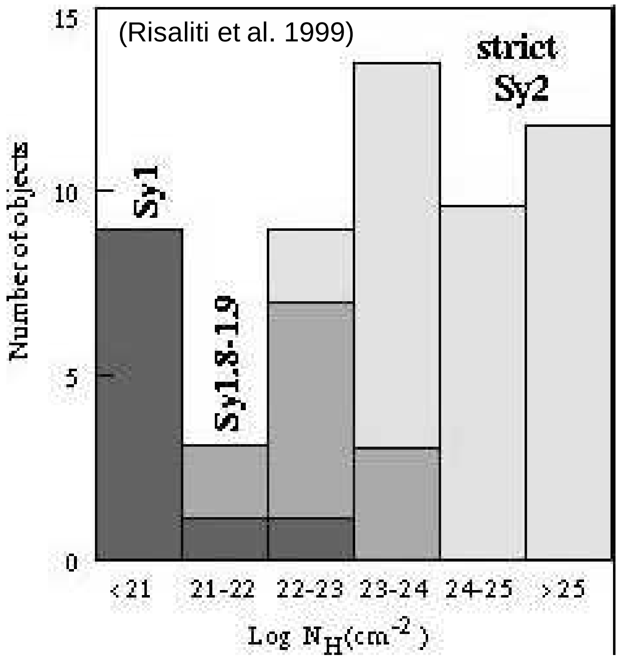

Sy 2s have the largest absorption columns, many of which imply the medium is Compton thick, so that X-rays are suppressed below 10 keV (Mushotzky 1982, Risaliti et al. 1999, Bassani et al. 1999).

Sy 2s also have colder IR colours than Sy 1s, as inferred from a sample of 10 Seyfert galaxies with ISO colours (Pérez-García et al. 1998):

T_{Sy2}=112 – 136 K $\quad\quad$ T_{Sy1}≈ 150 K

which can be explained if the torus is partially thick at mid-IR wavelengths.

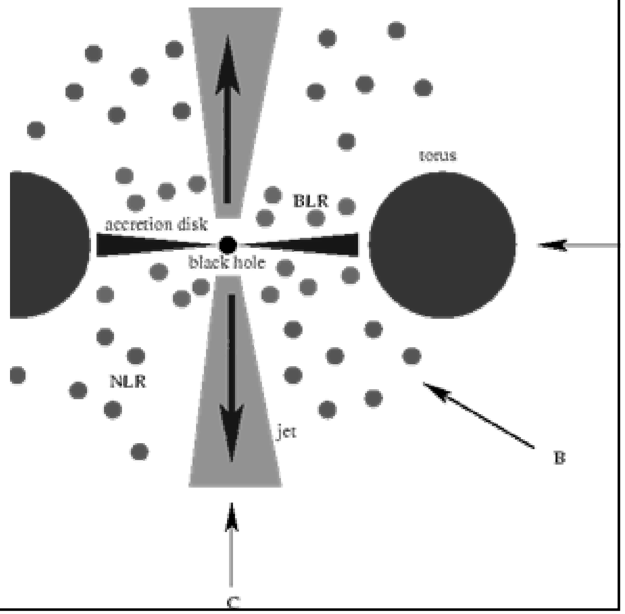

Support for unification: detection of tori?

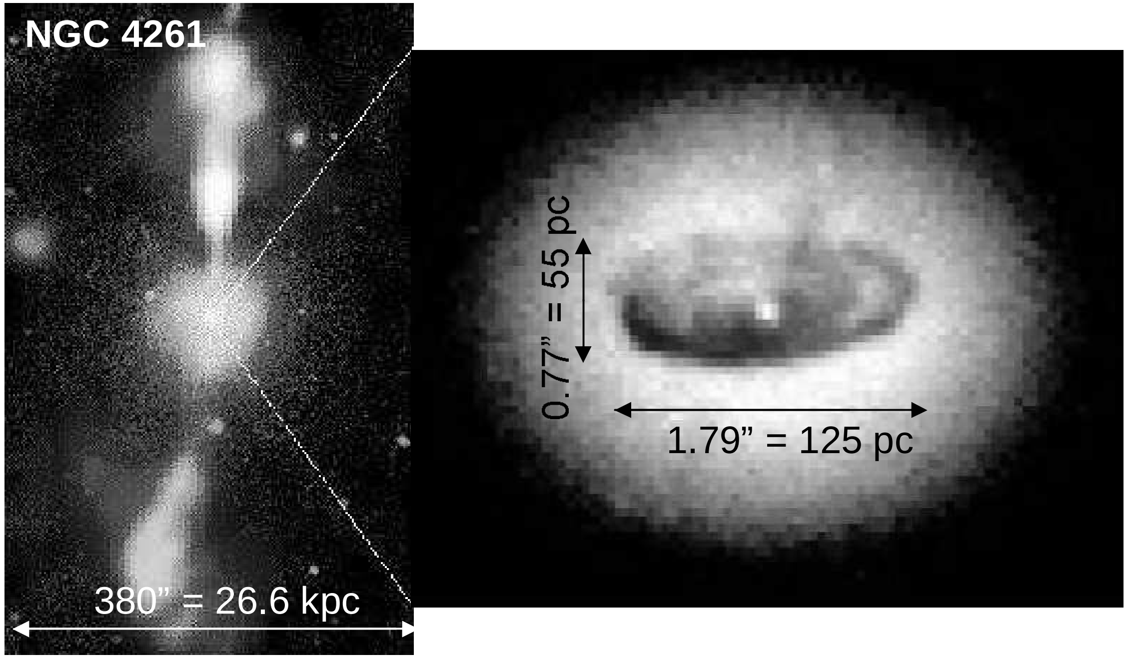

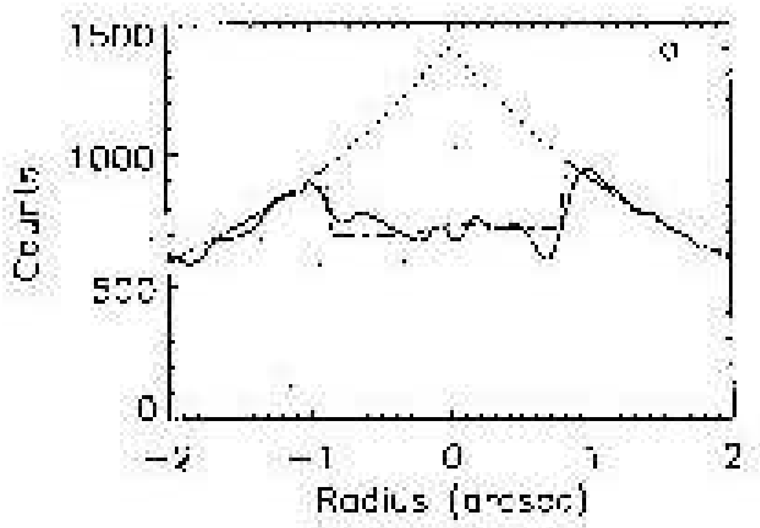

HST imaging of the radio galaxy **NGC 4261** at 5429 Å reveals a thin (≤20pc) extended (125pc along major axis) disk of obscuration (Jaffe et al. 1993, 1996).

Unification hypothesis:

Radio-loud:

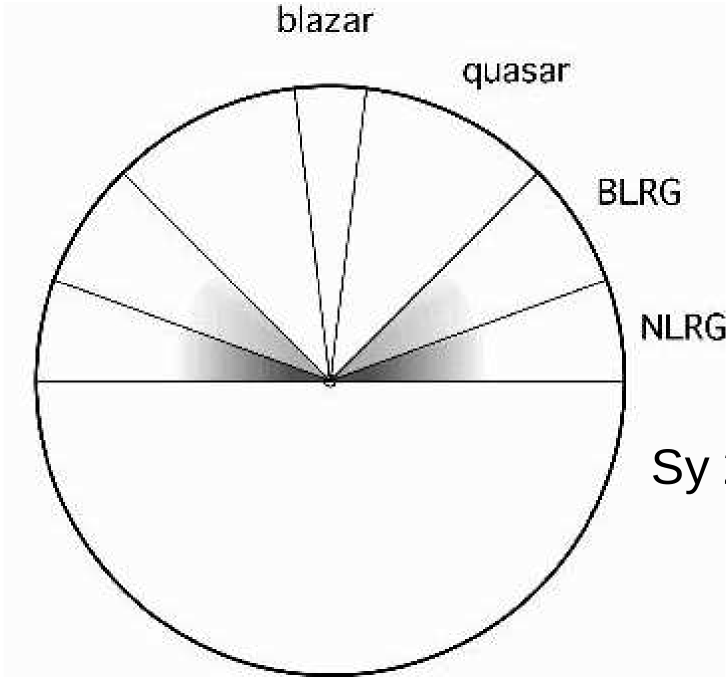

Sy 2

Radio-quiet:

Sy 1
QSO

RQs have radio jets very similar to those in RLs albeit at much lower power

(Goodrich 2001)

Particle acceleration at shocks
Blandford & Königl 1979, Blandford & Eichler 1982

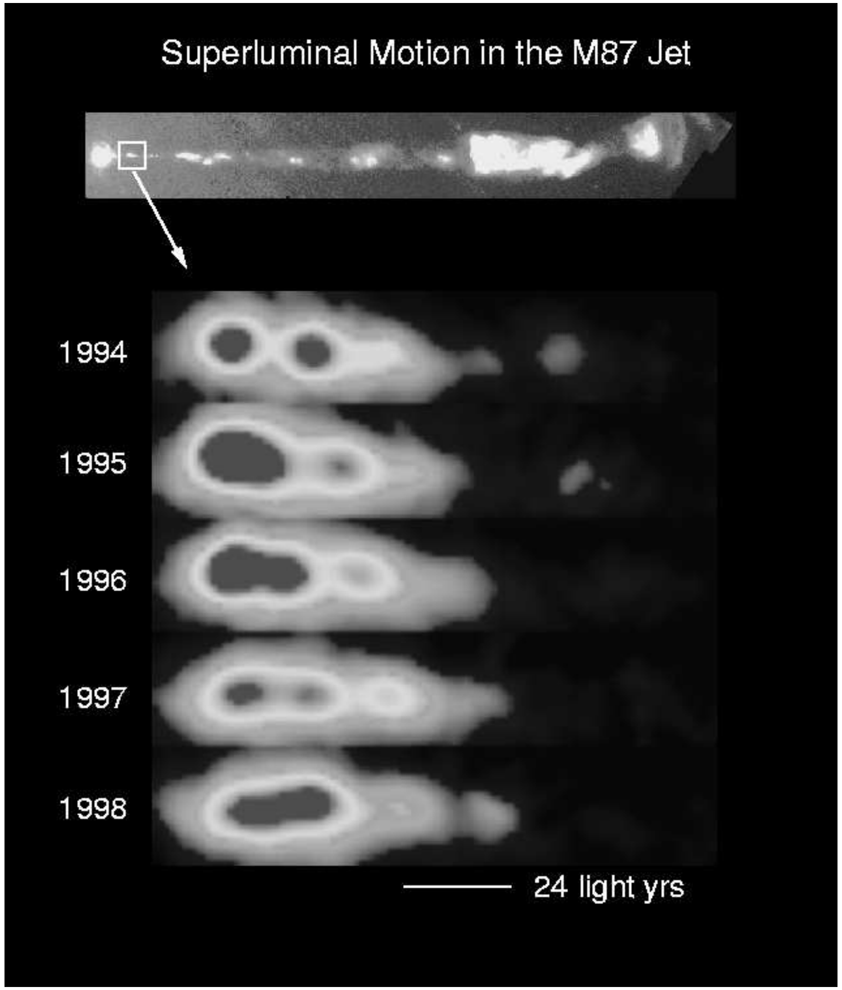

Relativistic propagation of acceleration zone → beaming, abberation

Power law spectra → in situ acceleration with Fermi-type spectra $dN/dE \sim E^{-2}$ (synchrotron spectral index ½)

Problems with spectral ageing away from the shock front

Shear acceleration? (Rieger & Mannheim 2003, Ostrowski 2003)

Composite spectra → multiple shocks in the jet

Blandford&Königl, Marsher&Gear, Mannheim&Biermann

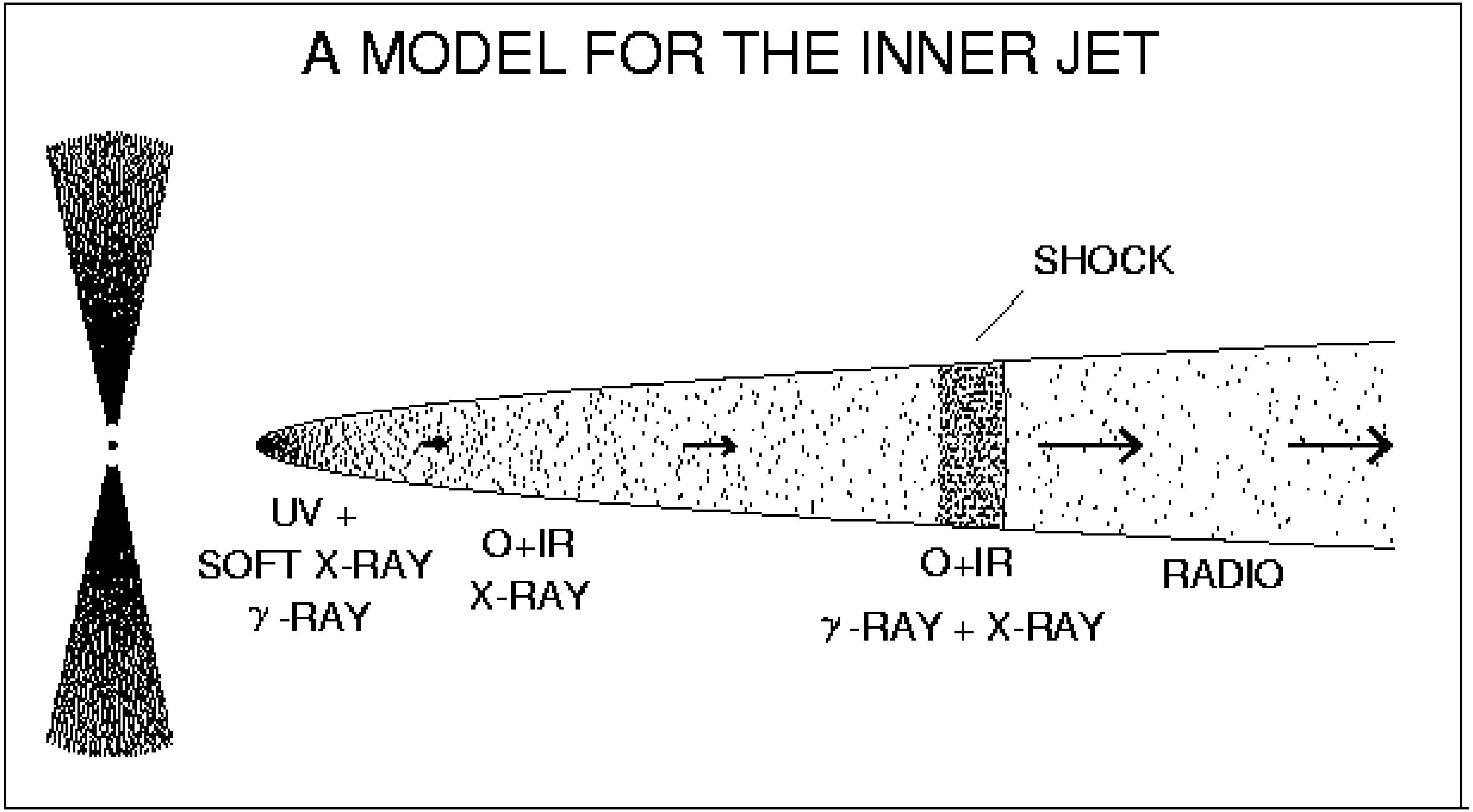

Spectral energy distributions

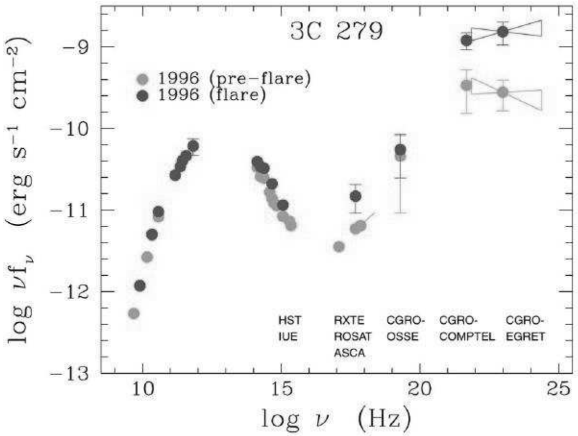

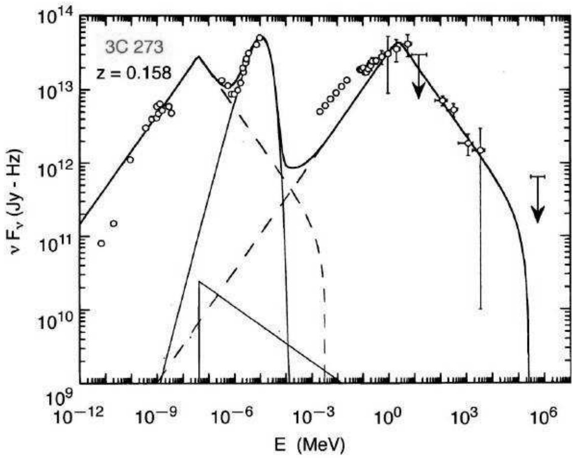

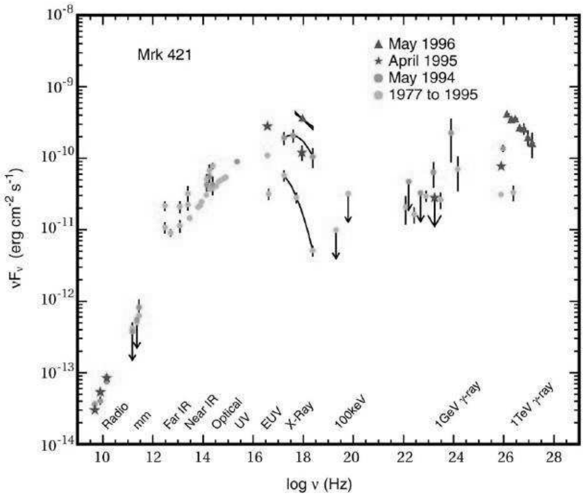

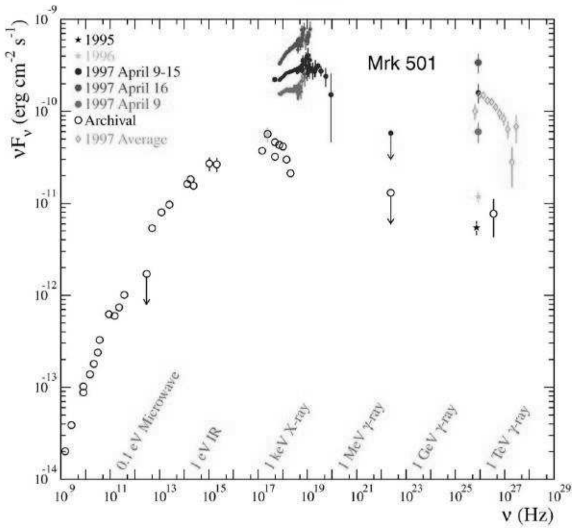

Flare spectra → single shock evolution

Kirk&Rieger, Dermer&Schlickeiser, Mücke(Reimer)&Protheroe

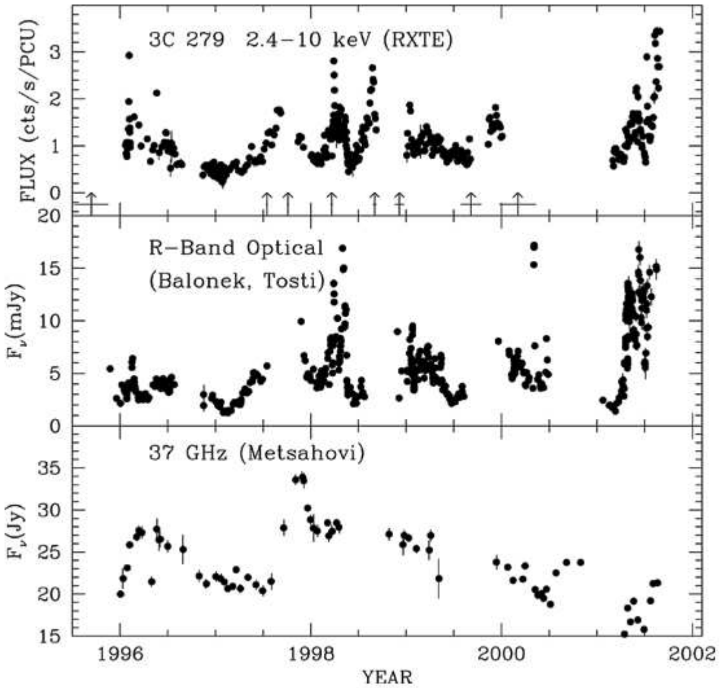

Periodic modulation due to binary black hole ?

Valtaoja

Rieger&Mannheim

Prompt Gamma-Ray Bursts

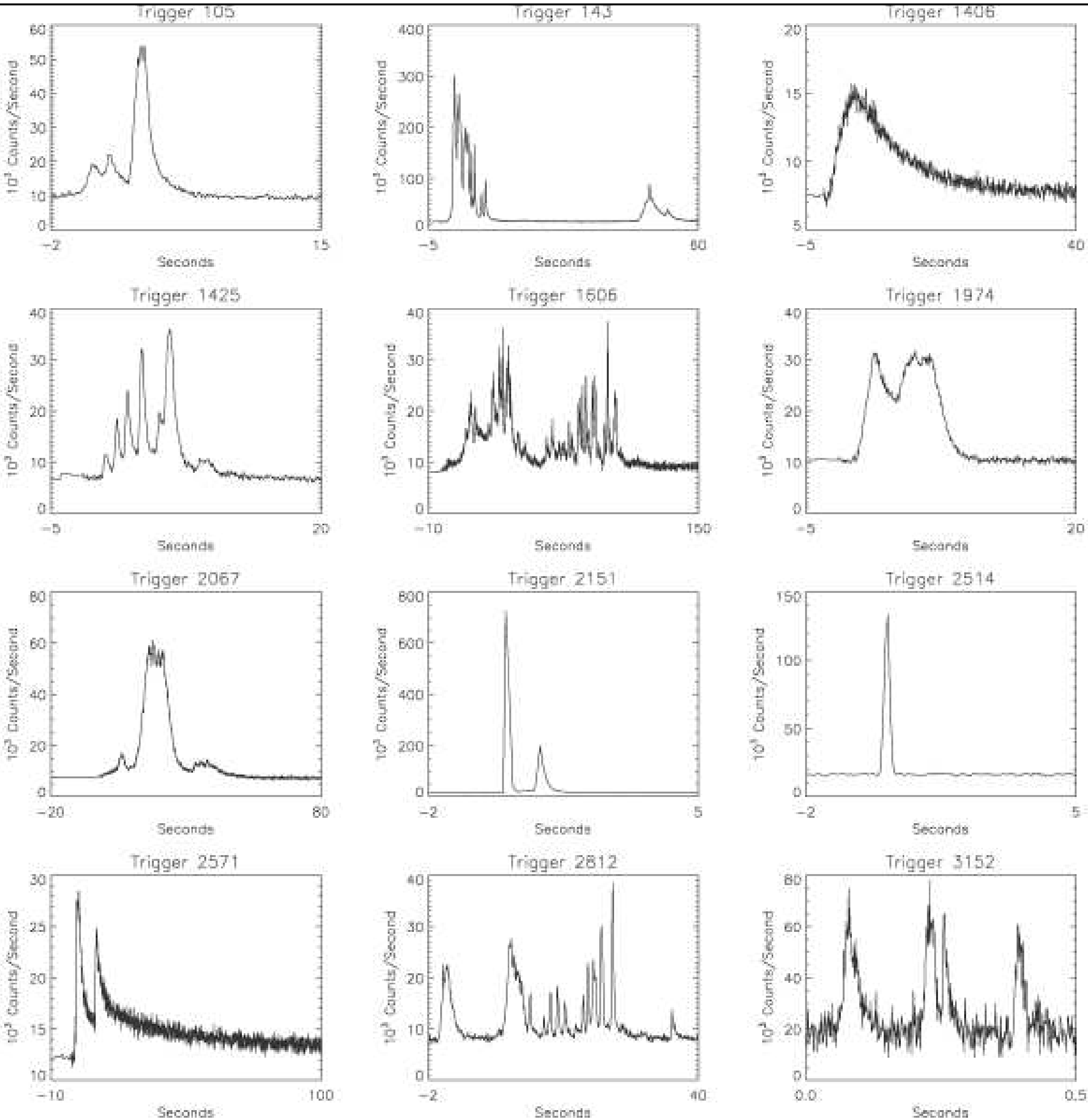
Trigger 105
Trigger 143
Trigger 1406
Trigger 1425
Trigger 1606
Trigger 1974
Trigger 2067
Trigger 2151
Trigger 2514
Trigger 2571
Trigger 2812
Trigger 3152
10^3 Counts/Second
Seconds

Bimodal distribution of the burst duration

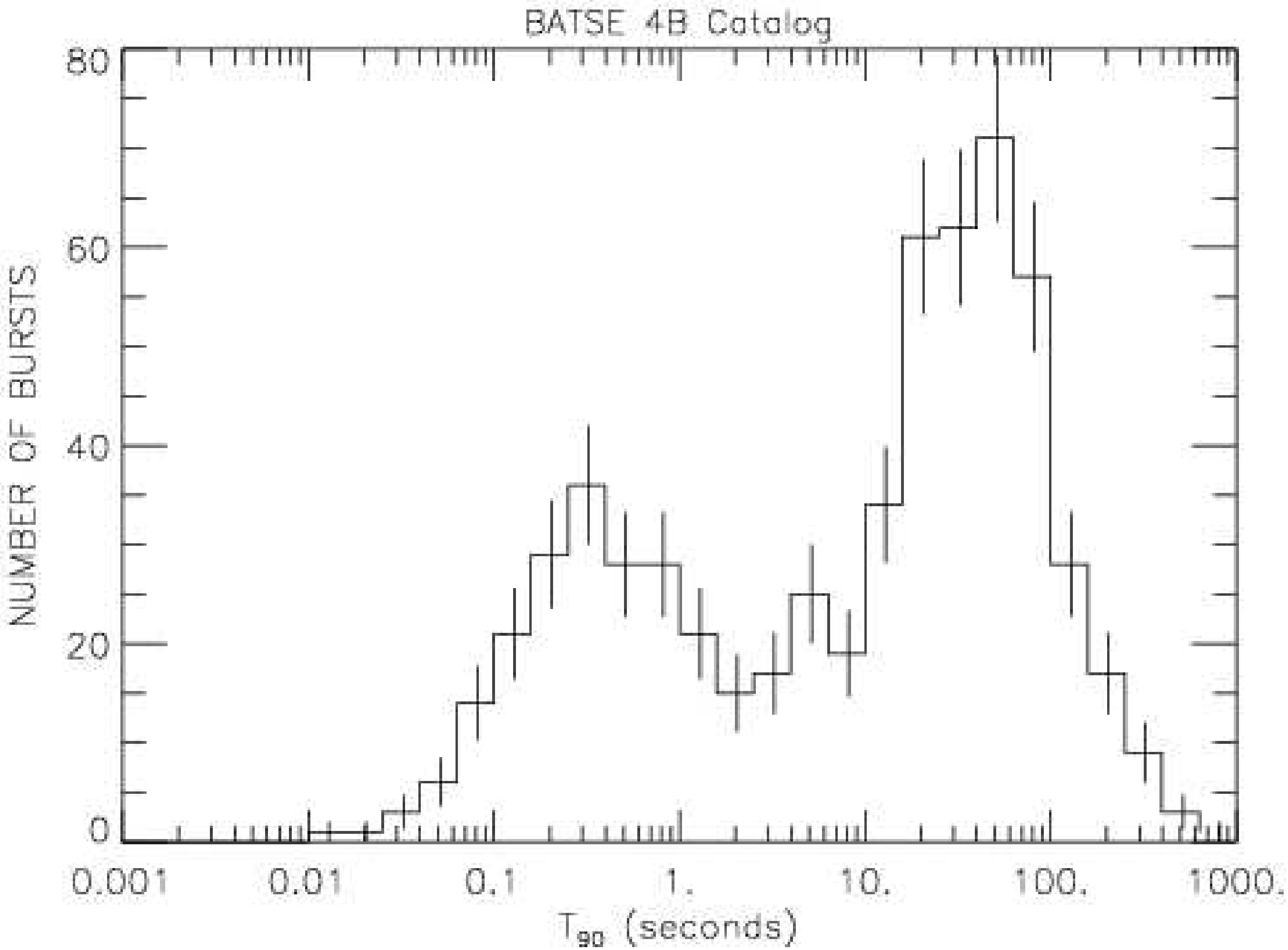

Current GRB Characterizations

- Gamma Ray Photon Energies > 100 keV
- GRB types, by duration/spectra:
  - Short and Hard < 2 seconds
  - Long and Soft > 2 seconds, some over 100 seconds
- Sources are now determined to be extra-galactic
  - up to redshifts of 5 have been observed
- Typically 10-1000 FOE released (isotropically)
  - i.e., large luminosities 10^{51-55} erg/s
- Power-law spectra
  - index of 1 at low energies
  - 2-3 above about 1 MeV, extending well above 1 GeV
- FRED time behavior – Fast Rise Exponential Decay

Temporal Variation

Walker, Schaefer and Fenimore, ApJ 537:264 (2000)

- Looking at isolated flares. Examined initial second of GRB light curves in a sample of 20 bursts.
- Timescales from 256 to 2048 μsec were observed.
  - Wavelet analysis showed power from 256 μsec to 33 ms
- Conclusions:
  - $R \leq 1200$ km along line of sight
  - Emission region as subtended from central source and collimation of jet must be less than 42” – implies a degree of polarization
  - Lorentz factors along a radius line must have dispersion of less than roughly 2%
  - External Shock scenario: impacted cloud must be smaller than 16 AU on average

Nakar & Piran, astro-ph/0103192

- Looking at 33 short pulses and 34 long pulses, came to similar conclusions:
  - On average 10 ms timescale variability (both short and long)
  - Unlikely to be external shock
  - 30% of short bursts are smooth

The Compactness Problem

(cf. discovery of 3C279 with EGRET: Bignami report in 1991 Nature "isotropic luminosity of 10^{49} erg/s" and first relativistic beaming model with baryonic energy transport by Mannheim&Biermann, AA Letter 1992)

- Consider isotropically emitting source at a distance *D*

$$E = 4\pi D^2 F = 0.1\,\mathrm{FOE}\left(\frac{D}{3\,\mathrm{Gpc}}\right)^2\left(\frac{F}{10^{-7}\ \mathrm{erg/cm^2}}\right)$$

- Temporal variations ➔ R < 1200 km
- Given high photon energy population, production of e^+e^- pairs likely. f_p is fraction of photon pairs that satisfy

$$\sqrt{E_1 E_2} > m_e c^2$$

- The average optical depth for this process is

$$\tau = 10^{13} f_p\left(\frac{F}{10^{-7}\ \mathrm{erg/cm^2}}\right)\left(\frac{D}{3\,\mathrm{Gpc}}\right)^2\left(\frac{\delta T}{10\,\mathrm{ms}}\right)^{-2}$$

Correction of optical depth due to relativistic beaming for source moving at Lorentz factor γ towards the observer:

$$\tau = \frac{10^{13}}{\gamma^{(4+2\alpha)}} f_p \left(\frac{F}{10^{-7}\ \mathrm{erg/cm^2}} \right) \left(\frac{D}{3\ \mathrm{Gpc}} \right)^2 \left(\frac{\delta T}{10\ \mathrm{ms}} \right)^{-2}$$

→ $\gamma \sim 300$

GRB Generic Model

This leads us to the following generic model:

I. *A hidden central inner engine which produces a relativistic outflow of energy*
   - NS-NS, NS-BH, BH-He, Collapsar, Hypernova

II. *Energy transport from the engine to an outer region where,*
   - Kinetic energy flux by relativistic particles is easiest

III. *there is a conversion of energy to the observed prompt radiation, i.e., the burst*
   - Kinetic energy is converted to thermal energy in shocks, then radiated away as gamma-rays. Two models: internal and external shocks.

IV. *Later, there is a conversion of the remaining energy into radiation, i.e., the afterglow*
   a) Inner engine of GRB shines for long time, produces both the pre-cursor as well as the afterglow
   b) Slowing down of relativistic shell by the ISM, i.e., an external shock, the Blandford-McKee self-similar solution

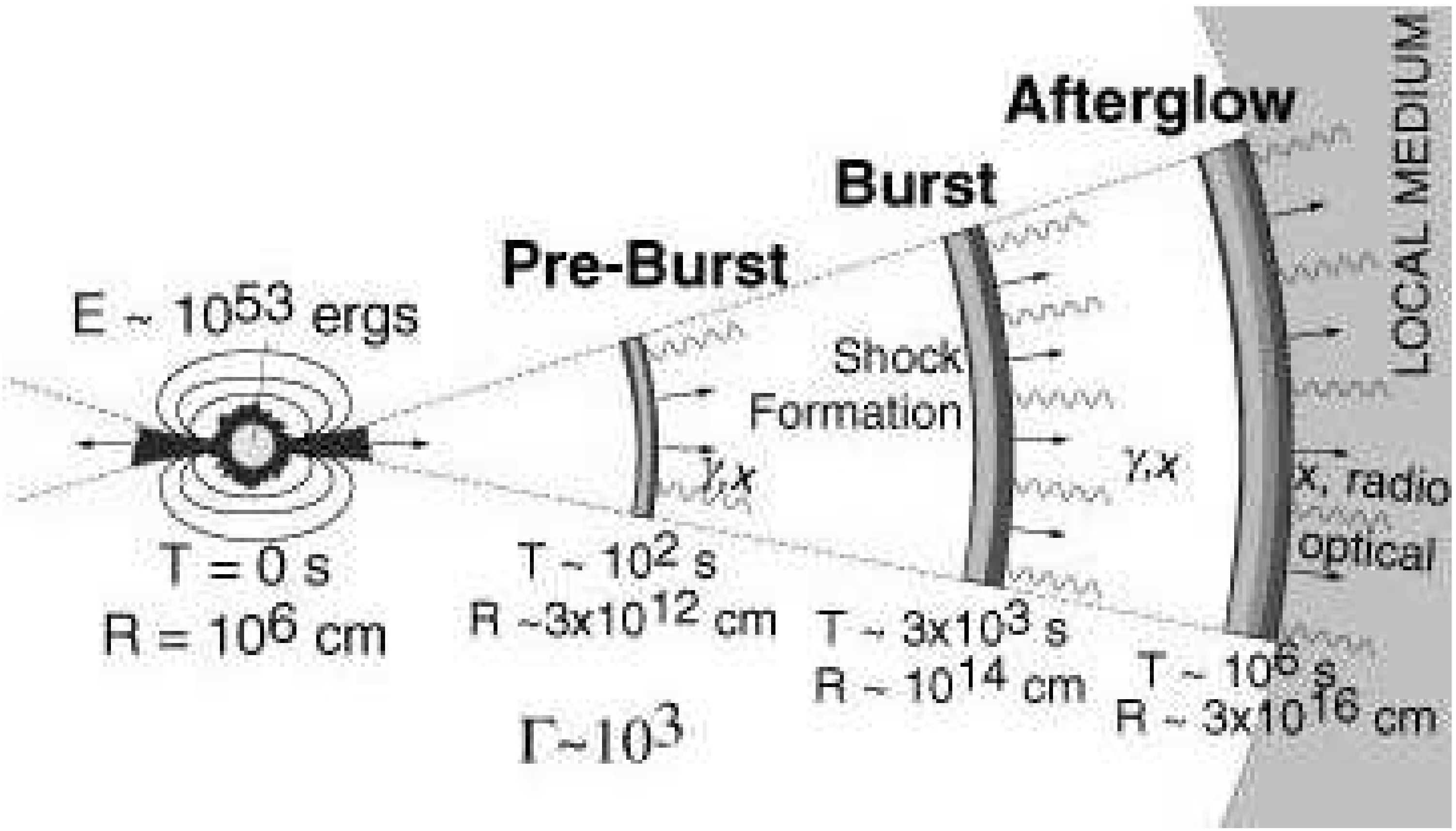

Afterglow
Burst
Pre-Burst
E ~ 10^53 ergs
T = 0 s
R = 10^6 cm
T ~ 10^2 s
R ~3x10^12 cm
Γ~10^3
Shock
Formation
γ,x
T ~ 3x10^3 s
R ~ 10^14 cm
γ,x
x, radio
optical
T ~ 10^6 s
R ~ 3x10^16 cm
LOCAL MEDIUM

Fireballs

- Large concentration of electromagnetic radiation in small region of space with small fraction of baryons
- Sudden release of high intensity gamma-rays produces e^+e^- pairs which create an opaque photon-lepton "fireball"
- If present, most energy goes into bulk motion of the baryons. Reach a Newtonian flow with

$$\mathrm{v} \cong \sqrt{2E/M}$$

Types of Fireballs

1. **Pure Radiation Fireball**

   Neglecting baryons, evolution is pure photon-lepton. When T=20keV, τ=1 and E>Mc^2, radiation dominated, energy escapes as radiation.

2. **Electron Dominated Opacity**

   In late stages, electrons associated with baryons dominate opacity. T<<20keV before τ=1. Eventually radiation dominated.

3. **Relativistic Baryonic Fireball**

   Matter dominated before optically thin. Energy is converted into bulk kinetic energy of baryons. Most interesting for GRBs.

4. **Newtonian Fireball**

   Expansion never becomes relativistic. An example is a supernova explosion where the energy is deposited into a massive envelope.

Energy Conversion

SNR

- order of FOE
- Solar mass of ejecta
- Non-relativistic flow
  - Several 1000 km/s
- Interaction with ISM
  - Over several pc
  - lasts for thousands of years

GRB

- order of FOE
- Small fraction of a solar mass of ejecta
- Very relativistic flow
- Internal collisions produce primary radiation
  - Over hundreds of AU
  - Lasts for fraction of a second
- ISM interactions produce afterglow
  - Over a fraction of a pc
  - Lasts for several days

Internal Shocks

- Take place when inner shell overtakes an outer shell (with lower velocity, γ). Collision takes place at $R_\delta \approx \gamma^2 \delta \approx 10^{14}\ \mathrm{cm}\ \delta_{10}\gamma_{100}^2$

  where δ_{10} is the initial separation by 10^{10} cm
- Internal shocks are important only if the bulk motion is not too fast (otherwise one would only get external shocks) $\gamma \leq 2800\, T_{10\mathrm{s}}^{-3/8}$
- Recall lower bound on velocity.
  - For Compton scattering of the photons on the shell's electrons: $\gamma \geq 130\, T_{10\mathrm{s}}^{-2/5} E_{52}^{1/5}$
  - For pair production, unity optical depth of 100MeV photon $\gamma \geq 570\, T_{10\mathrm{s}}^{-1/4}$
- This limits the radii at which the emission can take place

$$\left\{ 5\times10^{13}\ \mathrm{cm}\, T_{10\mathrm{s}}^{1/5}, 10^{15}\ \mathrm{cm}\, T_{10\mathrm{s}}^{1/2} \right\} \leq R_\delta \leq 3\times10^{16}\ \mathrm{cm}\, T_{10\mathrm{s}}^{1/4}$$

- Prediction: bursts with narrow peaks should not have high energy tails, very short bursts may have a softer spectrum

External Shocks with the ISM

- Characterized by the reverse shock which crosses inner outwardly moving shocks:
  - Newtonian
    - Reduces energy in each shock very little
  - Relativistic
    - Reduces significantly the kinetic energy of each layer that it crosses
- Mostly important in the afterglow effect

Emission Mechanisms and Limits

- Synchrotron Emission
  - Observed low energy spectra appear to resemble synchrotron spectra, power law index about 2.5
  - Electrons are tightly coupled to protons and therefore plasma waves.
  - Maximal velocity of electrons corresponds to the acceleration time equaling the magneto-sonic crossing time: $$t_{\mathrm{acc}} = \frac{cR_L}{\mathrm{v}_A^2}$$
  - Synchrotron Cooling Timescale: $$t_{\mathrm{synch}} = \frac{\gamma mc^2}{P_{\mathrm{synch}}}, \quad P_{\mathrm{synch}} = \frac{4}{3}\sigma_T c U_B \gamma^2$$
  - This yields γ-factors of 10^8, which if significantly higher than anything we're worried about. So we can ignore the upper cutoff. (recall HW)
- Given the characteristic photon energy $(h\nu_{\mathrm{synch}})_{\mathrm{obs}}$ (which is related to the Larmor frequency and the energy of the emitting electrons), we can compute the above synchrotron cooling time.
  - The observed cooling time is shorter by a factor of Γ.
  - We can obtain the cooling time scale as a function of the observed photon energy.

$$t_{\mathrm{synch}}(\nu) \propto B^{-3/2}\Gamma^{-1/2}\nu^{-1/2}$$

- This is a "universal" time since the energy of a particular electron is not present in the equation. This relation is very close to the observed GRB timescale of $\delta T \propto \nu^{-0.4}$
- Lower limit on variability of GRB. Source cannot spike on scales shorter than cooling time.
- FRED may be explained by rapid shock heating of the electrons, decay set by cooling

Synchrotron Self-Absorption

- Irrelevant during the GRB itself

  → Optically thin region

- More important at late times, i.e., afterglow

Synchrotron Self-Compton

- Only one IC scattering can take place
  - γ^2 factor in energy, energy relation no longer satisfied (Klein-Nishina)
- Large fraction of low energy radiation will be up-scattered by IC
  - Can have photon energies in the GeV or even TeV range
- Has the effect of shortening the cooling time (by extracting energy from the electrons)
- Reduces the efficiency of energy conversion by the Comptonization parameter $Y = \gamma^2\tau$ which can be large

GRB Central Engines
Requirements

Energy

1 FOE (anisotropic), accelerate approximately 10^{-5} solar masses to relativistic velocities, $\Gamma > 100$

Beaming

Most are beamed with opening angles 0.02 to 0.2 radians → collimated flow

But some have rather large opening angles, not well collimated

Long and Short Bursts

same mechanism?

Rates

1 per 10^7 $(4/\theta^2)$ year per galaxy, about 1/1000 the rate of supernovae, equivalent to about one per day

Time Scales

variability of say 1 ms, duration on the order of 50 s – cannot be produced from single explosion

Possible SN association

Some GRBs seem to be associated with SNe. GRB030329 shows SN spectrum, SN2003dh

Iron Lines

Observed in some X-ray afterglows. Must have large amount of iron at rest near central engine

Star Formation association

GRBs seem to be prevalent in star forming regions. Rates also seem comparable.

Distribution

Within galaxies, don't seem to be outside of galaxies (NS-NS)

No Windy Afterglow

"No evidence for a wind (n=2) in any of the aferglow light curves? Futhermore, most fits for the afterglow parameters show low ambient density."

GRB Engine Models
Collapsar and Hypernova

- Another end for stars, fits in with stellar evolution of massive stars

- Type I
  - Iron core collapse to BH
  - 0.01 – 0.1 solar mass per second for first 20 s
  - Variability down to 50 ms, duration of about 10 seconds
- Type II – "Failed Supernova"
  - Fallback of SN explosion onto NS/BH
  - 0.001 – 0.01 solar mass per second, no jet by neutrinos
  - Duration 10-100 times longer than Type I

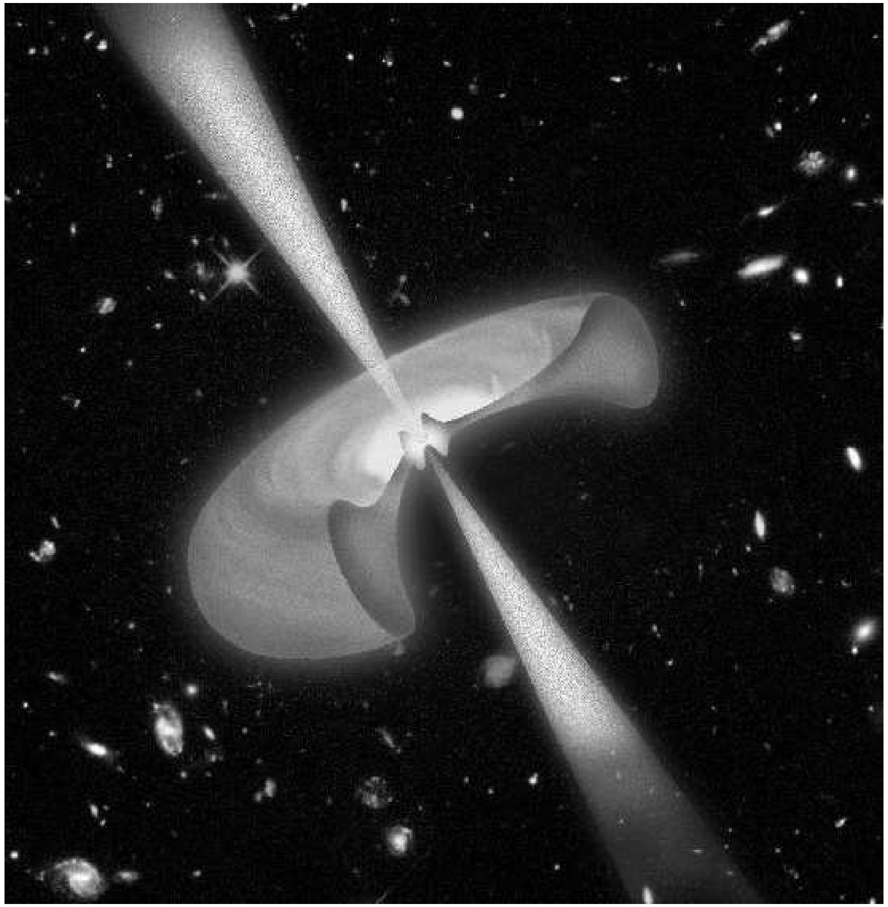

GRB Engine Models

Compact Object Merger

  - Promising for short and hard bursts, not so much for long and soft
- Direct Merger
  - NS-NS, NS-BH, BH-He star binary mergers
  - Very short burst
  - Could have variability of output flow during merger
- Tidal Disruption
  - BH torus system
  - similar to collapsar model
  - Blandford-Znajek

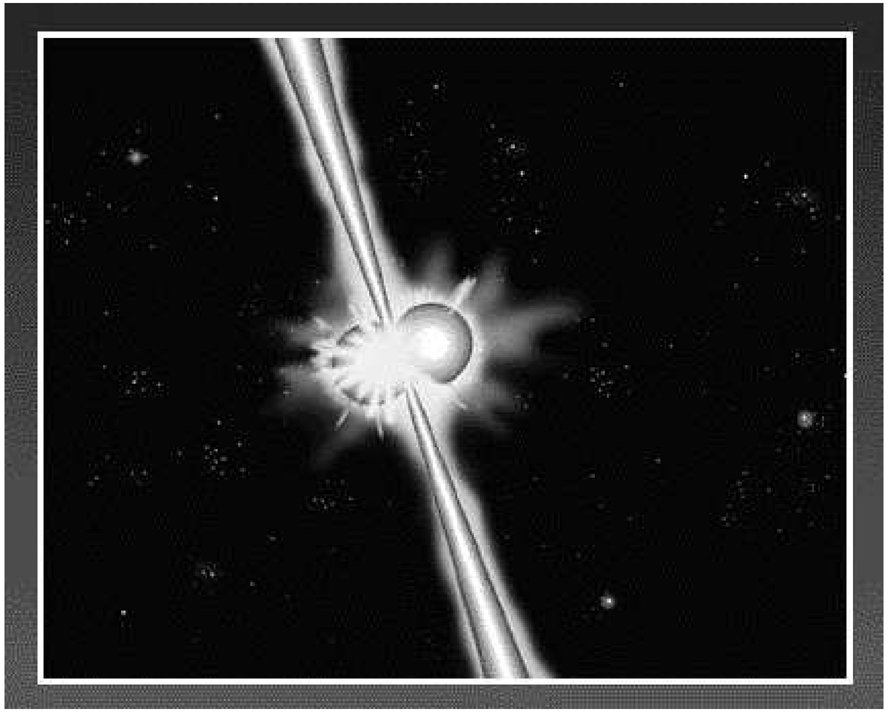

Association with star forming regions at high z favor SN Collapsar models

Probing the jet phase of a GRB

- Cosmic Rays
  - Possibility of 10^{19} eV cosmic rays from Fermi acceleration of protons in cosmological GRBs. E Waxman, ApJ 452, L1 (1995)
- Neutrino emission
  - 10^{14} eV neutrinos via photomeson production of pions in interactions between the fireball gamma rays and accelerated protons. E Waxman PRL 78:2292 (1997)
- Gravitational Wave Signature
  - All models have a predicted unique gravitational wave signature which should be detectable by advanced LIGO

Open Questions

- Fireball model has observational support
  - Predictions about early afterglow and the GRB-afterglow transition need to be confirmed
  - How do collisionless shocks work?
  - Source of large magnetic fields? ($10^{13\text{-}18}$ G)
  - Just the right amount of baryon contamination
- GRB Engine for acceleration of ejecta
  - Variability of ejecta, (shot-gun model?)
- Short vs. Long bursts – the same mechanism?

Part C) Particle acceleration

- Stoßfreies, magnetisiertes Plasma
- MHD Stoßwelle der thermischen Teilchen
- Suprathermische Testteilchen (Injektion)
- Plasmaturbulenz über gyroresonanten Wellenzahlenbereich (Diffusionskoeffizienten im Orts- und Impulsraum)
- Quasilineare Näherung
- Energieverluste < Energiegewinne
- Statistische Balance aus Entweichen und Beschleunigung

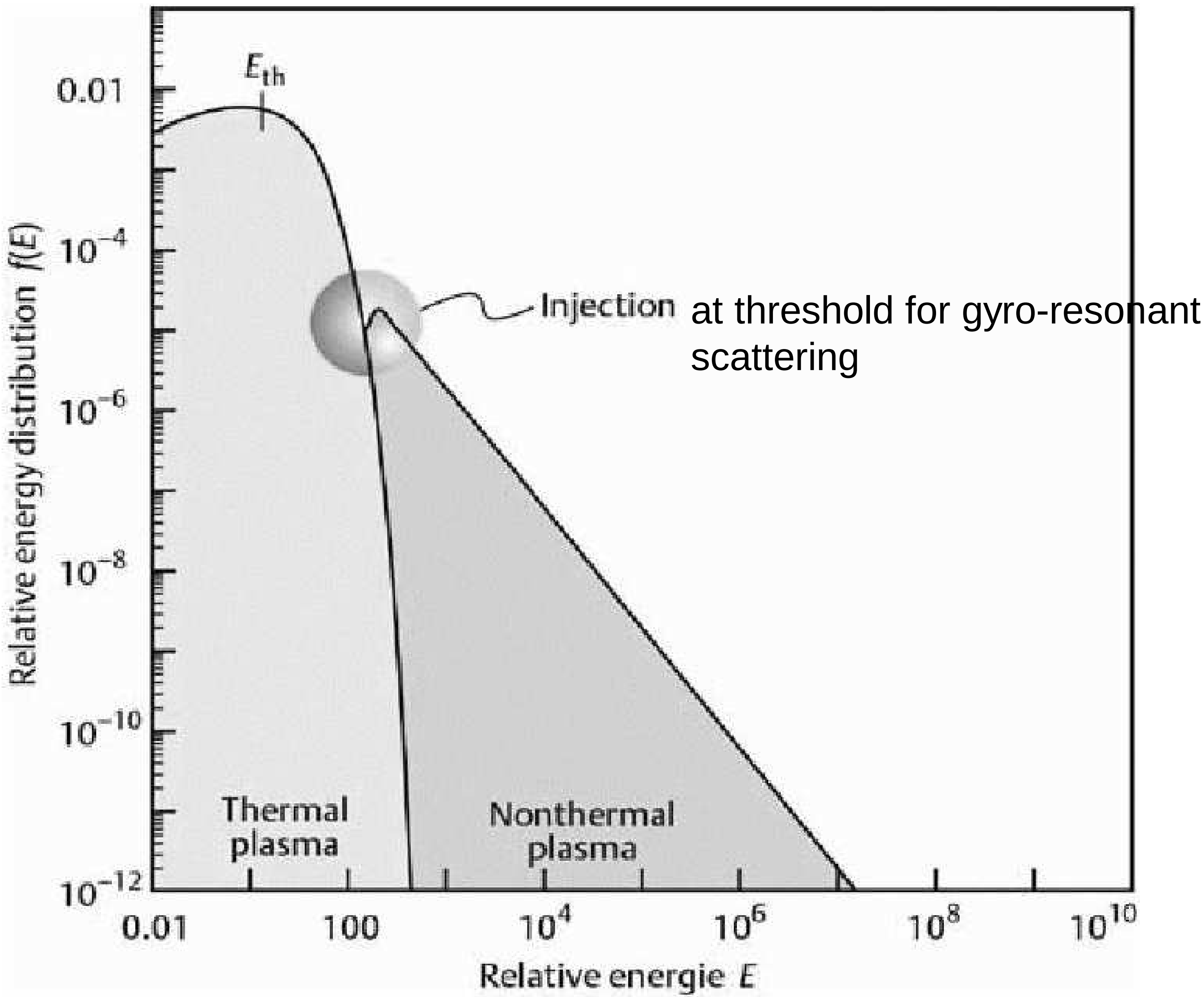
E_th
0.01
10^-4
10^-6
10^-8
10^-10
10^-12
Relative energy distribution f(E)
Injection
at threshold for gyro-resonant scattering
Thermal plasma
Nonthermal plasma
0.01
100
10^4
10^6
10^8
10^10
Relative energie E

Fermi Acceleration Mechanism

Stochastic energy gain in collisions with plasma clouds

2nd order :
randomly distributed magnetic mirrors

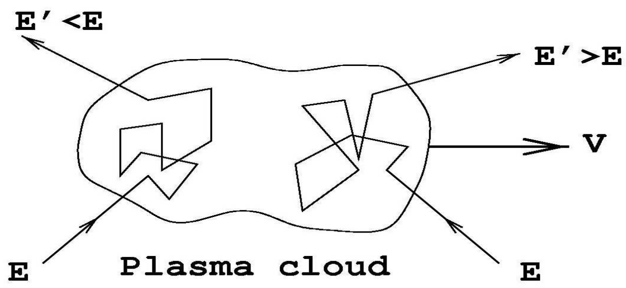

$$\frac{\Delta E}{E} \sim \beta^2 \qquad \beta = \frac{V}{c} \lesssim 10^{-4}$$

[Slow and inefficient]

1st order :
acceleration in strong shock waves (supernova ejecta, RG hot spots...)

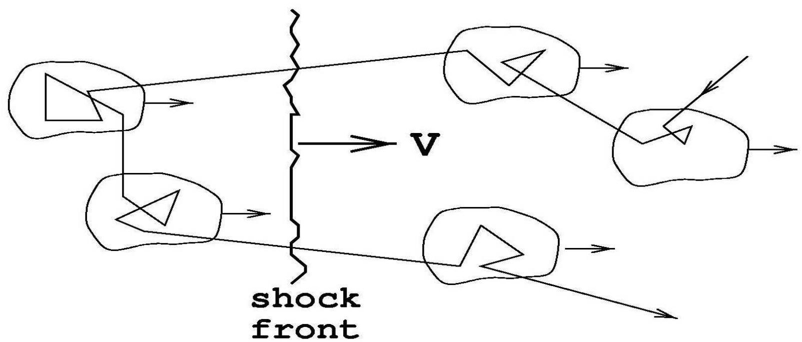

$$\frac{\Delta E}{E} \sim \beta \qquad \beta = \frac{V}{c} \lesssim 10^{-1}$$

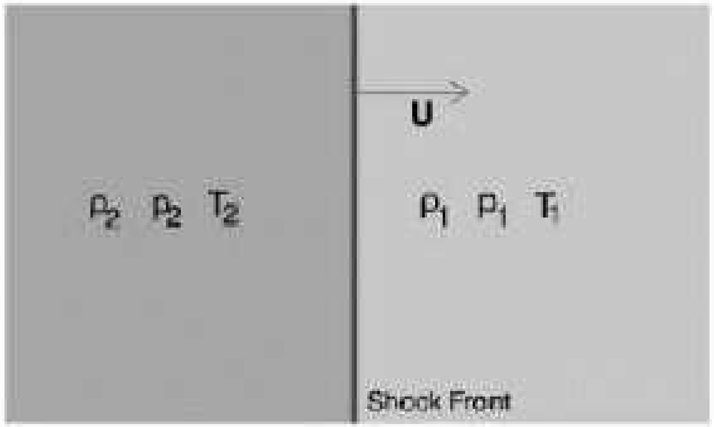

(a) Shock front traveling at speed **U**

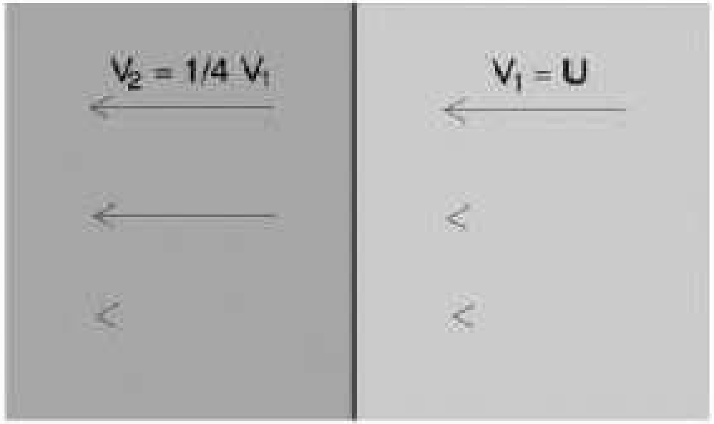

(b) seen in rest frame of shock front

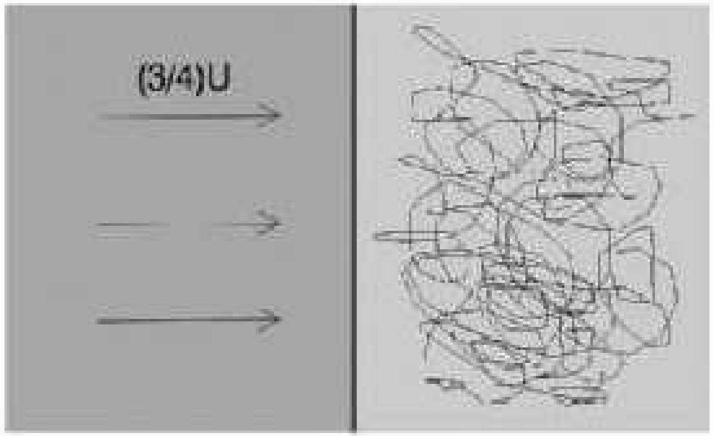

(c) rest frame of downstream medium

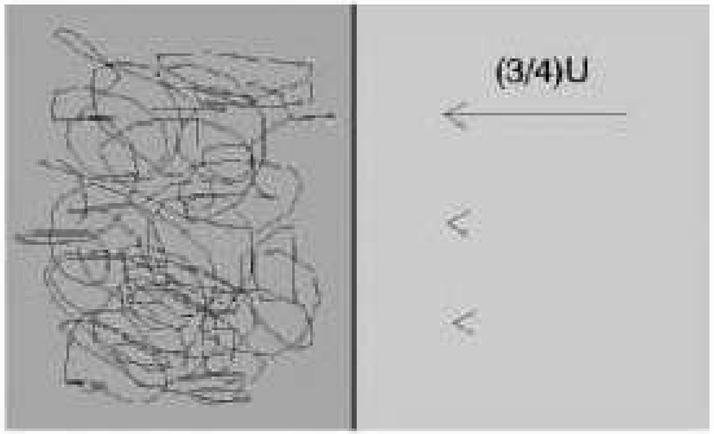

(d) rest frame of upstream medium

Does not work for relativistic shocks → anisotropies (Kirk)

Diffusions-Stosswellenbeschleunigung

Idee: ***Elastische Streuung zwischen sich aufeinander zu bewegenden Spiegeln***

(Fermi 1949,1954)

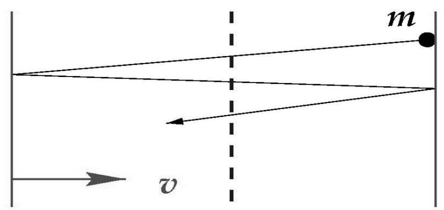

$$\frac{\Delta E}{E} = 2\,\frac{v}{c} = \xi$$

Pitchwinkel Streuung

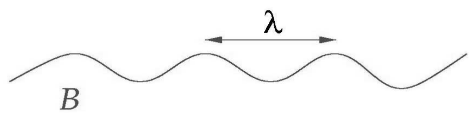

Gyroresonanz $r_g = \lambda$

⟶ *Diffusion + Konvektion (Wellenfortpflanzung)*

Stosswellen: *(Axford et al. 1977, Krimsky 1977)* *(Entweichwahrscheinlichkeit p)*

$$E_n = E_o\,(1+\xi)^n$$

$$N(>E) = \frac{(1-p)^n}{p} \longrightarrow \frac{dN}{dE} = \frac{1}{p}\left(\frac{E}{E_o}\right)^{-s} \qquad s = 2 + \frac{4}{M^2}$$

Maximalenergien: $t_{acc} = f\; r_g / c = Min[t_{cool}, t_{age}, t_{diff}]$

t_{cool} :

$$E^{(e)}_{max} = 4\,(f/10)^{-0.5}\,(B/1\,G)^{-0.5}\,(v/c)\ \ TeV$$

$$E^{(p)}_{max} = 1\,(f/10)^{-0.5}\,(B/1\,G)^{-0.5}\,(v/c)\ \ EeV$$

Summary of lecture on cosmic accelerators

- Nonthermal Universe hosts zoo of interesting objects
  - AGN most powerful population, UHE CR candidates
  - GRB most powerful objects, UHE CR candidates
  - SNR candidates for galactic CRs with problems
- Ubiquity of collisionless relativistic plasma
  - shock waves
  - magnetic fields and plasma turbulence
  - jets (collimated by z-pinch)
  - rotation
- Link between energy carried in cosmic rays, gamma rays, and neutrinos → observations and theory can be tied together
- New physics at high mass scale → anomalies ?